Cooperative Phenomena in Stochastic Neural Networks with Dynamic Synapses

Instituto Carlos I de Física Teórica y Computacional
y Depto. de Electromagnetismo y Física de la Materia
Universidad de Granada

Fenómenos Cooperativos en Autómatas Neuronales Estocásticos con Sinapsis Dinámicas

JESÚS M. CORTÉS DÍAZ

TESIS DOCTORAL

Granada, 22 de Febrero de 2005

Editor: Editorial de la Universidad de Granada
Autor: Jesús M. Cortés Díaz
D.L.: Gr. 353 - 2005
ISBN: 84-338-3291-3

To *Esther* . . .

Dr. D. Joaquín Marro Borau, catedrático del Departamento de Electromagnetismo y Física de la Materia de la Universidad de Granada, y Dr. D. Joaquín J. Torres Agudo, contratado *Ramón y Cajal* en el mismo departamento, CERTIFICAN que el presente trabajo ha sido realizado bajo su dirección y constituye la Tesis Doctoral de D. Jesús M. Cortés Díaz

Granada, a 22 de Febrero de 2005

Fdo: Joaquín Marro Borau

Fdo: Joaquín J. Torres Agudo

Acknowledgments

Una vez llegado hasta aquí, no sería justo ni honesto el no recordar ni agraceder a toda esa gente que han hecho posible el estar yo, ahora, acordándome de ellos. En primer lugar al profesor Joaquin Marro. Un gran entusiasta por el trabajo y que en todo momento me ha sabido transmitir ese motor de ilusión y sentido ante resultados siempre posibles, pero aún pendientes por hacer. Una tarea sin duda complicada y llevada a cabo de forma impecable. A Joaquin J. Torres, por apostar por mí de forma incondicional. Él me ha dado todo su apoyo y me ha enseñado todo lo que sé, que no es otra cosa que la única receta milagrosa para hacer ciencia es querer hacerla. A la demás gente del grupo de Física Estadística de la Universidad de Granada. A Pedro Garrido, por educarme para que me gusten los ordenadores. A Miguel Ángel Muñoz, por escucharme en muchos momentos un tanto delicados. Y a los demás, a Pablo, los dos Pacos, Omar, Manolo, Juan Antonio y David. Muchas gracias por hacer de nuestros despachos un lugar ideal para pensar, hablar y disfrutar del trabajo. Gracias a todos.

Fuera del ambiente de trabajo, no me puedo olvidar de la *otra gente* que a mi juicio, han contribuido de forma desinteresada y mucho en el desarrollo de esta tesis. A mis amigos, quienes me han dado clases magistrales de cómo ser práctico en la vida. A mis hermanos, por haberme enseñado que estudiar tiene también muchas satisfacciones y ventajas. A mis padres, por darme su apoyo siempre y para todo. De mi padre he aprendido que las matemáticas también pueder ser bellas. De mi madre, la importancia de pensar y ese espíritu crítico

que me caracteriza y que me ha ayudado tanto a la hora de resolver problemas. Y por último a Esther, quien sin ella nunca hubiera llegado a este momento. Y de esto estoy plenamente seguro. Esta tesis es parte de vosotros. Muchas gracias.

Contents

Figures

Chapter 1

Resumen en español

En esta tesis se ha estudiado mediante técnicas de Mecánica Estadística del No-Equilibrio cómo en redes neuronales recurrentes es posible que propiedades macroscópicas emerjan como resultado de la interacción entre neuronas y sinapsis. Algunos ejemplos de tales propiedades macroscópicas o colectivas pueden ser el reconocimiento de patrones, la aparición de memoria, la identificación y categorización de patrones de infomación y un fenómeno oscilante, por el cual el sistema estaría al recuperar información continuamente visitando todos los patrones almacenados en la regla de aprendizaje. Dichas propiedades dependen del grado de complejidad asumido para describir los mecanismos o interacciones sinápticas. Se ha estudiado cómo dichas propiedades emergen bajo tres diferentes niveles de descripción.

El nivel más alto y que asume un mayor realismo en las sinapsis se ha estudiado en el capítulo 3. El estudio se basa en un modelo fenomenológico de sinapsis dinámicas [Tsodyks et al., 1998]. Se asume que las intensidades sinápticas pueden o incrementar (dando lugar a la aparición de mecanismos facilitadores) o disminuir (mecanismos depresores) debido a la existencia de repetida activación presináptica, la cual, es necesaria para observar cierto grado de plasticidad sináptica [Abbott and Regehr, 2004]. Para estudiar los efectos de este modelo fenomenológico de sinapsis, se considera una red neuronal es-

tocástica con N diferentes neuronas. Cada una de ellas puede representar dos estados, el de disparo o excitacion y el de descanso y evoluciona en el tiempo con una dinámica probabilística del tipo de Glauber [Peretto, 1992] asociada a campos locales $h_i = \sum_j \omega_{ij} x_j s_j$. Tales campos, representan la intensidad presináptica total que recibe una neurona postsináptica genérica, s_i. Las variables ω_{ij} son sinapsis estáticas y representan la intensidad sináptica entre las neuronas i y j. En este modelo, son definidas a partir de una regla de aprendizaje standard, la regla de Hebb [Hertz et al., 1991]. La variable x_j is una cantidad que dinámicamente cambia con el tiempo y además representa el estado de la sinapsis y su probabilidad para producir una respuesta postsináptica. En particular, representa la fracción de neurotransmisores que están e un estado de recuperación, y que puede incluir mecanismos depresores o facilitadores. Cuando $x_j = 1$, para cualquier valor de j se recupera el modelo de Hopfield [Hertz et al., 1991], que bajo este escenario de sinapsis dinámicas es una red neuronal atractor con sinapsis estáticas. Para incluir mecanismos facilitadores es necesario incluir una nueva variable dinámica, $u_j(t)$, la cual incrementa después de cada disparo presináptico y tiene en cuenta la apertura de los canales de calcio en la neurona presináptica cerca de canales de liberación de neurotransmisores. Como una consecuencia, los iones Ca^2+ se introducen dentro de la célula y se unen a un aceptor [Bertram et al., 1996]. El sistema es caracterizado por un conjunto de de ecuaciones dinámicas donde ambas varibles $u_j(t)$ y $x_j(t)$ están acopladas y caracterizadas respectivamente por las constantes de tiempo τ_{fac} y τ_{rec} [Tsodyks et al., 1998]. Se estudian propiedades estáticas y dinámicas del modelo usando una teoría de campo medio y considerando técnicas similares a las explicadas en los trabajos [Hertz et al., 1991, Marro and Dickman, 1999, Pantic et al., 2002]. La solución de puntos fijos recupera en el límite de $\tau_{fac} \to 0$ los resultados obtenidos para el caso de sólo depresión [Torres et al., 2002]. El efecto de incorporar mecanismos facilitadores es apreciable únicamente cuando la probabilidad de liberación de neurotransmisores inicialmente (U_{SE}) es baja [Tsodyks et al., 1998]. Facilitación y depresión coexisten en las sinapsis con un peso relativo que depende fuertemente del valor de

U_{SE}. Un valor alto o bajo favorece respectivamente a mecanismos depresores o facilitadores.

Otra cantidad medida en el estado estacionario y que en redes neuronales atractor toma una especial importancia la *capacidad crítica* de la red neuronal, que es el máximo número de patrones que el sistema es capaz de almacenar y recuperar. Para calcularla, usamos técnicas similares a las presentadas en el trabajo [Hertz et al., 1991]. Aquí se asume que en el estado estacionario la red tiene un número finito de overlaps de orden $\mathcal{O}(1)$ (patrones condesados) y el resto de los overlaps son de orden $\mathcal{O}(1/\sqrt{N})$ (patrones no condesados). Además, utilizamos aproximaciones similares a las mostradas en el trabajo [Torres et al., 2002]. El resultado es un conjunto cerrado de ecuaciones macroscópicas para los parámetros de orden $\mathbf{m}, \mathbf{q}, \mathbf{r}$, que son llamados respectivamente el overlap, el parámetro de Edwards-Anderson (EA) y el Amit-Gutfreund-Sompolinsky (AGS) [Amit et al., 1987, Hertz et al., 1991]. Nosotros obtenemos resultados que son más generales a los existentes en la literatura. Así, tomando el límite de $\tau_{fac} \to 0$ se recupera el resultado de la capacidad crítica del modelo de Hopfield o sinapsis estáticas. Por otro lado, haciendo el límite $\tau_{rec} \to 0$ se recuperan los resultados de sólo consideran mecanismos depresores [Torres et al., 2002]. Lo que incorpora el considerar mecanismos facilitadores es un desceso drástico de la capacidad crítica de la red neuronal (veáse la figura 1.1). Esto es debido a que después de incorporar facilitación, la depresión se hace más intensa, y así la estabilidad de los atractores disminuye considerablemente. Por lo tanto, existen dos fuentes bien diferenciadas de ruido a tener en cuenta en el cálculo de la capacidad crítica. La contribución estándar y usual debido al aumento del número de patrones almacenados en la regla de aprendizaje y una nueva contribución, ocasionada por la depresión. Siguiendo este razonamiento, el caso de sinapsis estáticas es el que mayor capacidad crítica posee [Hertz et al., 1991]. Le sigue el caso de sólo mecanismos depresores [Torres et al., 2002] y por último el caso estudiado aquí de incluir junto con depresión, facilitación.

Con relación al estudio de propiedades dinámicas, en este capítulo se estudia para el caso de $\alpha = 0$ la estabilidad local alrededor de los estados esta-

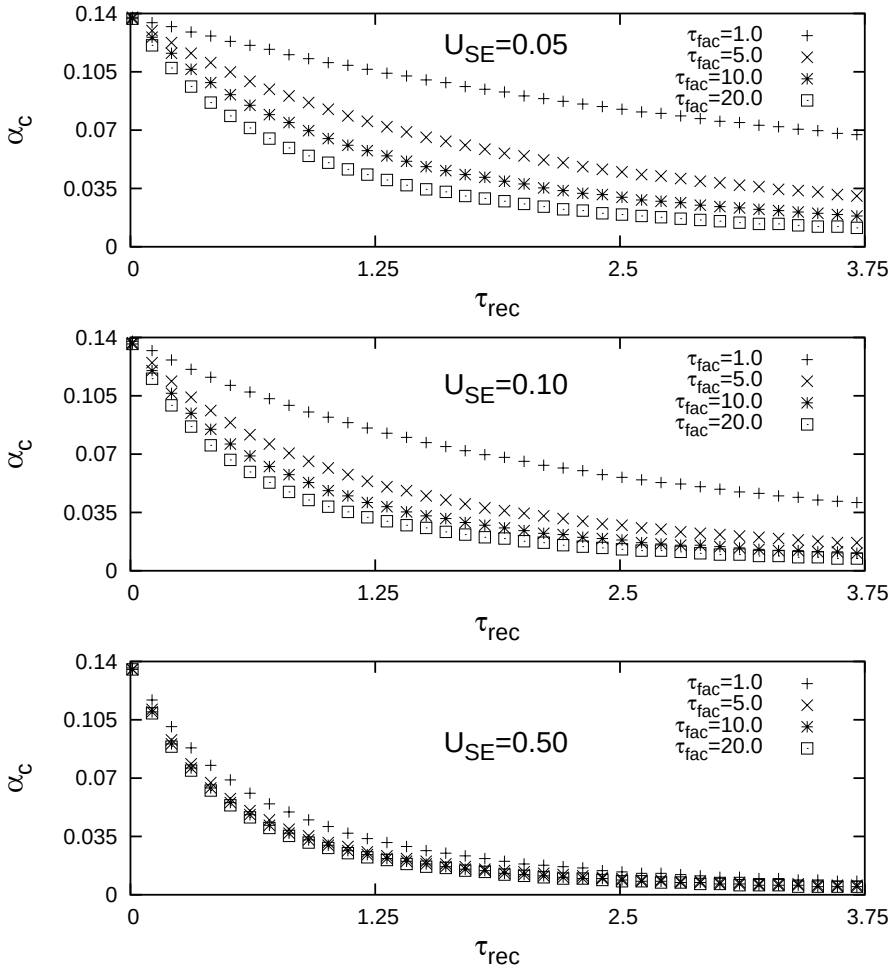

Figure 1.1: Capacidad crítica (α_c) del modelo calculada en aproximación de campo medio para diferentes valores de τ_{rec}, τ_{fac} y U_{SE}. La facilitación aumenta considerablemente la drepresión de las sinapsis. Consequentemente, la capacidad crítica en presencia de facilitación disminuye mucho comparado con el caso de considerar sólo depresión[Torres et al., 2002]. Esto se oberva sólo para valores de U_{SE} muy pequeños.

cionarios. Como una novedad, después de incluir sinapsis dinámicas aparece una fase oscilante que tiene especial importancia y donde el sistema está continuamente saltando entre los diferentes patrones almacenados. A este comportamiento le llamaremos *switching.* Para estudiar esta fase, al igual que en el trabajo [Pantic et al., 2002], introducimos dos puntos críticos o de bifurcación, τ^{*}_{rec} y τ^{**}_{rec}. Para $\tau_{rec} < \tau^{*}_{rec}$, el sistema tiene tres puntos fijos, de los cuales dos son estables (solución con memoria o ferromagnética) y otro inestable (solución sin memoria o paramagnética). Para $\tau^{*}_{rec} < \tau_{rec} < \tau^{**}_{rec}$ el sistema presenta oscilaciones que son estables (solución tipo atractor ciclo límite). Finalmente, para $\tau_{rec} > \tau^{**}_{rec}$ la solución paramagnética (punto fijo) se hace estable. Por lo tanto, además de soluciones punto fijo (ferro y para), el sistema presenta un atractor ciclo límite, el cual permite que la red describa un comportamiento oscilatorio periódico. Si comparamos esta situación con el caso de sinapsis estáticas (también para $\alpha = 0$), dónde sólo existen las fases ferromagnética y paramagnética, vemos cómo en esta nueva fase ciclo límite el sistema es capaz de saltar entre los diferentes patrones almacenados, y además lo hace sin necesidad de estimulación externa. Otro hecho muy importante que el incorporar facilitación produce es un rescalamiento no trivial y complejo de los puntos de bifurcación τ^{*}_{rec} y τ^{**}_{rec}, comparado con la situación de considerar sólo mecanismos depresores. El valor crítico τ^{*}_{rec} decrece a medida que τ_{fac} crece. Esto consigue que la fase oscilante se anticipe mucho (con respecto a sólo depresión) y además produce una disminución drástica de la anchura de la fase ferromagnética. La anchura de la fase oscilante también dismunuye a medida que se la facilitación se hace más intensa. Sin embargo, la frecuencia de las ocilaciones es más alta, y consequentemente puede mejorar la habilidad de la red a responder a estímulos que son altamente cambiantes y recibidos del entorno.

Un nivel intermedio de interacción de las sinapsis asume la presencia de un ruido dependiente de la actividad presináptica afecta a las sinapsis. Este hecho puede modelar plasticidad de corto alcance o *memoria de trabajo* [Abbott and Regehr, 2004] y también *errores* en transmisiones en sinapsis reales [Zador, 1998]. El caso de *updating secuencial* ha sido estudiado en el capítulo 4. Hay

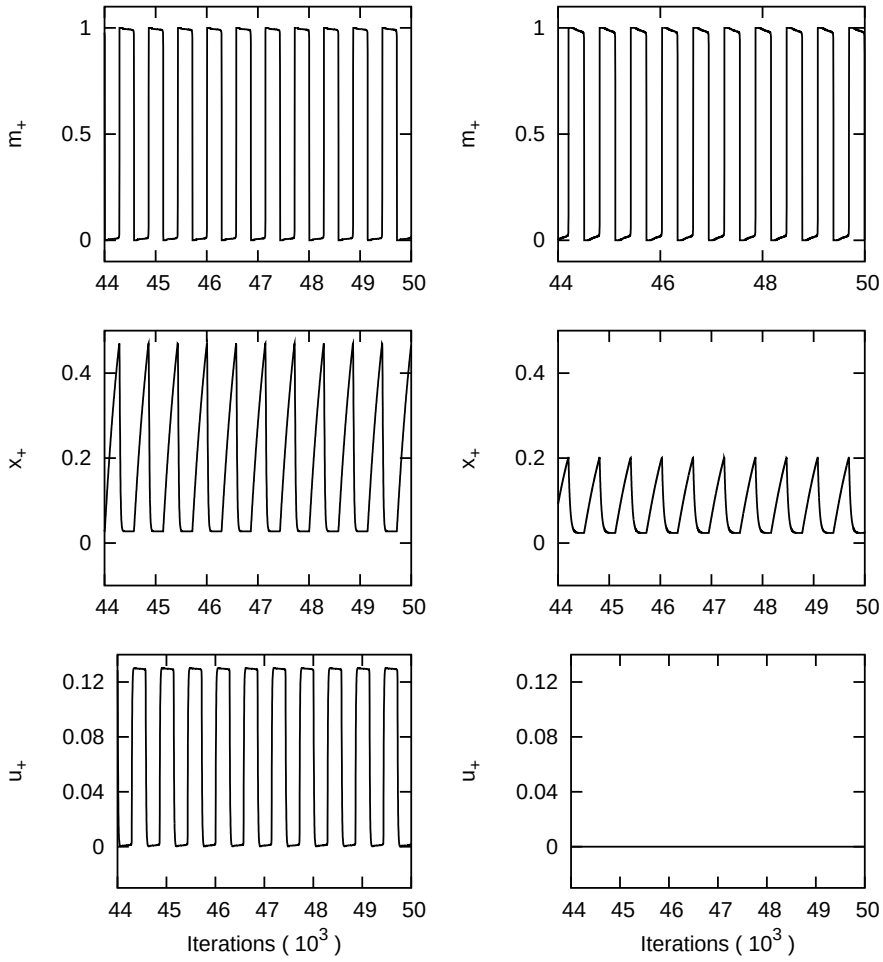

Figure 1.2: El efecto de considerar facilitación y depresión (panel de la izquierda) es comparado con el caso de considerar sólo depresión (panel de la derecha) para $U_{SE} = 0.03$ y $\beta = 100$. Arriba, variando el parámetro τ_{rec} se observa cómo las oscilaciones para m_+ parecen ser similares en ambos casos. Sin embargo, en los gráficos del medio, se observa cómo la facilitación consigue intensificar la depresión, ya que la amplitud de la oscilación para x_+ crece en presencia de facilitación. Finalmente, en los gráficos de más abajo, se ilustra cómo en presencia de sólo depresión la variable dinámica u_+ es constante en el tiempo e igual a 0.

muchas recientes evidencias que nos dicen que las sinapsis juegan un papel fundamental para determinar el complejo procesamiento de información que ocurre en el cerebro. Es posible entender algunas observaciones recientes si se asume que la respuesta post-sináptica puede o decrecer (dando lugar al mecanismo de depresión) o crecer (facilitación) dependiendo la actividad neuronal presináptica [Thomson et al., 2002, Tsodyks et al., 1998]. Es razonalbe esperar, que estos efectos que ocurren en una escala temporal muy pequeña, sean la base de una eficiente cooperación entre neuronas. En este modelo, los valores asignados a las intensidades sinápticas y que vienen dados por una regla de aprendizaje (por ejemplo, la regla de Hebb) son constantemente perturbados por la presencia de un ruido microscópico y rápido. Se introduce un parámetro que controla la intensidad de dicho ruido y que además permite transiciones continuas entre sinapsis depresoras y estáticas. El modelo es una red neuronal en que la dinámica estocástica local es constantemente influenciada por ruido sináptico. La dinámica es formulada usando una ecuación maestra. En el caso de considerar fluctuaciones de ruido muy rápidas, las neuronas evolucionan en el tiempo en presencia de una distribución estacionaria para dicho ruido. Esta dinámica es caracterizada por una probabilidad de transición por unidad de tiempo que es efectiva y que puede ser interpretada como una competición entre varios mecanismos elementales. Cada uno de ellos, tiende a conducir al sistema hacia un estado de equilibrio. En general, la competición de entre todos, impide al sistema el alcanzar el equilibrio termodinámico, y lo que alcanza es un estado de estacionario de no-equilibrio [Marro and Dickman, 1999]. Estos estados, son mucho más generales y frecuentes que aquellos asociados a la condición de equilibrio.

En este capítulo se estudian dos escenarios diferentes; el primero asume distribuciones estacionarias de probabilidad que son dependientes en actividad neuronal local y el segundo asumen una dependencia global. Bajo ciertas condiciones y en el primero de los casos, el sistema es descrito por medio de un Hamiltoniano Efectivo. Consecuentemente, este sistema se reduce al modelo de Hopfield con pesos y umbral rescalados. El modelo de Hopfield, es en

términos de ruido rápido, una red neuronal en ausencia de dicho ruido. Un caso mucho más interesante es el segundo de ellos que asume que el ruido depende de la corriente presináptica total que llega a la corriente postsináptica. Este caso se analiza por medio de simulaciones Monte Carlo y por una teoría de campo medio. Ambos estudios estás en total acuerdo. Nuestro modelo queda caracteriado por dos parámetros, la temperatura, T, que controla la estocasticidad de las neuronas y Φ que controla la intensidad del ruido rápido. Un resultado importante es que la presencia de ruido rápido induce la aparición de un punto tricirítico para ciertos valores de dichos parámetros $(T_c, \Phi_c) = (1, -4/3)$. En el límite de $\alpha \to 0$, dicho punto tricrítico separa transiciones de primer de las de segundo orden entre las fases de recuerdo (ferromagnética) de las de no recuerdo (paramagnética) (ver la figura 1.3).

Otra consecuencia estudiada en este modelo, es que la presencia de ruido rápido mejora muy considerablemente la sensibilidad de la red frente a estimulación externa. Se explica cómo el ruido provoca la inestabilidad del atractor, conduciendo al sistema a otro. En particular, se observa tanto para un sólo patrón (saltando al antipatrón) y para varios patrones (saltando entre todos ellos). Esta propiedad es interesante pues mejora la habilidad de la red a cambiar frente a estímulus que pueden ser muy cambiantes; por otro lado, se observa como esta dependencia es independiente a la condición inicial de la red. Nosotros sugerimos que en la naturaleza, procesos que se dan en reconocimiento de patrones tales como clasificación y categorización pueden seguir una estrategia similar. Así, cada atractor podría corresponder a diferentes objetos y una dinámica convenientemente perturbada por ruido rápido puede incluir una visita continuada entre patrones que pertenecen a una misma clase, la cual es caracterizada por cierto grado de correlación entre sus elementos. En realidad, un mecanismo similiar parece ser la base de los comienzos de procesos olfativos en insectos [Laurent et al., 2001], y además, una misma clase de inestabilidades han sido descritas en la actividad neuronal del cortex de un tipo de mono [Abeles et al., 1995].

En el capítulo 5, estudiamos las consecuencias del ruido rápido formu-

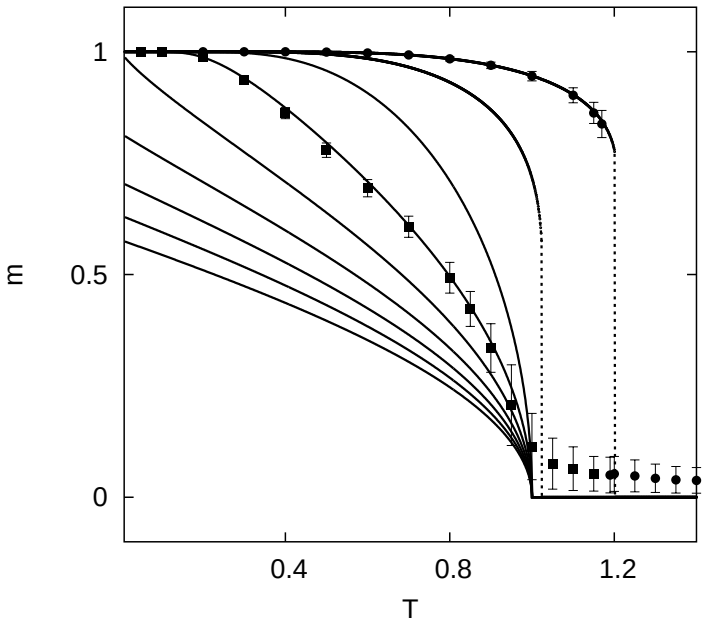

Figure 1.3: Resultados de campo medio para el overlap estacionario en función de la temperatura, $m^*(T)$, para diferentes valores en la intensidad del ruido rápido. A saber, $\Phi = -2.0, -1.5, -1.0, -0.5, 0.0, 0.5, 1.0, 1.5, 2.0$, respectivamente, de arriba a abajo. El caso de $\Phi = -1$ se corresponde con el modelo de Hopfield. El gráfico muestra transiciones de segundo orden (líneas continuas) entre las fases de recuerdo ($m \neq 0$) y las de no recuerdo ($m = 0$) y también de primer orden (líneas discontinuas). Los símobolos son para simulaciones Monte Carlo para una red neuronal de $N = 1600$ neuronas y para $\Phi = -0.5$ (cuadrados) y $\Phi = -2.0$ (círculos).

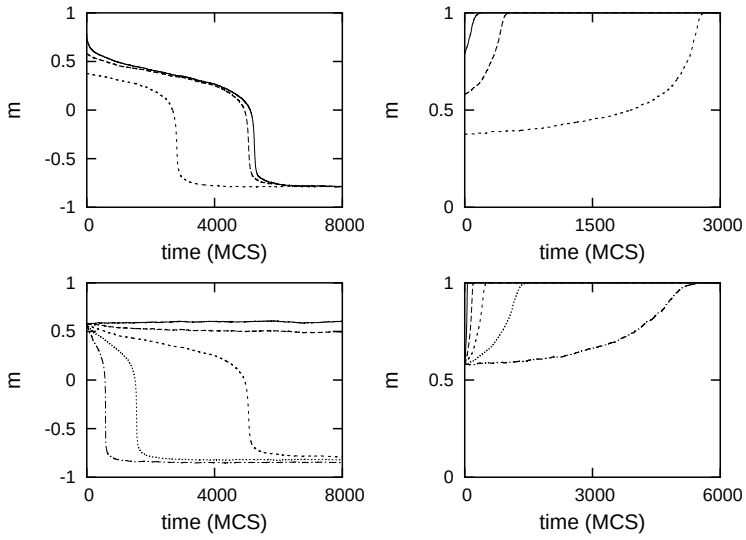

Figure 1.4: Simulaciones Monte Carlo del sistema muestran la evolución temporal del overlap entre la actividad neuronal y el único patrón almacenado. El tamaño de la red es $N = 3600$ y la temperatura es tomada igual a $T = 0.1$. Estudiamos el efecto del ruido rápido ante estimulación externa (cuantificada por δ) por comparar dos casos $\Phi = 1$ (a la izquierda) y $\Phi = -1$ (a la derecha), ya que este último caso equivale al modelo de Hopfield, que es una red neuronal atractor en ausencia de ruido rápido. Cada gráfico, definido por un par de valores (δ, Φ), muestra diferentes curvas para diferentes evoluciones cada uno correspondiendo a una condición inicial. Los gráficos de arriba son para $\delta = 0.3$ y $\Phi = 1$ (a la izquierda) y $\Phi = -1$ (a la derecha). Para el caso de ruido rápido (izquierda), nótese la gran sensibilidad de la red ante la estimulación externa. Abajo, hacemos el mismo tipo de experimentos pero fijando la condición inicial vamos variando la intensidad de la estimulación externa (para valores de arriba a abajo de $\delta = 0.1, 0.2, 0.3, 0.4$, y 0.5).

lado en el capítulo anterior en redes que son cambiadas simultáneamente para un gran número de neuronas. Situamos en cada nodo de una red una neurona binaria y asumimos que sus configuraciones vienen representadas por $\mathbf{S} \equiv \{s_i = \pm 1\}_{i=1}^{N}$, y que las intensidades sinápticas son dadas por w_{ij}. Dichas intensidades vienen definidas por $w_{ij} = \overline{w}_{ij} x_j$, donde x_j es una variables estocástica y $\overline{w}_{ij}$ son intensidades fijas o pesos y son determinados en un proceso previo de aprendizaje. Después de definir los campos locales como $h_i = \sum_{j \neq i} w_{ij} x_j s_j$, la dinámica en ausencia de temperatura es determinista y asegura que $\mathrm{sig}(h_i) = s_i$. Nosotros introducimos un parámetro temperatura, $T \equiv \beta^{-1}$, que nos permite introducir errores, y hace que la dinámica sea estocástica. Es interesante destacar que debido a que las intensidades $w_{ij} = \overline{w}_{ij} x_j$ son asimétricas, el comportamiento del sistema no puede ser descrito por una descripción Hamiltoniana o de equilibrio. En el límite de ruido presináptico muy rápido, es posible describir la dinámica del sistema en términos de *campos locales efectivos*. El principal resultado, comparado con el capítulo 4 es que ahora el sistema sí es capaz de mostrar comportamiento oscilante entre todos los patrones y sin necesidad de estimulación externa. Éste es el efecto de considerar dinámicas donde simultáneamente se mueve a un gran número de neuronas (nosotros llamaremos a estos sistemas autómatas neuronales) frente a aquellos sistemas donde la dinámica es secuencial (los llamemos red neuronal). Para detalles y definiciones de estos tipos de dinámicas Monte Carlo veáse por ejemplo [Marro and Dickman, 1999, Peretto, 1992].

Nosotros discutimos dos tipos de autómatas neuronales estocásticos, caracterizados por considerar diferentes números de sitios cambiados $N^*(t)$ en la dinámica Monte Carlo. La primera familia, asume $N^*(t) = N$ y es equivalente a la dinámca paralela [Peretto, 1992]. La segunda, toma N^* variable en el tiempo y satisfaciendo que $N^*(t) < N$. Para el primer caso, presentamos teoría de campo medio y simulaciones Monte Carlo en total acuerdo. Para el segundo, sólo simulaciones Monte Carlo. Ambas situaciones ilustran un comportamiento emergente que es complejo, así aparecen puntos fijos, P-ciclos y *switching* que puede llegar incluso a ser caótico.

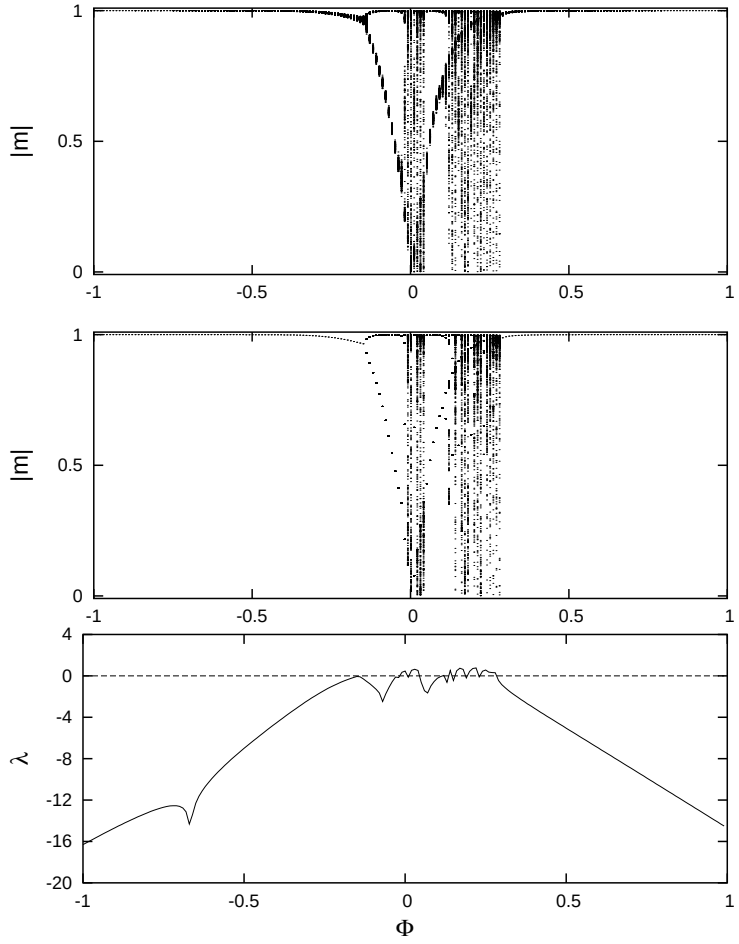

Figure 1.5: Diagrama de bifurcación para el overlap estacionario en función de la intensidad de ruido rápido Φ. Sólo hay un solo patrón almacenado en la regla de aprendizaje. El gráfico de más arriba presenta dicho overlap directamente medido de simulaciones Monte Carlo para una red de $N = 10000$ neuronas. El gráfico del medio, se corresponde con las soluciones para el overlap estacinario obtenidas después de realizar una teoría de campo medio. Ambos teoría y simulación están en perfecto acuerdo. El gráfico de más abajo muestra el exponente de Lyapunov, λ, en función del nivel de intensidad de ruido rápido (obtenido también bajo la aproximación de campo medio). Valores positivos de λ, indican que el sistema se hace caótico.

La dinámica caótica es aperiódica, y esto puede ser de gran utilidad para almacenar y recuperar diferentes y nuevos patrones espacio temporales [Freeman, 1994]. Como ejemplo de sistemas en la naturaleza utilizando la dinámica caótica para este fin veáse por ejemplo [Freeman, 1987] dónde se estudia cómo en el bulbo olfactivo de los insectos se puede diferenciar olores. Por otro lado, es importante destacar que esta nos es la primera vez que modelos de memoria asociativa aparece caos. Así por ejemplo en [Bolle and Vink, 1996, Dominguez, 1996] se estudia cómo la forma de las funciones transferencia (relación entrada/salida para cada neurona) puede ser modelada por parámetros de control. La principal consecuencia es que cuando estas funciones transferencia se hacen no monótonas aparece caos. Esto es también observado en nuestros autómatas neuronales. El punto fuerte de nuestro modelo, es que después de incluir un ruido rápido que es observado en experimentos y motivado por el fenómeno de depresión, nuestras funciones transferencias se hacen no monótonas, y consecuentemente conducen a un comportamiento caótico para el sistema. Para poder cuantificativamente estas oscilaciones , usamos una medida de entropía S utilizando el algoritmo FFT (*Fast Fourier Transform*). Su significado radica en que si S disminuye cuantifica una regularización de la serie temporal. Por el contrario, si S crece indica mayor coplejidad o caoticidad en la serie temporal. Proponemos que un autómata neuronal convenientemene perturbado por ruido rápido puede resolver muchos problemas en la naturaleza. Así hay ejemplos donde el caos puede mejorar y ser eficiente para resolver problemas [Lu et al., 2003, Schweighofer et al., 2004, Stam et al., 1994]. En cambio, en otros sistemas es interesante controlar el caos y regularizar la actividad neuronal [Schiff et al., 1994]. Esto es precisamente el comportamiento de nuestro autómata neuronal, dependiendo de la intensidad del ruido rápido presináptico el sistema puede manifestar o bien un comportamiento altamente caótico o bien un comportamiento casi-regular y donde la caoticidad es pequeña.

Finalmente, el nivel más bajo de complejidad asumido en las interacciones sinápticas ha sido estudiado en el capítulo 6 y las principales consecuencias computacionales de esta dinámica han sido explorados en el capítulo 7. En

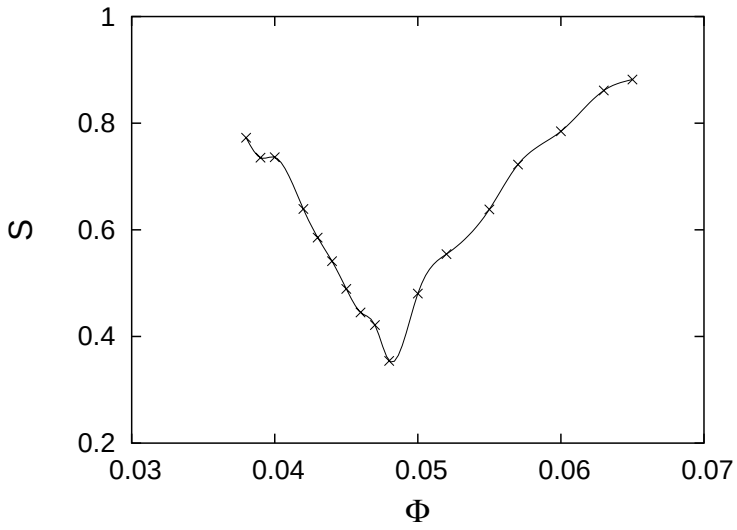

Figure 1.6: Función entropía directamente medida de series temporales de la evolución temporal del overlap entre la actividad neuronal y el único patrón almacenado en la regla de aprendizaje para diferentes valores de intensidad de ruido rápido. Un decremento en la entropía es una medida de regularización de la serie, mientras que un aumento siginifica que la complejidad o caoticidad de la serie aumenta.

el capítulo 6, se formula otro autómata neuronal estocástico, el cual tiene en cuenta dos dinámicas independientes que compiten, una para la actividad de las neuronas y la otra para las intensidades sinápticas y donde ambas son conducidas respectivamente por diferentes temeperaturas T_0 y T_1. Consideramos N neuronas binarias con estados dados por $s_i = \pm 1$, cada dos unidas mediante sinapsis con intensidades dadas por w_{ij}, con $i, j = 1, \ldots, N$. El interés está en las configuraciones $\mathbf{S} \equiv \{s_i\}$ y $\mathbf{W} \equiv \{w_{ij}\}$. Para tener una referencia bien establecida, las interacciones son determinadas por medio de una función energía igual que para el modelo de Hopfield. Además, consistente con que la memoria es un fenómeno dinámico global, consideramos que en cada iteración temporal para las neuronas las sinapsis quedan definidas en un solo patrón de entre todos los almacenados en la regla de aprendiazaje. Se presentan simulaciones Monte Carlo de este modelo las cuales revelan un escenario muy intrigante. Dependiendo de los valores T_0 y T_1 diferentes régimenes ocurren. Para estudiarlos, se introduce el overlap (**m**) y el número total de saltos (j). Aparecen 3 diferentes fases: (1) la ferromagnética, satisface que $\mathbf{m} \neq 0$ y $j = 0$. El sistema aquí tiene memoria asociativa que llamaremos estática, lo que significa que una vez en el proceso de recuperación de información el sistema recupera un patrón, nunca escapará de él. (2) La paramagnética, donde no existe ningún tipo de memoria asociativa. Aquí, se da que $\mathbf{m} = 0$ y $j = 0$ y por último, (3) la oscilatoria, en la que existe swiching entre patrones y donde for $\mathbf{m} = 0$, $j \neq 0$. Aquí existe memoria asociativa, pero ahora es un proceso dinámico en el sentido que una vez se ha alcanzadado un atractor, correspondiente a uno de los patrones almacenados, el sistema es capaz de saltar a otro diferente. Debido a que la probabilidad de cambiar entre patrones depende de los overlaps, este mecanismo es un proceso complejo. Para estudiar los detalles de esta fase oscilante, calculamos el tiempo $\tau_{\nu\gamma}$ en el que el sistema está en el patrón νth antes de saltar al γth. Esto permite diferenciar dos tipos de comportamiento oscilatorio. El primero satisface que $\tau_{\nu\gamma} \simeq \tau$, independientemente de ν y γ. Así el sistema permanece igual tiempo en todos los diferentes patrones. La dinámica de saltos es un proceso descorrelacionado en el tiempo.

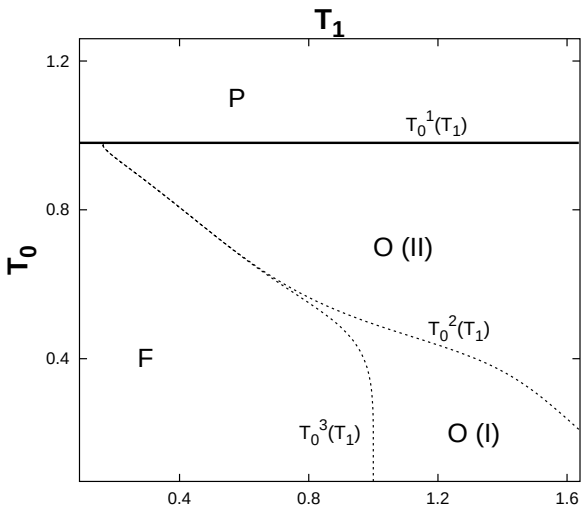

Figure 1.7: Diagrama de fases para el autómata neuronal estocástico conducido por diferentes temperaturas. Las diferentes fases son explicadas en el texto. Las líneas continuas representan transiciones de fase de segundo orden y las discontinuas de primer orden. Aquí, nosotros tomamos $N = 16384$ y $P = 3$ patrones que son correlacionados y cuyo overlap entre cada dos es del 20%.

En cambio, cuando T_0 es baja, aparecen correlaciones temporales no triviales en la dinámica de saltos entre patrones. A saber, $\tau_{\nu\gamma}$ depende de ambos ν and γ. Este comportamiento tan peculiar sugiere utilizar este algoritmo para codificar información espacio temporal.

Para explicar la fenomenología observada en simulaciones Monte Carlo, desarrollamos un procedimiento de *coarse-graining*. Directamente desde la ecuación maestra para probabilidades dadas en representación de **S** es posible obtener cómo cualquier observable evoluciona en el tiempo[1]. De forma alternativa, se puede calcular la probabilidad en representación de los overlaps **m**. Esto reduce el número de grados de libertad, de $2^N + 1$ para la representación $(\mathbf{S}, \mu)$ a $P + 1$ para $(\mathbf{m}, \mu)$. Después de realizar un procedimiento de coarse-graining la evolución temporal del sistema es conducida por una probabilidad de saltar efectiva, la cual permite tener dos mecanismos independientes de evolución. El primero, dado un patrón definiendo una configuración de intensidad de sinapsis, nos dice cómo el sistema cambia de configuración de la actividad neuronal a través de sus overlaps. El segundo, es responsable de los cambios entre diferentes patrones dada una cierta configuración de overlaps. Un resultado importante, es que después de aplicar el procedimiento de coarse-graining, no es necesario autopromediar en patrones, como es típico en modelos de memoria asociativa Hertz et al. [1991], Peretto [1992].

En el capítulo 7, se presenta un estudio computacional del autómata neuronal estocástico formulado en el capítulo 6. En realidad, este capítulo puede entenderse como una extensión de aquel. La motivación de estas simulaciones se basan en multitud de aplicaciones técnicas que requieren la categorización, esto es, la asignación de objetos a cero o más clases predefinidas anteriormente. Estos modelos requiriendo categorización, utilizan un almacenaje de información que es muy alto y que después debe ser consultado. En los últimos años, la aplicación más demandada es categorización de texto en buscadores de internet, ya que existe un gran número de documentos en formato digital

[1] Para ejemplos en diferentes sistemas de cómo hacerlo véase [Marro and Dickman, 1999].

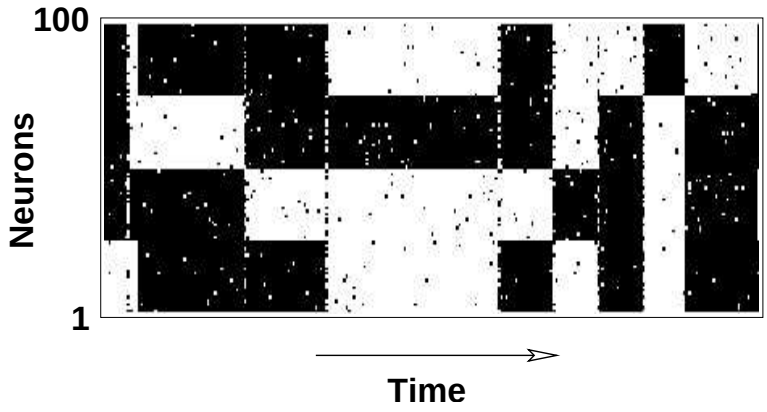

Figure 1.8: Actvidad neuronal frente al tiempo para $N = 100$ neuronas y $P = 4$ patrones. Here, $T_0 = 0.9T_0^c$ and $T_1 = 1.69T_1^c$, donde T_0^c y T_1^c son las correspondientes temperaturas críticas.

y consecuentemente, existe una gran necesidad para organizarlos de tal forma que adquieran un uso más fácil. Algunos ejemplos incluyen la clasificación de documentos webs, o buscadores de artículos o investigadores en bases de datos de ciencia [Berners-Lee et al., 1994]. El más ambicioso objetivo es conseguir desarrollar software capaz de aprender categorías a partir de un conjunto no clasificado de documentos [Aphinyanaphongs et al., 2004, Doolittle, 2004]. En biotecnología, no existe todavía un sistema preciso y automatizado para la clasificación de proteínas, debido a la extrema diversidad entre sus miembros [Cheng et al., 2005]. También existen dispositivos con interés en la industria que necesitan de algoritmos capaces de solventar con éxito el problema de la categorización. Así por ejemplo, las narices electrónicas, que son sensores químicos con un sistema de reconocimiento de patrones (normalmente una red neuronal aritificial) y que estás siendo utilizadas para deteción automática y clasificación de olores, vapores y gases, y que pueden jugar un papel importante en defensa en las llamadas *guerras químicas*. Pero también existen aplicaciones civiles que usan las narices electrónicas, como por ejemplo la industria de la alimentación. Aquí se usan como herramientas de control de calidad de alimentos [Vazquez et al., 2004]. Además, hay muchos otros escenarios en bi-

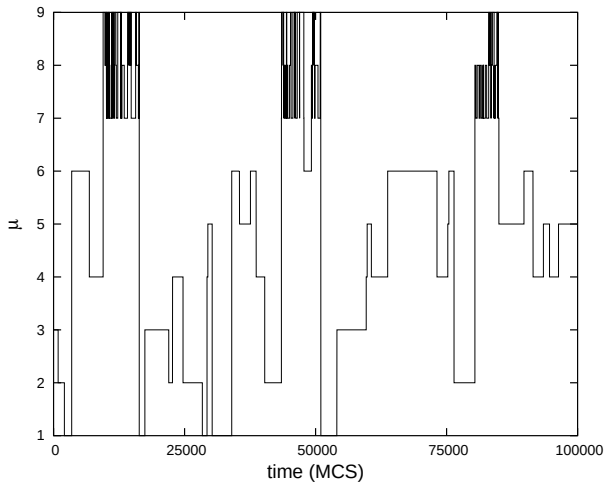

Figure 1.9: Evolución temporal del autómata neuronal estocástico. En el eje de las ordenadas aparece el índice que indica en que patrón de entre todos los que definen la regla de aprendizaje se encuentra el sistema. En el de las abscisas el tiempo (en unidades de pasos Monte Carlo). Como puede observarse, el autómata neuronal es capaz de identificar los patrones 7, 8 y 9 y clasificarlos por constituir la misma familia.

ología que demandan algoritmos óptimos para categorización, por ejemplo el procesamiento temprano de olores en el bulbo olfativo de los insectos [Laurent et al., 2001]. En vez de métodos de aprendizaje artificial, como por ejemplo árboles de decisión y clasificadores bayesianos, nosotros presentamos una alternativa basada en un autómata neuronal estocástico. Computacionalmente exploramos la compleja estructura dinámica espacio temporal. Para diferentes familias de patrones, mostramos cómo la trajectoria seguida por el autómata puede ser una herramienta para resolver categoriazación. Dependiendo de las correlaciones entre los patrones definiendo la regla de aprendizaje, el autómata neuronal es capaz de describir trayectorias que establecen una cierta jerarquía en la corrrelación entre sus elementos.

Resumiendo, en esta tesis se ha estudiado propiedades estacionarias y dinámicas de redes neuronales recurrentes fuera del equilibrio termodinámico. Estas

Figure 1.10: Diferentes familias asociados a diferentes individuos. Cada familia está formada por distintas posturas del mismo individuo. En la tesis, se presentan distintas simulaciones Monte Carlo que prueban cómo el autómata neuronal puede utilizarse para identificar y clasificar familias tales como la ilustrada aquí. Estas fotos han sido tomadas de The Laboratory for Communications Engineering within the Cambridge University Department of Engineering.

propiedades dependen fuertemente de la complejidad asumida para explicar las interacciones entre neuronas dadas por una matriz de intensidades sinápticas. Se ha estudiado tres diferentes niveles de descripción. El caso más realista ha sido estudiado en el capítulo 3 y corresponde a considerar el sinapsis dinámicas dadas por el modelo fenomenológico de [Tsodyks et al., 1998]. Aquí aparecen mecanismos tanto depresores como facilitadores los cuales influyen en el comportamiento de la red neuronal atractor. Es la primera vez que se incorporan mecanismos facilitadores en redes de memoria asociativa. Nosotros resolvemos este caso, y presentamos un modelo general capaz de recuperar resultados obtenidos previamente para el caso de sólo de considerar mecanismos depresores [Pantic et al., 2002]. Nuestros resultados refuerzan la idea de que facilitación incrementa la intensidad de la depresión y consecuentemente, mejora la capacidad de saltar entre patrones en la dinámica de resuperación de información. El caso de complejidad intermedio en las interacciones sinápticas ha sido estudiado en los capítulos 4 y 5. En el capítulo 4 se estudia mediante simulaciones Monte Carlo y teoría de campo medio el efecto de ruido presináptico

rápido afectando la transmisión de información a través de las intensidades sinápticas. Este hecho está inspirado en recientes observaciones en neurobiología, las cuales muestran cómo la intensidad en las sinapsis puede aumentar o disminuir, en una escala temporal muy pequeña y dependiendo de la actividad neuronal presináptica. De esta forma modelamos plasticidad de corto alcance o memoria de trabajo [Abbott and Regehr, 2004] y errores en las transmisiones sinápticas [Zador, 1998] y describimos un mecanismo por el cual el ruido presináptico rápido mejora la sensibilidad de la red ante estimulación externa. La razón por la que esto ocurre, es que el ruido presináptico rápido induce un comportamiento de no equilibrio y consequentemente, el espacio de puntos fijos es modificado de tal forma que el sistema puede escapar de un atractor a el resto. Así, además de identificación en el reconocimiento de patrones, el sistema muestra clasificación y categorización, lo que puede ser relevante para la comprensión de algunos de los procesos más complejos en el cerebro. En el capítulo 5, presentamos una familia de autómatas neuronales estocásticos que son afectados por el ruido rápido estudiado en el capítulo 4. Dependiendo del parámetro que controla la intensidad de dicho ruido, el sistema presenta diferentes tipos de comportamiento, que van desde totalmente periódico a caótico. En el capítulo 6 presentamos otro autómata neuronal estocástico en el que las fluctuaciones de la actividad neuronal y de las intensidades sinápticas son conducidas por diferentes parámetros temperatura. La competición entre las dos temperaturas impide el alcanzar el equilibrio termodinámico [Marro and Dickman, 1999]. La dinámica compleja y no lineal es resuelta usando un procedimiento de coarse-graining. La red muestra varias fases, incluyendo switching entre los diferentes atractores, el cual puede ser descorrelacionado o correlacionado en el tiempo. En el capítulo 7, presentamos un estudio computacional de estas correlaciones temporales observadas en la fase oscilante. Se analiza el sistema en dicha fase oscilante por combinar la dinámica mesoscópica obtenida en el capítulo 6 y simulaciones Monte Carlo. Este comportamiento oscilante o switching ha sido estudiado en diferentes partes de la tesis. En particular, en los capítulos 3,5 y 6. La principal

conclusión es que es ventajoso porque mejora la habilidad de la red para detectar estímulos cambiantes recibidos del entorno. Algunas veces este switching es producido de forma autónoma y sin necesidad de estimulación externa. La dinámica en esta fase es compleja, y presenta bien puntos fijos, P-ciclos e incluso comportamiento caótico. Computacionalmente es muy ventajoso el poder codificar y decodificar ciertos inputs, estímulos o patrones en la dimension temporal, que junto con la información espacial que es susceptible de ser almacenada y recuperada en modelos de memoria asociativa, permite el poder identificar y clasificar patrones espacio temporales que pueden ser importantes por ejemplo en procesos olfativos [Laurent et al., 2001]. Diferentes olores pueden ser codificados en diferentes atractores y el sistema neuronal es capaz de extraer y segmentar las distintas componentes de estos patrones espacio temporales de la actividad neuronal. Notar que categorización asume que previamente ha habido un proceso de identificación de los diferentes patrones, para luego ser consituidos a formar una misma familia.

Bibliography

L. F. Abbott and W. G. Regehr. Synaptic computation. *Nature*, 431:796–803, 2004. 1, 5, 21

M. Abeles, H. Bergman, I. Gat, I. Meilijson, E. Seidemann, N. Tishby, and E. Vaadia. Cortical activity flips among quasi-stationary states. *Proc. Natl. Acad. Sci. USA*, 92:8616–8620, 1995. 8

D. J. Amit, H. Gutfreund, and H. Sompolinsky. Statistical mechanics of neural networks near saturation. *Ann. Phys.*, 173:30–67, 1987. 3

Y. Aphinyanaphongs, I. Tsamardinos, A. Statnikov, D. Hardin, and C. F. Aliferis. Text categorization models for high quality article retrieval in internal medicine. *J. Am. Med. Inform. Assoc.*, Nov 23, 2004. 18

T. Berners-Lee, R. Cailliau, A. Luotonen, H. F. Nielsen, and A. Secret. The world-wide web. *Communications of the ACM*, 37:76–82, 1994. 18

R. Bertram, A. Sherman, and E. F. Stanley. Single-domain/bound calcium hypothesis of transmitter release and facilitation. *J. Neurophysiol.*, 75:1919–1931, 1996. 2

D. Bolle and B. Vink. On the dynamics of analogue neurons with nonsigmoidal gain functions. *Physica A*, 223:293–308, 1996. 13

B. Y. Cheng, J. G. Carbonell, and J. Klein-Seetharaman. Protein classification based on text document classification techniques. *Proteins*, Jan 11, 2005. 18

D. R. C. Dominguez. Inference and chaos by a network of nonmonotonic neurons. *Phys. Rev. E*, 54:4066–4070, 1996. 13

N. D. Doolittle. State of the science in brain tumor classification. *Semin. Oncol. Nurs.*, 20:224–230, 2004. 18

W. J. Freeman. Simulation of chaotic eeg patterns with a dynamic model of the olfactory system. *Biol. Cybern.*, 56:139–150, 1987. 13

W. J. Freeman. Neural networks and chaos. *J. Theor. Biol.*, 171:13–18, 1994. 13

J. Hertz, A. Krogh, and R.G. Palmer. *Introduction to the theory of neural computation*. Addison-Wesley, 1991. 2, 3, 17

G. Laurent, M. Stopfer, R.W. Friedrich, M.I. Rabinovich, A. Volkovskii, and H.D.I. Abarbanel. Odor encoding as an active, dynamical process: Experiments, computation and theory. *Annual Review of Neuroscience*, 24:263–297, 2001. 8, 19, 22

Q. Lu, G. Shen, and R. Yu. A chaotic approach to maintain the population diversity of genetic algorithm in network training. *Comput. Biol. Chem.*, 27: 363–371, 2003. 13

J. Marro and R. Dickman. *Nonequilibrium Phase Transitions in Lattice Models*. Cambridge University Press, 1999. 2, 7, 11, 17, 21

L. Pantic, J.J. Torres, H.J. Kappen, and S.C.A.M. Gielen. Associative memmory with dynamic synapses. *Neural Comp.*, 14:2903–2923, 2002. 2, 5, 20

P. Peretto. *An Introduction to the modeling of neural networks*. Cambridge University Press, 1992. 2, 11, 17

S. J. Schiff, K. Jerger, D. H. Duong, T. Chang, M. L. Spano, and W. L. Ditto. Controlling chaos in the brain. *Nature*, 370:615–620, 1994. 13

N. Schweighofer, K. Doya, H. Fukai, J. V. Chiron, T. Furukawa, and M. Kawato. Chaos may enhance information transmission in the inferior olive. *Proc. Natl. Acad. Sci. USA*, 101:4655–4660, 2004. 13

K. J. Stam, D. L. Tavy, B. Jelles, H. A. Achtereekte, J. P. Slaets JP, and R. W. Keunen. Non-linear dynamical analysis of multichannel eeg: clinical applications in dementia and parkinson's disease. *Brain Topogr.*, 7:141–150, 1994. 13

A.M. Thomson, A.P. Bannister, A. Mercer, and O.T. Morris. Target and temporal pattern selection at neocortical synapses. *Philos. Trans. R. Soc. Lond. B Biol. Sci.*, 357:1781–1791, 2002. 7

J.J. Torres, L. Pantic, and H.J. Kappen. Storage capacity of attractor neural networks with depressing synapses. *Phys. Rev. E.*, 66:061910, 2002. xvii, 2, 3, 4

M. V. Tsodyks, K. Pawelzik, and H. Markram. Neural networks with dynamic synapses. *Neural Comp.*, 10:821–835, 1998. 1, 2, 7, 20

M. J. Vazquez, R. A. Lorenzo, and R. Cela. Chlorophenols identification in water using an electronic nose and anns (artificial neural networks) classification. *Water Sci. Technol.*, 49:99–105, 2004. 18

A. Zador. Impact of synaptic unreliability on the information transmitted by spiking neurons. *J. Neurophysiol.*, 79:1219–1229, 1998. 5, 21

Chapter 2

Motivation and Antecedents

2.1 Statistical Mechanics

Statistical mechanics deals with large systems of stochastically interacting microscopic elements (particles, neurons, ion-channels, magnets, polymers, genes, vehicles in traffic models, etc.). The strategy of statistical mechanics is to abandon any ambition to solve exact and simultaneously all the involved equations of motion at the microscopic level, and to use the individual microscopic laws to describe the behavior of a suitably chosen of *macroscopic* observables. To achieve it, it is necessary to capture the *essential physics* under study, such as, for instance, symmetries, scaling and conservation laws, etc. The toolbox of statistical mechanics consists of methods to perform this reduction from the microscopic to macroscopic level, which are all based on efficient ways to compute probabilities. In general, formal and mathematical solutions to this problem do not exist. The experiences tell us what to expect, and serve as a guide to find the macroscopic observables and to see the differences between relevant mathematical properties and irrelevant ones. As in any statistical theory, clean and transparent mathematical laws can be expected to emerge only for (preferable infinitely) large systems. In this limit, one often encounters *phase transitions*, i.e. drastic changes in the system's macroscopic behavior at specific

values of global control parameters. In this thesis, we apply statistical mechanics to neural networks. We consider that neurons evolve stochastically in time connected by synapses of intensity also evolving in time as a dynamical variable.

2.2 Non-Equilibrium vs. Equilibrium

Under the *detailed balance* condition [Marro and Dickman, 1999], the stochastic process of evolving neuron states and static synapses leads towards an equilibrium situation where the microscopic state probabilities are known, and where techniques of *equilibrium statistical mechanics* can be applied in different forms. Although some of these techniques can provide much detailed quantitative information on the behavior of neural networks, they have serious restrictions. The first one is that, by definition, they will only provide information on network properties in the stationary state. The second and more serious restriction, is that detailed balance translates to symmetric interactions or strength of synapses, which from a physiological point of view, is clearly unacceptable. For non-symmetric networks, where the asymptotic (stationary) statistics are not known, dynamical techniques from *non-equilibrium statistical mechanics* are the only tools available for analysis, even to analyze stationary properties. The *natural* set of macroscopic quantities (or *order parameters*) to be calculated can be defined in practice as the smallest set which obey closed deterministic equations in the limit of an infinitely large network.

In this thesis, we discuss particular non-equilibrium situations with *conflicting dynamics* applied to the field of attractor neural networks. These models have been studied in the last decade by different researchers in a large variety of systems, and a nice review is the chapter 8 of the book [Marro and Dickman, 1999]. These systems are characterized by a spin-flip dynamics which is a linear superposition of transition rates. Each individual rate is associated for instance to a different temperature and/or extern field (thresholds) and attempts to drive the system asymptotically to a thermodynamic equilibrium. The com-

petition between the different dynamics makes a kind of *dynamical frustration* to appear and the stationary state is, in principle, a non-equilibrium one. These non-equilibrium steady states present a much more varied and complex picture than equilibrium ones. In this context, a non-equilibrium system is built by superposing several equilibrium rates. Lonely under certain assumptions, and choosing particular functional forms for the transition rates, it is possible to construct an *effective-Hamiltonian* and therefore the non-equilibrium description is lacking. The stationary state is a Gibbsian one with an effective Hamiltonian with coupling constants depending on the microscopic-details of the dynamics.

2.3 Recurrent vs. Layered Neural Networks

We restrict our study to *recurrent neural networks*, i.e. neural networks with synaptic feedback loops. Statistical mechanics can solve this kind of networks assuming a large size of the system. They are characterized for having a high degree of connectivity (synaptic-links) among different neurons and therefore, collective phenomena measured by a few numbers of observables, as for instance, (long-term) memory, pattern recognition, identification and categorization, emerge from cooperation between the whole system. Here, the microscopic stochastic dynamical variables are the firing states of the neurons or their membrane potentials. One is mostly interested in quantities such as average state correlations and global information processing quality, which are measured by macroscopic observables. In contrast to layered networks, for models of recurrent neural networks one cannot simply write down the values of successive neuron states. They must be solved from (mostly stochastic) coupled dynamic equations.

2.4 Lattice Models in Binary States

Lattice models have played a central role in equilibrium statistical mechanics, particularly in understanding phase transitions and critical phenomena. Equally, detailed investigation of phase transitions in lattice models of non-equilibrium has blossomed over the last decade [Marro and Dickman, 1999]. The models studied are oversimplified representations of caricatures of nature. However, they may capture some of the essential features in real systems. The pillars of lattice models are: (1) make the system most amenable to precise analysis by using well-formulated techniques, (2) allow to isolate specific features of a system and connect them with macroscopic properties, and (3) are exactly well-defined in a computer. This last feature makes them very intriguing and stimulating. One observes how (infinitely) large systems with very simple and well-understood rules of interaction among their constituents, can be implemented on the computer and show a very complex and non-trivial collective behavior. Thus, in this thesis we shall consider several cases of recurrent neural networks on a lattice. In each node we represent a neuron with two-states, firing or being silent. Although, in principle, this can seem very unrealistic, different works in the literature, show how this low-degree of description on the neural activity can be enough in order to explain some macroscopic properties and/or cooperative behavior which have been observed in other more realistic levels of description, as for instance, integrate and fire models [Abbott and Kepler, 1990, Mueller and Herz, 1999, Tsodyks, 1999].

2.5 Associative Memory

Associative memory illustrates the simplest possible manner in which collective neural computation can work. This property may be said to initiate, mathematically well-formulated, with the Hopfield model [Amit et al., 1987, Hopfield, 1982]. The basic problem is to store a set of different stimuli or patterns in the network, in such way that when a new pattern is presented, the net-

work dynamics drives the system to one of the stored patterns most *similar* to the new one. The meaning of similar is to be close according to a previously defined distance. The main idea behind a Hopfield network is that, during a learning stage, a long-acting stimulus is used to modify specific sets of connections before getting the steady state associated to that stimulus. As a consequence, it is said that the system has stored a pattern or stimulus, which can be retrieved during a particular dynamics. This means, that a retrieved, and previously memorized pattern, is an attractor. Through training, each stimulus thus generates its own attractor. After learning, this trained, autonomous system becomes multistable; for recognition, future incoming stimuli will simply play the role of initial conditions. The number of different attractors determine the number of different stimuli or patterns that the system can store and retrieve. The most familiar types of recurrent neural network models are the attractor neural networks for associative memory, designed to store and retrieve information in the form of neural firing patterns and/or sequences of neural firing patterns. Attractor neural networks are high-dimensional and non-linear systems with extensive feedback. Generally, they are dominated by a wealth of steady solutions (fixed-point, limit-cycles, or even chaotic), and the practical use of such neural networks (in both biology and engineering) lies in the potential for creation and manipulation of these attractors through adaptation of the network parameters (synapses and thresholds).

2.6 Dynamic Synapses

Many different variants and applications of attractor neural networks, including asymmetric synapses, dilution and non-detailed balance, have been studied in the last decades [Amit, 1989, Geszti, 1990, Hertz et al., 1991]. Here, neurons are considered to be the computational and essential engines for coding and processing the information, and (static) synapses solely acting as connections and messengers among neurons. Very recently, it has been emphasized that a lonely neural dynamics is clearly incomplete and undefined [Ab-

bott and Regehr, 2004]. Neural dynamics wellcomes to the *Synaptic Computation*. Diverse types of synaptic plasticity and the range of timescales over which they operate suggest that synapses have the most active role in information processing. Therefore, it is necessary to have both neural and synaptic descriptions. Synaptic plasticity can be divided in three categories: (1) long-term plasticity, involving in changes of hours or longer, is thought to underpin learning and memory [Brown and Milner, 2003, Lynch, 2004, Morris, 2003], (2) homeostatic plasticity of both synapses and neurons allows neural circuits to mantain appropriate levels of excitability and connectivity despite changes brought about by protein turnover and experience-dependent plasticity [Turrigiano et al., 1998, Turrigiano and Nelson, 2004], and (3) short-term plasticity, occurs over milliseconds to minutes and allows synapses to perform critical computational functions in neural circuits [Abbott and Regehr, 2004].

The dynamic synapses are activity-dependent processes. The postsynaptic potential or response can either decrease (depression) or increase (facilitation) due to rapid repeated presynaptic activation [Tsodyks et al., 1998]. Directly extracted from [Tsodyks et al., 1998], in figure 2.1 is shown the effect of both facilitating and depressing mechanisms. These effects are fundamental for the development and adaptation of the nervous system, and are believed to be the basis of such higher functions as learning and memory. The effect of only (short-term) depressing synapses in attractor neural networks was studied in previous works [Bibitchkov et al., 2002, Pantic et al., 2002]. In chapter 3 we incorporate facilitating mechanisms in associative memory models. Facilitation gets a stronger depression which influences on the stability of patterns changing it considerably. This is shown to be advantageous for processing of patterns sequences and for switching between the stored patterns, which enhances the network response to changing stimuli.

There are several applications of neural networks (both feedback recurrent and feedforward layered) with dynamic synapses in industrial and technological devices:

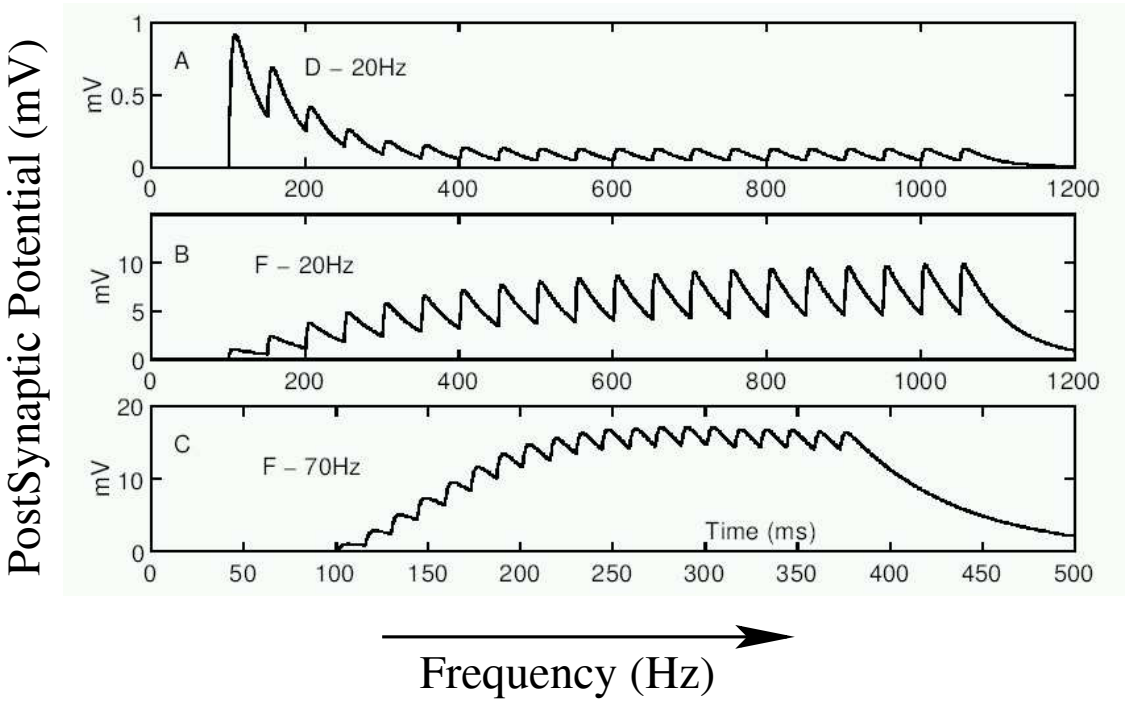

Figure 2.1: (A) Simulated postsynaptic potential generated by a regular spike train at a frequency of 20 Hz transmitted through a depressing synapse. (B)The same as A for facilitating synapse. (C) The same as B but for a presynaptic frequency of 70 Hz. REMARK: Both, caption and figure, have been directly taken from the work [Tsodyks et al., 1998] in order to illustrate the behavior of a realistic and phenomenological model of dynamic synapses.

1. They can approximate a large class of non-linear filters [Natschläger et al., 2001], including high-pass, low-pass and band-pass. The first (second) ones, need a very low (high) initial probability of release. The third ones are the most effective at transmitting impulses when there is an intermediate range of presynaptic activity. The filtering characteristics of a given synapse are not fixed; they can be adjusted through modulation of the initial release probability or other aspects of synaptic transmission [Dittman et al., 2000]. For instance, many neuromodulators activate presynaptic receptors, and the result is often a reduction in the probability of release. Thus, it decreases the amount of neurotransmitter released and the filtering characteristics of the modulated synapse are altered. In this way, depression makes a smaller contribution to synaptic dynamics and facilitation becomes more prominent. Consequently, presynaptic inhibition can convert a synapse from a low-pass filter to a band-pass filter, or from band-pass filter to a high-pass filter.

2. They allow the extraction of statistically significant features from noisy and variable temporal patterns [Liaw and Berger, 1996]. For instance, consider the case of sensory inputs arriving to a neuron A, which excites a neuron B through a depressing synapse. Even if a prolonged sensory stimulus activates neuron A, the response of neuron B may only be prominent at the beginning of the stimulation because synaptic depression produces a synaptic-specific decrease in the drive to neuron B. These results in a neuron that only respond to new stimuli improve adaptation and enhancement of transients.

3. And more specific consequences of previous items 1 and 2 as for instance sound localization [Cook et al., 2003], coincidence detection of signals [Kuba et al., 2002, Pantic et al., 2003] or decorrelation and burst detection [Goldman et al., 2002, Lisman, 1997].

2.7 Switching Phenomena

In attractor neural networks, and in special in the original Hopfield case, associative memory appears as a collective behavior depending on the (thermal) noise parameter [Amit et al., 1987, Hopfield, 1982]. Upper than a critical value, there is no any kind of memory observed, and this situation is corresponded with the (fixed-point) paramagnetic solution. On the contrary, and for low number of patterns [1], lower than the critical value, it is possible to retrieve information previously stored in the synapses intensities e.g. (fixed-point) ferromagnetic solution. Although a Hopfield network is a dynamical system, is static (or stationary) after convergence. Time does not play an intrinsic role in the encoding or decoding the input. However, there are experimental evidences in neuroscience that show how time takes a main role, for instance, in the early olfactory processing (see [Laurent et al., 2001] for a review) or hippocampus [Scarpetta et al., 2002]. Therefore, in order to be possible to study with attractor neural networks such systems mentioned above, where temporal information has a main role, in this thesis we incorporate new ingredients and reformulate the classical and artificial Hopfield situation. Considering these biology-based modifications, we observe *switching behavior*, e.g after a time in which one of the stored pattern is retrieved, the system jumps to another possible attractor, and keeps indefinitely doing so. This oscillatory behavior is an advantage because improves the network ability to detect changing stimuli which are received from the environment. Mathematically, the reason is that the fixed point in the ferromagnetic phase becomes unstable, and the system is driven to another attractor. The solution is a limit cycle attractor. Therefore, now is possible to code and/or decode in the temporal dimension. Furthermore, spatial information in attractor neural networks is stored in synapses. Hence, this mechanism can explain and interpret identification and categorization of spatio-temporal patterns which can be relevant, for in-

[1] For large number of patterns, in addition of ferromagnetic and paramagnetic solutions, the spin-glass phase appears [Amit et al., 1987].

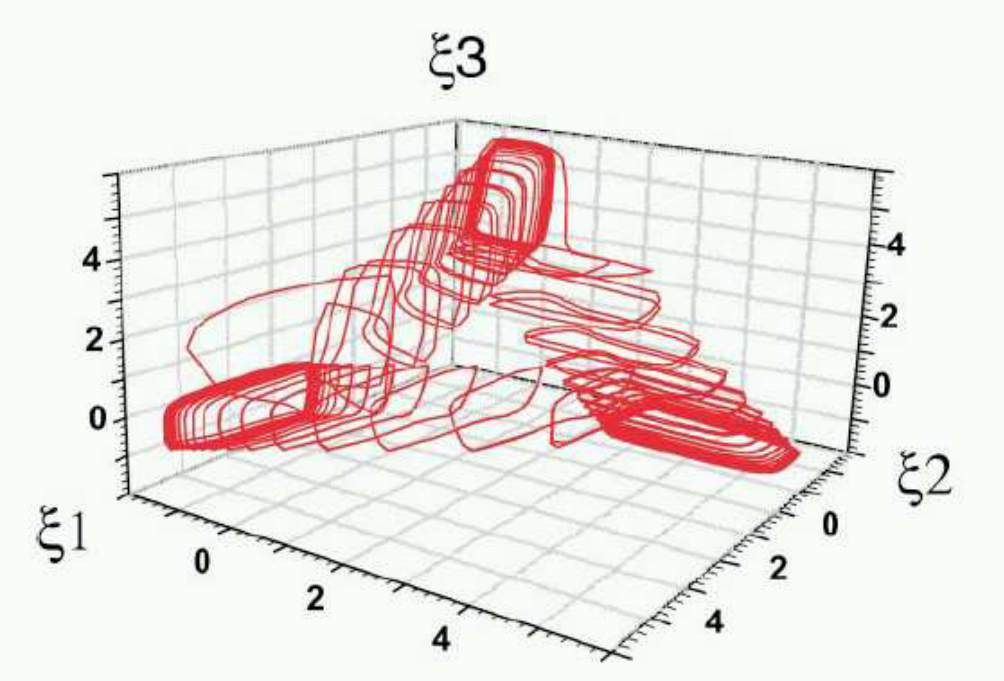

Figure 2.2: Heteroclinic loop for a simple network of three oscillating projection neurons (PNs), activated by a given pattern. Each axis maps the activity of one PN through a state variable ξ. The sequence connecting saddle limit cycles and the intervals between them are functions of the stimulus. A different stimulus would thus be represented by a different orbit and thus, a different temporal pattern of activation of the PNs.REMARK: Both, caption and figure, have been directly taken from the work [Laurent et al., 2001] in order to illustrate the behavior of a neural network model to understand early olfactory processes in insects.

stance, to the understanding of early olfactory processing [Laurent et al., 2001]. Thus, different odors could be coded in different attractors and the hierarchical discrimination of an odor is made by recognizing the components in order of decreasing response strengths [Oyamada et al., 2000].

In this thesis, we present and study switching or oscillatory behavior under three different degrees of description for dynamic synapses. The highest level is studied in the chapter 3, and incorporates a phenomenologycal model for real synapses [Tsodyks et al., 1998]. This model is susceptible to be analyzed under a mean field assumption and by doing Monte Carlo simulations. The intermediate-level is studied in the chapters 4 and 5. Here, we introduce a (fast) noise motivated by feedforward (short-term) plasticity, which assumes that elevated presynaptic activity can cause either an increase (facilitation) or a decrease (depression) by rapid repeated presynaptic activation which is typically required to produce appreciable synaptic plasticity [Abbott and Regehr, 2004]. We present Monte Carlo simulations of the system and a stochastic formulation based on a master equation [Marro and Dickman, 1999]. This allows to obtain (mean-field) dynamical equations for the order parameters e.g. overlaps between the network activity and the different patterns stored. Finnally, the lowest level, or equivalently, the most artificial system, is formulated and studied in the chapters 6 and 7. Here, activity of neurons and synaptic intensities are stochastically driven by different (temperature) parameters. The competition between baths impedes the system from reaching thermal equilibrium. In general, the asymptotic state is a non-equilibrium state, which is more realistic than an equilibrium one [Marro and Dickman, 1999]. The stochastic dynamics of synapses intensities is controlled by a different temperature, whose transition rate depends on the overlaps, or equivalently on the total presynaptic current arriving to the postsynaptic neuron. There is a oscillatory phase, where the dynamics may keep visiting different time-correlated attractors belonging to a class which is characterized by a certain degree of correlation between its elements.

In the chapter 5 we introduce a family of stochastic neural automatas, where

is possible to describe a switching dynamics which is chaotic, which may play a critical role in the Hebbian learning processes. On the one hand, in the construction of a new pattern or stimulus to encode. Let be an example, returning to olfactory processing, if an insect inhales air which does not contain a known odorant but a novel one, then there are no bursts, and the spatiotemporal patters are disordered. An existing pattern is not accessed, and therefore a recognizable spatial pattern fails, e.g. neural activity does not converge to any pre-existing spatial pattern. The strengthening of Hebbian synapses requires correlated activity in pre- and postsynaptic neurons. If a new pattern is going to be created for a new class of stimuli, then the activity that drives synapses must be also new. A chaotic generator appears to be a feasible way than the bulb can do this [Freeman, 1994]. On the other hand, chaotic motions explore a broad sector of the system state space and gives a means to explore the opportunities available to the system when the environment changes, and thus acts as a precursor to adaptative, reliable, and robust behavior for living systems. The instability inherent in chaotic motions, or more precisely in the non-linear dynamics of systems with chaos, facilitates the extraordinary ability of neural systems to adapt, make transitions from one pattern of behavior to another when the environment is altered, and consequently to create a rich variety of patterns [Rabinovich and Abarbanel, 1998]. It is important to remark that both chaos and noise are able to organize the irregular behavior of individual neurons or neural assemblies. However, the principal difference is that the dynamical chaos is a controllable irregularity and for that, it possesses structure in state space, while noise is an uncontrollable action of dynamical systems. This feature is extremely important for information processing.

2.8 Plan of the Report

In chapter 3, we introduce the effect of facilitating synapses in binary attractor neural networks. Motivated by the work in [Tsodyks et al., 1998], we use a realistic model of synaptic dynamics, in which both short-term facilitating

and depressing mechanisms operate on synapses. Compared to the situation previously studied of only depressing synapses [Pantic et al., 2002], facilitation increases the strength of depression. The attractors of the dynamics become highly unstable and consequently, the system enhances easier switching among the different stored patterns.

In chapter 4, we study both analytically and numerically the influence of presynaptic noise on the transmission of information in attractor neural networks. The noise occurs on a very short–time scale compared to that for the neurons activity. This is inspired in recent neurobiological findings that show that synaptic strength increases or decreases on a short–time scale depending on presynaptic activity. We thus describe a mechanism by which fast presynaptic noise enhances the neural network sensitivity to an external stimulus. The reason is that the presynaptic noise affects the stability of fixed points and consequently the system is able to scape from the attractor, which allows for categorization and may be relevant, for instance, to the understanding of early olfactory processing.

In chapter 5, we present a computational study of a stochastic neural automata with associative memory whose dynamics is formulated by using a master equation. The jumping probability takes into account the presence of presynaptic noise in a time scale shorter than neural activity. This noise is biologically motivated and incorporates activity dependent processes taken place at synapses intensities. In particular, our choice ranges from short-term depression to static synapses. Monte Carlo simulations of such system depict steady states which are complex. For instance, it shows switching phenomena and chaotic hopping between stored patterns. The chaoticity can be regulated by tuning a parameter which controls the intensity of fast noise. This can be quantitatively measured by computing the entropy for the harmonics of the oscillations. We suggest that this mechanism might be one of the strategies in brain to self-control chaos and may mimic some behavior in nature.

In chapter 6 we present a stochastic neural automata in which activity fluctuations and synaptic intensities evolve at different temperature, the latter mov-

ing trough a set of stored patterns. The complex non-linear dynamics of coupled neurons and synapses is solved exactly via coarse–graining procedure which is complemented by Monte Carlo simulations. The network exhibits various retrieval phases, including one which depicts continuous switching among different attractors. The switching may be either random or more complex, depending on the system parameters values.

In chapter 7, we (computationally) explore the oscillatory time-trajectory of the neural automata defined in chapter 6. We analyse the system by combining the mesoscopic dynamics obtained in chapter 6 with Monte Carlo simulations. We suggest that the resulting dynamics dynamics can be an efficient procedure to classify and generalize large sets of different patterns organized in families. This is relevant for biological systems and it may have also important technological applications.

Bibliography

L. F. Abbott and T. B. Kepler. Model neurons: From hodgkin-huxley to hopfield. In L. Garrido, editor, *Statistical Mechanis of Neural Networks*, pages 5–18. Springer-Verlag, 1990. 30

L. F. Abbott and W. G. Regehr. Synaptic computation. *Nature*, 431:796–803, 2004. 31, 32, 37

D. J. Amit. *Modeling brain function: the world of attractor neural network*. Cambridge University Press, 1989. 31

D. J. Amit, H. Gutfreund, and H. Sompolinsky. Statistical mechanics of neural networks near saturation. *Ann. Phys.*, 173:30–67, 1987. 30, 35

D. Bibitchkov, J.M. Herrmann, and T. Geisel. Pattern storage and processing in attractor networks with short-time synaptic dynamics. *Network: Comput. Neural Syst.*, 13:115–129, 2002. 32

R. E. Brown and P. M. Milner. The legacy of Donald O. Hebb: more than the hebb synapse. *Nat. Rev. Neurosci.*, 4:1013–1019, 2003. 32

D. L. Cook, P. C. Schwindtt, L. A. Grande, and W. J. Spain. Synaptic depression in the localization of sound. *Nature*, 421:66–70, 2003. 34

J. S. Dittman, A. C. Kreitzer, and W. G. Regehr. Interplay between facilitation, depression, and residual calcium at three presynaptic terminals. *J. Neurosci.*, 20:1374–1385, 2000. 34

W. J. Freeman. Neural networks and chaos. *J. Theor. Biol.*, 171:13–18, 1994. 38

T. Geszti. *Physical Models of Neural Networks*. World Scientific, 1990. 31

M.S. Goldman, P. Maldonado, and L.F. Abbott. Redundancy reduction and sustained firing with stochastic depressing synapses. *J. Neurosci.*, 22:584–591, 2002. 34

J. Hertz, A. Krogh, and R.G. Palmer. *Introduction to the theory of neural computation*. Addison-Wesley, 1991. 31

J.J. Hopfield. Neural networks and physical systems with emergent collective computational abilities. *Proc. Natl. Acad. Sci. USA*, 79:2554–2558, 1982. 30, 35

H. Kuba, K. Koyano, , and H. Ohmori. Synaptic depression improves coincidence detection in the nucleus laminaris in brainstem slices of the chick embryo. *Eur. J. Neurosci.*, 15:984–990, 2002. 34

G. Laurent, M. Stopfer, R.W. Friedrich, M.I. Rabinovich, A. Volkovskii, and H.D.I. Abarbanel. Odor encoding as an active, dynamical process: Experiments, computation and theory. *Annual Review of Neuroscience*, 24:263–297, 2001. xx, 35, 36, 37

J. S. Liaw and T. W. Berger. Dynamic synapse: a new concept of neural representation and computation. *Hippocampus*, 6:591–600, 1996. 34

J. E. Lisman. Bursts as a unit of neural information: making unreliable synapses reliable. *Trends Neurosci.*, 20:38–43, 1997. 34

M. A. Lynch. Long-term potentiation and memory. *Physiol. Rev.*, 84:87–136, 2004. 32

J. Marro and R. Dickman. *Nonequilibrium Phase Transitions in Lattice Models*. Cambridge University Press, 1999. 28, 30, 37

R. G. Morris. Long-term potentiation and memory. *Philos. Trans. R. Soc. Lond. B Biol. Sci.*, 358:643–647, 2003. 32

R. Mueller and A. V. M. Herz. Content-addressable memory with spiking neurons. *Phys. Rev. E*, 59:330–3338, 1999. 30

T. Natschläger, W. Maass, and A. Zador. Efficient temporal processing with biologically realistic dynamic synapses. *Network: Comput. Neural Syst.*, 12: 75–87, 2001. 34

T. Oyamada, Y. Kashimori, O. Hoshino, and T. Kambara. A neural mechanism of hierarchical discrimination of odors in the olfactory cortex based on spatiotemporal encoding of odor information. *Biological Cybernetics*, 83:21–33, 2000. 37

L. Pantic, J.J. Torres, and H.J. Kappen. Coincidence detection with dynamic synapses. *Network: Comput. Neural Syst.*, 14:17–33, 2003. 34

L. Pantic, J.J. Torres, H.J. Kappen, and S.C.A.M. Gielen. Associative memmory with dynamic synapses. *Neural Comp.*, 14:2903–2923, 2002. 32, 39

M. I. Rabinovich and H. D. I. Abarbanel. The role of chaos in neural systems. *Neuroscience*, 87:5–14, 1998. 38

S. Scarpetta, L. Zhaopin, and J. Hertz. Hebbian imprinting and retrieval in oscillatory neural networks. *Neural Comp.*, 14:2371–2396, 2002. 35

M. Tsodyks. Attractor neural network models of spatial maps in hippocampus. *Hippocampus*, 9:481–489, 1999. 30

M. V. Tsodyks, K. Pawelzik, and H. Markram. Neural networks with dynamic synapses. *Neural Comp.*, 10:821–835, 1998. xx, 32, 33, 37, 38

G. G. Turrigiano, K. R. Leslie, N. S. Desai, L. C. Rutherford, and S. B. Nelson. Activity-dependent scaling of quantal amplitude in neocortical neurons. *Nature*, 26:892–896, 1998. 32

G. G. Turrigiano and S. B Nelson. Homeostatic plasticity in the developing nervous system. *Nat. Rev. Neurosci.*, 5:97–107, 2004. 32

Chapter 3

Attractor Neural Networks with Dynamic Synapses

3.1 Introduction

Associative memory illustrates the simplest possible manner in which collective neural computation can work. This property may be said to initiate, mathematically well-formulated, with the Hopfield model [Amit et al., 1987, Hopfield, 1982]. The basic problem is to store a set of different stimuli or patterns in the network, in such way that when a new pattern is presented, the network dynamics drives the system to one of the stored patterns most *similar* to the new one. The meaning of similar is to be close according to a previously defined distance. Therefore, the retrieval of stored patterns during the dynamics appears. This means that a retrieved, and previously memorized pattern, is an attractor. The number of different attractors determines the number of different stimuli or patterns that the system can store and retrieve. Many different variants and applications, including asymmetric synapses, dilution and non-detailed balance, have been studied in the last decades [Amit, 1989, Geszti, 1990, Hertz et al., 1991]. Here, neurons are considered to be the computational

and essential engines for coding and processing of information. The role of synapses is to act as connections and messengers of neural transmissions. Very recently, it has been emphasized that neural dynamics with static synapses is incomplete and undefined [Abbott and Regehr, 2004]. Diverse types of synaptic plasticity and the range of timescales over which they operate suggest that synapses have the most active role in information processing and therefore it is necessary both neural and synaptic dynamical descriptions.

In this work, we study the effect of the inclusion of a phenomenological model[Tsodyks et al., 1998] of dynamic synapses on the emergent properties of attractor neural networks. The dynamic synapses are activity-dependent processes. That is, the postsynaptic potential or response can either decrease (depression) or increase (facilitation) due to rapid repeated presynaptic activation. These effects are fundamental for the development and adaptation of the nervous system, and are believed to be on the basis of such higher functions as learning and memory. The effect of only (short-term) depressing synapses in attractor neural networks was studied in previous works [Bibitchkov et al., 2002, Pantic et al., 2002]. Depression affects on the the stability of patterns changing it considerably. Consequently, the storage capacity of memorized (stable) patterns is reduced [Torres et al., 2002]. On the contrary, it is shown to be advantageous for processing of sequences of patterns and it allows for switching between the stored patterns. This feature enhances the network response to continuosly changing stimuli. However, the study of facilitating mechanisms in such networks still hast not been reported. Here, we study the emergent properties of attractor neural networks with dynamic synapses including short-term depression and facilitation. Facilitation gets a stronger depression and the network ability to switch among the patterns increases. This high facility could be interesting to code both spatial and temporal information, and could explain, for instance, the classification and categorization on the spatio-temporal patterns in the early olfactory processes in insects [Laurent et al., 2001].

3.2 The Model

Lets us consider a stochastic neural network of N binary neurons with state variables given by $s_i = \{1, 0\}$. Each state represents a firing (silent) neuron. We assume that the state of each neuron evolve in time with the following probabilistic discrete dynamics

$$\text{Prob}\{s_i(t+1) = 1\} = \frac{1}{2}\{1 + \tanh[2\beta(h_i(t) - \theta_i)]\}, \tag{3.1}$$

where the local fields $h_i = \sum_j \omega_{ij} x_j s_j$ represent the total presynaptic current arriving to the postsynaptic neuron i, θ_i is the threshold of neuron i to fire, and $\beta \equiv \frac{1}{T}$ represents the level of noise in the network affecting neuron activity. The variables ω_{ij} are static weights representing the synaptic strength between neurons i and j. They are defined according to the standard covariance rule

$$\omega_{ij} = \frac{1}{Nf(1-f)} \sum_{\nu=1}^{P} (\xi_i^\nu - f)(\xi_j^\nu - f), \tag{3.2}$$

where $\xi^\nu, \nu = 1 \ldots, P$ are P random patterns stored in the network with average activity $\langle \xi_i^\mu \rangle = f = 1/2$. The variable x_j is a dynamical quantity representing the current state of the synapse and its probability to produce a postsynaptic response [Tsodyks et al., 1998]. In particular it represents the fraction of neurotransmitters that are in a *recovering* state. Depending of its dynamics this variable can include short term depression and facilitation mechanisms. When $x_j = 1$, for any j we recover the standard Hopfield model with static synapses.

The general equation describing the dynamical behavior of the state of synapses is given, according to [Tsodyks et al., 1998], by

$$\frac{dx_j(t)}{dt} = \frac{1 - x_j(t)}{\tau_{rec}} - x_j(t) s_j(t) \bar{U}_{SE,j}(t) \;\; \forall j = 1, \ldots, N, \tag{3.3}$$

where $\bar{U}_{SE,j}(t)$ is the maximum amount of neurotransmitter released by each spike arriving from the presynaptic neuron j. In absence of any facilitating mechanism one has

$$\bar{U}_{SE,i}(t) = \begin{cases} U_{SE} & t = t_{sp} \\ 0 & t \neq t_{sp} \end{cases} \tag{3.4}$$

for all presynaptic spikes, where t_{sp} denotes the time at which the spike arrives to the postsynaptic neuron, and U_{SE} is the maximum amount of neurotransmitter released after the first spike, assuming resting conditions (or equivalently, when the frequency of the presynaptic spike train is very low). If one wants to include facilitation, it is necessary to use a new dinamical variable $u_i(t)$ which is increasing after each presynaptic spike and that takes into account the opening of calcium channels in the presynaptic neuron near the neurotransmitter release sites. As a consequence, Ca^2+ ions enter into the cell and binds to an acceptor near the release sites gating the neurotransmitter quantal release [Bertram et al., 1996]. Using the model of synaptic facilitation introduced in [Tsodyks et al., 1998], the dynamics of the variable u can be written in the form

$$\frac{du_i(t)}{dt} = \frac{-u_i(t)}{\tau_{fac}} + U_{SE}[1 - u_i(t)]s_i(t) \;\; \forall i = 1, \ldots, N. \tag{3.5}$$

The equation (3.5) is coupled to equation (3.3) taken into account the fact that from (3.5) one has

$$\bar{U}_{SE,i}(t) = \begin{cases} u_i(t)(1 - U_{SE}) + U_{SE} & t = t_{sp} \\ 0 & t \neq t_{sp} \end{cases} . \tag{3.6}$$

Then, we can rewrite equation (3.3) as follows:

$$\frac{dx_i(t)}{dt} = \frac{1 - x_i(t)}{\tau_{rec}} - x_i(t)s_i(t)U_{SE} - u_i(t)x_i(t)(1 - U_{SE})s_i(t). \tag{3.7}$$

Thus, the equations (3.5) and (3.7) define the dynamics of synapses including both short-term depression and facilitation.

3.3 Mean-field Analysis

In this section we report on the mean-field analysis of the model. The set of equations (3.1),(3.5) and (3.7) constitutes the system under study. Due to the fact that the dynamics in (3.1) is discrete and syncrhonous it will convenient for our analysis to discretize the set of equations (3.5) and (3.7).

In order to develop a mean-field framework for our system, it is convenient to define the mean activity of the network for the units which are active and inactive in a particular pattern ν. Thus, we define the following two order parameters, $m_+^\nu \equiv \frac{1}{Nf}\sum_{j\in Act(\nu)} s_j$ and $m_-^\nu \equiv \frac{1}{N(1-f)}\sum_{j\notin Act(\nu)} s_j$. With these definitions one can easily see that the overlap of the network activity with a stored pattern ν relates with m_+^ν and m_-^ν as follows

$$m^\nu \equiv \frac{1}{Nf(1-f)}\sum_i (\xi_i^\nu - f)s_i = m_+^\nu - m_-^\nu, \quad \forall\nu. \tag{3.8}$$

Similarly one can assume that all neurons which are active or inactive in the pattern ν have the same degree of depression and/or facilitation. Then, we can assume that x_i and u_i only take, respectively, two possible values, $\{x_+^\nu, x_-^\nu\}$ and $\{u_+^\nu, u_-^\nu\}$. Under these hypothesis, the local field h_i representing the total synaptic current arriving to a particular neuron i can be written as follow:

$$h_i = \sum_{\nu=1}^{P} (\xi_i^\nu - f)[x_+^\nu m_+^\nu - x_-^\nu m_-^\nu]. \tag{3.9}$$

Finally, considering random patterns ($f = 1/2$) and under a standard mean-field approach our set of equations becomes the following coupled map:

$$\begin{aligned}
x_\pm^\nu(t+1) &= x_\pm^\nu(t) + \frac{1-x_\pm^\nu(t)}{\tau_{rec}} - U_{SE}x_\pm^\nu(t)m_\pm^\nu(t) - (1-U_{SE})u_\pm^\nu(t)x_\pm^\nu(t)m_\pm^\nu(t),\\
u_\pm^\nu(t+1) &= u_\pm^\nu(t) - \frac{u_\pm^\nu(t)}{\tau_{fac}} + U_{SE}[1-u_\pm^\nu(t)]m_\pm^\nu(t),\\
m_\pm^\nu(t+1) &= \frac{1}{N}\sum_{i\{\substack{\in\\ \notin}\}Act(\nu)}\left[1 \pm \tanh\left\{\beta\left(\left[x_+^\nu(t)m_+^\nu(t) - x_-^\nu(t)m_-^\nu(t)\right]\right.\right.\right.\\
&\qquad \left.\left.\left. \pm \sum_{\mu\neq\nu}(2\xi_i^\mu - 1)\left[x_+^\mu(t)m_+^\mu(t) - x_-^\mu(t)m_-^\mu(t)\right]\right)\right\}\right],\\
m^\nu(t+1) &= \frac{1}{N}\sum_i (2\xi_i^\nu - 1)\left[1+\tanh\left\{\beta\sum_\mu (2\xi_i^\mu - 1)\left[x_+^\mu(t)m_+^\mu(t) - x_-^\mu(t)m_-^\mu(t)\right]\right\}\right].
\end{aligned} \tag{3.10}$$

In the thermodynamic limit ($N \to \infty$) the fixed point equations for the coupled dynamics of neurons and synapses is given in the mean field approxima-

tion as

$$
\begin{aligned}
x_{\pm}^{\nu} &= \frac{1}{1 \,+\, \tau_{rec}\; m_{\pm}^{\nu}\; U_{SE} \,+\, (1-U_{SE})\; u_{\pm}^{\nu}\; \tau_{rec}\; m_{\pm}^{\nu}}, \\
u_{\pm}^{\nu} &= \frac{\tau_{fac}\; m_{\pm}^{\nu}\; U_{SE}}{1 \,+\, \tau_{fac}\; m_{\pm}^{\nu}\; U_{SE}}, \\
m_{\pm}^{\nu} &= \frac{1}{2}\left[1 \pm \frac{2}{N} \sum_{i\left\{\begin{smallmatrix}\in\\ \notin\end{smallmatrix}\right\}Act(\nu)} \tanh\left\{\beta\left(\left[x_{+}^{\nu} m_{+}^{\nu} - x_{-}^{\nu} m_{-}^{\nu}\right] \pm \sum_{\mu\neq\nu} \epsilon_{i}^{\mu}\left[x_{+}^{\mu} m_{+}^{\mu} - x_{-}^{\mu} m_{-}^{\mu}\right]\right)\right\}\right], \\
m^{\nu} &= \frac{1}{N}\sum_{i} \epsilon_{i}^{\nu} \tanh\{\beta \sum_{\mu} \epsilon_{i}^{\mu}[x_{+}^{\mu} m_{+}^{\mu} - x_{-}^{\mu} m_{-}^{\mu}]\},
\end{aligned}
\tag{3.11}
$$

where $\epsilon_{i}^{\mu} \equiv 2\xi_{i}^{\mu} - 1$.

One can substitute the expressions for u_{+}^{ν} and u_{-}^{ν} into the other equations to reduce the dimensionality of the system (3.11). Thus, we obtain

$$
\begin{aligned}
m_{\pm}^{\nu} &= \frac{1}{2}\left[1 \pm \frac{2}{N} \sum_{i\left\{\begin{smallmatrix}\in\\ \notin\end{smallmatrix}\right\}Act(\nu)} \tanh\left\{\beta\left(\left[x_{+}^{\nu} m_{+}^{\nu} - x_{-}^{\nu} m_{-}^{\nu}\right] \pm \sum_{\mu\neq\nu} \epsilon_{i}^{\mu}\left[x_{+}^{\mu} m_{+}^{\mu} - x_{-}^{\mu} m_{-}^{\mu}\right]\right)\right\}\right], \\
m^{\nu} &= \frac{1}{N}\sum_{i} \epsilon_{i}^{\nu} \tanh\{\beta \sum_{\mu} \epsilon_{i}^{\mu}[x_{+}^{\mu} m_{+}^{\mu} - x_{-}^{\mu} m_{-}^{\mu}]\}, \\
x_{\pm}^{\nu} &= \frac{1 \,+\, \tau_{fac}\; m_{\pm}^{\nu}\; U_{SE}}{1 \,+\, \tau_{fac}\; m_{\pm}^{\nu}\; U_{SE} \,+\, \tau_{rec}\; m_{\pm}^{\nu}\; U_{SE} \,+\, \tau_{rec}\; \tau_{fac}\; U_{SE}\; [m_{\pm}^{\nu}]^{2}}.
\end{aligned}
\tag{3.12}
$$

Note that the limit of τ_{fac} going to 0 recovers the previous results of only depression appearing [Torres et al., 2002]. This is,

$$
\lim_{\tau_{fac}\to 0} x_{\pm}^{\nu} = \frac{1}{1 + \tau_{rec}\; U_{SE}\; m_{\pm}}. \tag{3.13}
$$

In the following, we report on different features in an attractor neural network. Attending to stationary behavior, we compute the mean-field storage capacity. In relation to dynamical properties, we study the local stability around the steady states and we investigate an oscillatory phase, where the system is

able to jump between the stored patterns in the retrieval dynamics.

3.3.1 The Storage Capacity for $\alpha \neq 0$

In the study of attractor neural networks the calculation of the maximum number of stable patterns that the system is able to store and retrieve takes a main role. In order to compute this storage capacity we use the standard method so well explained in [Hertz et al., 1991]. We will take into account that in the steady state the network have a macroscopic overlap, $\mathcal{O}(1)$, with a finite number of patterns (condensed patterns) whereas the overlap is $\mathcal{O}(1/\sqrt{N})$ for the rest (non-condensed patterns). Let assume that we have only one condensed pattern, namely $\mu = 1$. Then, following the same reasoning used in [Torres et al., 2002] we have that $m_{\pm}^1$ is $\mathcal{O}(1)$, $m_{+}^1 + m_{-}^1 \approx 1$, $m_{\pm}^\nu$ is $\mathcal{O}(1/\sqrt{N})\forall\nu \neq 1$, and $x_{\pm}^\nu = 1 - \mathcal{O}(\frac{1}{\sqrt{N}})\ \forall\nu \neq 1$. In addition, if we define $M^\nu \equiv x_{+}^\nu m_{+}^\nu - x_{-}^\nu m_{-}^\nu$ then $M^\nu \approx m^\nu$ in the thermodynamic limit. The small order parameters M^μ can be considered as independent random variables with mean zero and variance $\alpha r/P$ where $r \equiv \frac{1}{\alpha}\sum_{\mu\neq 1} {M^\mu}^2$, and $\alpha = P/N$.

Besides we shall consider that $\epsilon_i^\mu \epsilon_i^1$ is random and independent of M^μ and therefore $z \equiv (1/\sqrt{\alpha r})\sum_{\mu\neq 1,\nu} \epsilon_i^\mu \epsilon_i^1 M^\mu$ is a Gaussian noise with zero mean and variance 1, the average $1/N\sum_i$ appearing in the fixed point equations reduces to an average over the Gaussian noise z. This argument can be also applied to the sums over neurons that are active (inactive) in the condensed pattern 1 [Torres et al., 2002]. Then, the steady-state system of equations (3.12) becomes:

$$\begin{aligned} \nu &= \int \frac{dz}{\sqrt{2\pi}} e^{-z^2/2} \tanh[\beta(f[\nu, \tau_{rec}, \tau_{fac}] + \sqrt{\alpha r} z)], \\ q &= \int \frac{dz}{\sqrt{2\pi}} e^{-z^2/2} \tanh^2[\beta(f[\nu, \tau_{rec}, \tau_{fac}] + \sqrt{\alpha r} z)], \\ r &= \frac{q}{[1-\beta(1-q)]^2}, \end{aligned} \tag{3.14}$$

where

$$q \equiv \frac{1}{N}\sum_i \tanh^2\left\{\beta \sum_\mu \epsilon_i^\mu M^\mu\right\} \tag{3.15}$$

is the *spin-glass* order parameter [Amit et al., 1987], $\nu \equiv 2m_+^\nu - 1$ and the function f is defined as

$$f[\nu, \tau_{rec}, \tau_{fac}] \equiv \frac{4\nu\Phi_1[\nu, \tau_{rec}, \tau_{fac}]}{4 + 4\gamma\Phi_2[\nu, \tau_{rec}, \tau_{fac}] + \gamma^2(1-\nu^2)\Phi_3[\nu, \tau_{rec}, \tau_{fac}]}, \tag{3.16}$$

being

$$\begin{aligned}
\gamma &\equiv \tau_{rec}\, U_{SE}, \\
\Phi_1[\nu, \tau_{rec}, \tau_{fac}] &= 1 + \tfrac{\gamma^2\tau_{fac}(\tau_{fac}+\tau_{rec})(1-\nu^2)+\gamma\tau_{fac}\tau_{rec}(4-\tau_{rec}+\tau_{rec}\nu^2)}{4\tau_{rec}^2}, \\
\Phi_2[\nu, \tau_{rec}, \tau_{fac}] &= 1 + \tfrac{\tau_{fac}}{2\tau_{rec}}(2 + \tau_{rec} + \tau_{rec}\nu^2), \\
\Phi_3[\nu, \tau_{rec}, \tau_{fac}] &= 1 + \tfrac{\tau_{fac}}{\tau_{rec}}(2 + \tau_{rec}) + \tfrac{\tau_{fac}^2}{\tau_{rec}^2}[1 + \tau_{rec} + \tfrac{\tau_{rec}^2}{4}(1-\nu^2)].
\end{aligned} \tag{3.17}$$

From equation (3.17), it is straightforward to obtain the limits

$$\begin{aligned}
\lim_{\tau_{rec}\to 0} f[\nu, \tau_{rec}, \tau_{fac}] &= \nu, \\
\lim_{\tau_{rec}\to \infty} f[\nu, \tau_{rec}, \tau_{fac}] &= 0, \\
\lim_{\tau_{fac}\to 0} f[\nu, \tau_{rec}, \tau_{fac}] &= \tfrac{4\nu}{4+4\gamma+\gamma^2(1-\nu^2)}, \\
\lim_{\tau_{fac}\to \infty} f[\nu, \tau_{rec}, \tau_{fac}] &= \tfrac{4\nu}{4+4\tau_{rec}+\tau_{rec}^2(1-\nu^2)}.
\end{aligned} \tag{3.18}$$

The first one coincides with the static synapse case, that is the Hopfield model situation [Hertz et al., 1991], the second gives a paramagnetic solution, the third recovers the previously obtained result in the case of considering only depressing synapses [Torres et al., 2002], and the fourth and last coincides with the third case with $U_{SE} = 1$.

The maximum (critical) storage capacity is achieved at zero temperature when increasing the loading parameter α the (ferromagnetic) solution $\nu \neq 0$ disappears. In the limit of $T = 0$ ($\beta \to \infty$) we use the approximations $\int \frac{dz}{\sqrt{2\pi}} e^{-z^2/2}(1-\tanh^2 \beta[az+b]) \approx \sqrt{\frac{2}{\pi}} \frac{1}{a\beta} e^{-b^2/2a^2}$ and $\int \frac{dz}{\sqrt{2\pi}} e^{-z^2/2} \tanh \beta[az+$

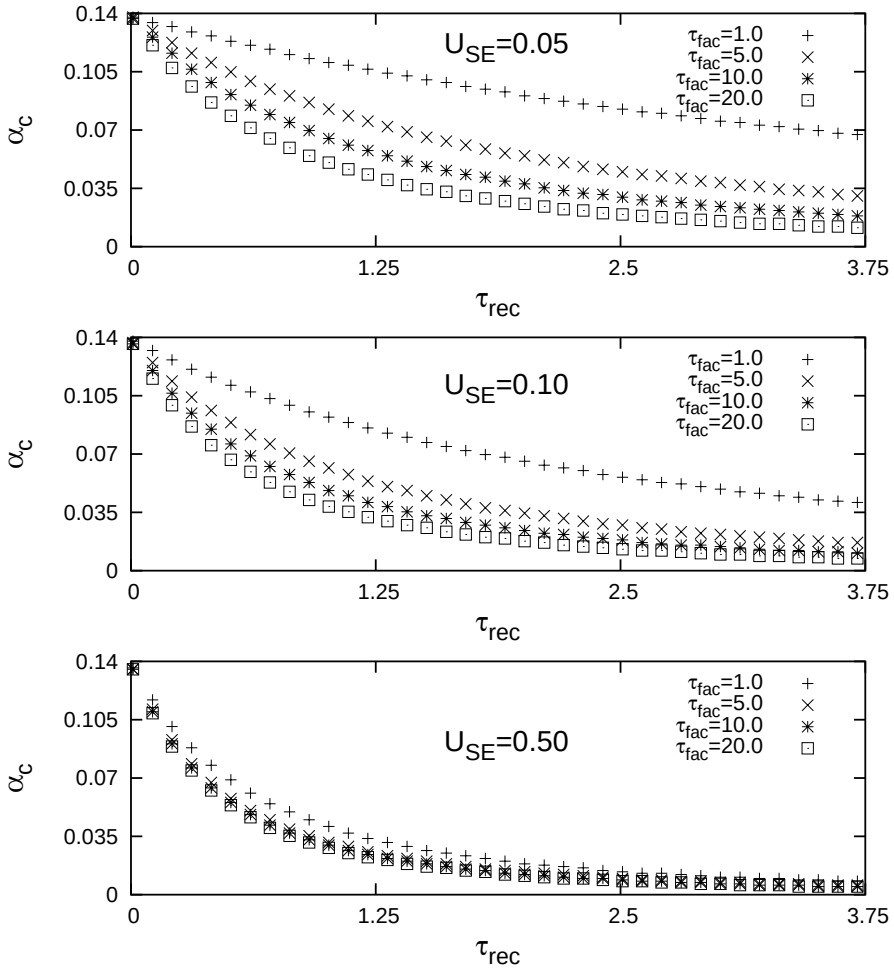

Figure 3.1: Mean field storage capacity α_c vs τ_{rec}, for different values of τ_{fac} and U_{SE}. In order to observe facilitating mechanisms we need very low values of U_{SE}. Facilitation gets a stronger depression, and consequently decreases the storage capacity compared to the situation of only depressing synapses [Torres et al., 2002].

$b]) \approx \mathrm{erf}(\frac{b}{\sqrt{2}a})$. Then, introducing a new variable $y = f[\nu, \tau_{rec}, \tau_{fac}]/\sqrt{2\alpha r}$ the system of steady-state equations (3.14) reduces to the single transcendental equation

$$y\left(\sqrt{2\alpha} + \frac{2}{\sqrt{\pi}} e^{-y^2}\right) = f[\mathrm{erf}(y), \tau_{rec}, \tau_{fac}]. \tag{3.19}$$

Given a set of parameters $(\tau_{rec}, \tau_{fac}, U_{SE},)$ the value of α at which appear non-trivial solutions of that equations, that is $y \neq 0$, gives the critical storage capacity for the network. In figure 3.1 we shows the effect produced by the facilitating mechanisms on the maximum storage capacity of the networks for different values of U_{SE}. We observe, firstly, that the effect of facilitation in the steady states, modulated by the parameter τ_{fac} is considerable only when U_{SE} is low [Tsodyks et al., 1998]. Secondly, that in any case of including facilitating mechanisms, the storage capacity of stable patterns decreases, compared to the situation of only depressing synapses [Torres et al., 2002]. As we show in the next section, this is due to facilitation achieves a stronger depression, and the stability of the attractors is changed considerably. Consequently, there is a superposition between the standard noise implied in the calculation of the storage capacity (originated by a increase of the number of patterns) and a new contribution due to the unstability of patterns. This superposition of two different sources of noises gets a meaningful decrease in the critical value for the storage capacity. Following this reasoning, the case of static synapses or Hopfield situation [Hertz et al., 1991, Hopfield, 1982], recovered in the limit $\tau_{rec} \to 0$, gives the largest storage capacity, $\alpha_c = 0.138$. This can be observed in the figure 3.1 at the left-top corner of the graph. The next value corresponds to the case of only depressing synapses [Torres et al., 2002] and finally, the smallest storage is achieved when both depressing and facilitating mechanisms are incorporated.

3.3.2 Local Stability around the Steady States for $\alpha = 0$

In this section we are going to study the local stability of the dynamics system (3.10) around the steady-state solutions (3.11) for $\alpha = 0$. In the case of only one

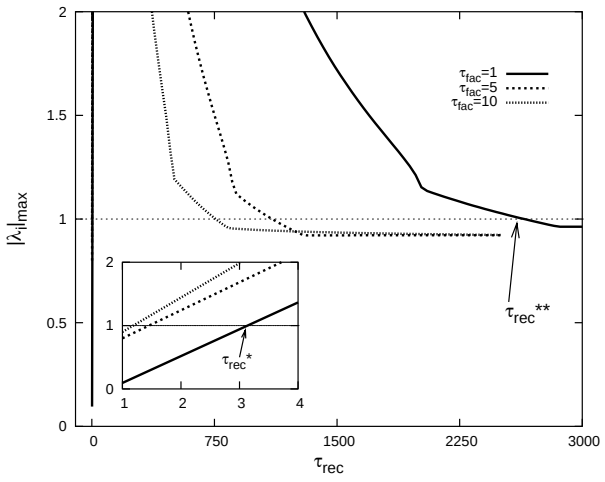

Figure 3.2: The maximum absolute value for the set of eigenvalues corresponding to the linearized (stability) matrix (3.22) evaluated in the steady states or fixed points (3.21) versus τ_{rec} and different values of τ_{fac}. The figure illustrates three different macroscopic phases limited by the bifurcation points or critical values τ^{*}_{rec} and τ^{**}_{rec}. When $\tau_{rec} < \tau^{*}_{rec}$ the ferromagnetic or memory solution $m_{+} \neq 0.5$ is stable, and fullfills that its $|\lambda|$ associated is less than 1. For $\tau_{rec} > \tau^{**}_{rec}$ only the paramagnetic or no-memory solution $m_{+} = 0.5$ is stable. Between of them and satisfying $\tau^{*}_{rec} < \tau_{rec} < \tau^{**}_{rec}$ exists an oscillatory phase, where the solution $m_{+} \neq 0.5$ exists, is unstable and obeys that $|\lambda| > 1$. The system describes continuous hopping among the different stored patterns (in the case of $P = 1$ from pattern to antipattern). These three different phases coincide with those shown in the work [Pantic et al., 2002] with only depressing synapses. Facilitation incorporates, moreover, both non-trivial rescaling of the critical values τ^{*}_{rec} and τ^{**}_{rec}, and consequently influences strongly in the stability of the fixed points. Here, we take the (inverse) noise parameter fixed to $\beta = 100$ and $U_{SE} = 0.05$.

random pattern stored the discrete map (3.10) reduces to

$$\begin{aligned} m_\pm(t+1) &= \frac{1}{2}\{1 \pm \tanh[\beta x_+(t)m_+(t) - \beta x_-(t)m_-(t)]\}, \\ x_\pm(t+1) &= x_\pm(t) + \frac{1-x_\pm(t)}{\tau_{rec}} - x_\pm(t)m_\pm(t)U_{SE} - u_\pm(t)x_\pm(t)(1-U_{SE})m_\pm(t), \\ u_\pm(t+1) &= u_\pm(t) - \frac{u_\pm(t)}{\tau_{fac}} + U_{SE}[1-u_\pm(t)]m_\pm(t). \end{aligned} \tag{3.20}$$

Note that for this particular case the constraint $m_+(t) + m_-(t) = 1$ is satisfied at any time. The steady-state solution (fixed point) of this discrete map is

$$\begin{aligned} m_\pm &= \frac{1}{2}\{1 \pm \tanh[\beta x_+ m_+ - \beta x_- m_-]\}, \\ x_\pm &= \frac{1}{1 + \tau_{rec}U_{SE}m_\pm + \tau_{rec}(1-U_{SE})u_\pm m_\pm}, \\ u_\pm &= \frac{\tau_{fac}U_{SE}m_\pm}{1 + \tau_{fac}U_{SE}m_\pm}. \end{aligned} \tag{3.21}$$

In order to study local stability of the system defined by (3.20) around the steady state (3.21) it is necessary to obtain the first derivative matrix $D \equiv \left(\frac{\partial \overrightarrow{f}}{\partial \overrightarrow{y}}\right)_{\overrightarrow{y}_{st}}$, being $\overrightarrow{f} \equiv \{f_i\}_{i=1}^6$ the functions appearing at the right side of (3.20) and $\overrightarrow{y} \equiv \{y_i\}_{i=1}^6 = (m_+, m_-, x_+, x_-, u_+, u_-)$. The result is

$$D = \begin{pmatrix} 2\beta m_+ m_- x_+ & -2\beta m_+ m_- x_- & 2\beta m_+^2 m_- & -2\beta m_+ m_-^2 & 0 & 0 \\ -2\beta m_+ m_- x_+ & 2\beta m_+ m_- x_- & -2\beta m_+^2 m_- & 2\beta m_+ m_-^2 & 0 & 0 \\ A_+ & 0 & B_+ & 0 & C_+ & 0 \\ 0 & A_- & 0 & B_- & 0 & C_- \\ D_+ & 0 & 0 & 0 & E_+ & 0 \\ 0 & D_- & 0 & 0 & 0 & E_- \end{pmatrix} \tag{3.22}$$

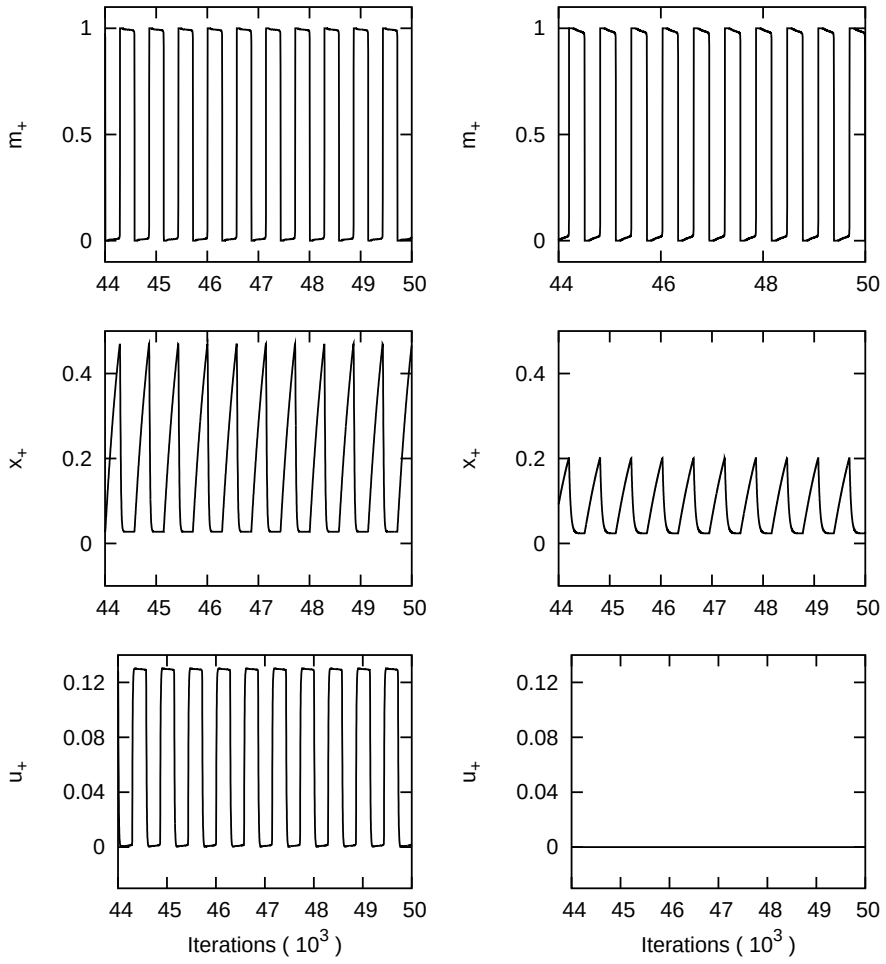

Figure 3.3: Facilitation and depression (left panel) is presented against only depression (right panel) for $U_{SE} = 0.03$ and $\beta = 100$. On the top, tuning the parameter τ_{rec}, and monitoring the variable m_+ both behaviors seem being similar. Nevertheless, the middle graphs show that facilitation gets a stronger depression, because the amplitude of the oscillation for x_+ grows in presence of facilitation. Finnally, we show on the bottom the time evolution for u_+, which illustrates how in the case of solely depression is constant and equal to 0. The left panel has been computed taking $\tau_{rec} = 229.0$ and $\tau_{fac} = 5.0$ and the right one using $\tau_{rec} = 1400.0$ Note that, in order to show, qualitatively, the same frequency on the oscillations for the variable m_+ appearing on the top, in the situation of lonely depression is necessary to increment drastically the parameter τ_{rec}.

where

$$\begin{aligned} A_{\pm} &= -U_{SE}x_{\pm} - (1 - U_{SE})u_{\pm}x_{\pm} \\ B_{\pm} &= 1 - \tfrac{1}{\tau_{rec}} - U_{SE}m_{\pm} - (1 - U_{SE})u_{\pm}m_{\pm} \\ C_{\pm} &= x_{\pm}(1 - U_{SE})m_{\pm} \\ D_{\pm} &= U_{SE}(1 - u_{\pm}) \\ E_{\pm} &= 1 - \tfrac{1}{\tau_{fac}} - U_{SE}m_{\pm}. \end{aligned} \tag{3.23}$$

After substituting the steady solutions of $x_{\pm}$ and $u_{\pm}$ appearing on (3.21) as a function of m_{+} and m_{-} and considering the constraint $m_{-} = (1 - m_{+})$ we obtain the eigenvalues and then take the absolute values. If $|\lambda_i|$ is less or more than 1 the system is respectively stable or unstable near to the associated fixed point y_i. The interest is on the maximum of them, because it determines, starting around the fixed points, the trajectories divergence between any two close initial conditions of the dynamic system defined by (3.20). Fixing β and U_{SE}, the figure 3.2 represents this maximum as a function of τ_{rec} and different values of τ_{fac}. Similar to the results reported in [Pantic et al., 2002], the graph shows that there are two critical or bifurcation values of τ_{rec} , namely, τ^{*}_{rec} and τ^{**}_{rec}, where $|\lambda_i|_{max}$ crosses the value 1. For $\tau_{rec} < \tau^{*}_{rec}$, the system has three fixed points, two stable, $\pm m_{+} \neq 0.5$, which correspond with the memory solution or ferromagnetic, and one unstable, $m_{+} = 0.5$, which gives the no-memory solution or paramagnetic. For $\tau^{*}_{rec} < \tau_{rec} < \tau^{**}_{rec}$ stable oscillations occur (limit cycle attractor). Finally, when $\tau_{rec} > \tau^{**}_{rec}$ only the paramagnetic fixed point is stable. In sum, we see that the network dynamics, in addition to the fixed-point (ferromagnetic and paramagnetic) attractors, reveals the limit cycle attractor, which enables a periodic kind of behavior. In the next section we study the effects of facilitating mechanisms on this oscillatory phase.

3.3.3 Oscillatory Phase for $\alpha \neq 0$

We have explained above that an attractor neural network in presence of both facilitating and depressing dynamic synapses shows three different regions or phases, which are ferromagnetic, paramagnetic and oscillatory. In this section

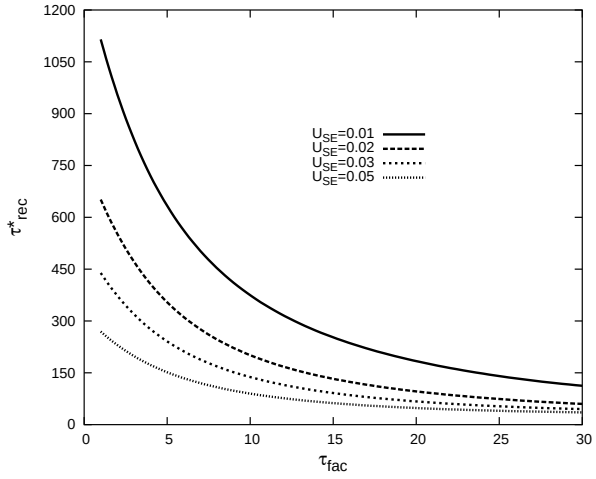

Figure 3.4: The mean-field critical value τ^*_{rec} versus different values of τ_{fac} and U_{SE}. The width of the ferromagnetic phase ($\tau_{rec} < \tau^*_{rec}$) is strongly reduced when facilitation is incorporated. Consequently, the oscillatory phase appears before when τ_{fac} is incremented. Here, we fix the inverse-noise parameter $\beta = 100.$.

we pay special attention to the last one. To obtain a qualitative description of these oscillations, we iterate the discrete map (3.20) and we represent in figure 3.3 the cycle limit solutions for m_+, x_+ and u_+. We compare the effects of considering only depressing synapses (right panel) with the case of incorporating both facilitating and depressing mechanisms (left panel). The middle graphs shows that facilitation gets a stronger depression [Tsodyks et al., 1998], because the amplitude of oscillations for x_+ appearing on the left grows considerably. The variable u_+ in the case of facilitation changes in time and for depression is constant and equal to 0. Mathematically, this can be understood simply taking the two limits of $u_\pm \to 0$ (or equivalently making $\tau_{fac} \to 0$) in the set of dynamical and steady equations (3.20) and (3.21).

The oscillatory behavior is found inside the region $\tau^*_{rec} < \tau_{rec} < \tau^{**}_{rec}$ (see figure 3.2 for details). The system here undergoes stable oscillations in the retrieval dynamics. Compared to static synapses ($\tau_{rec} \to 0$) for $\alpha = 0$, which lonely shows the ferromagnetic and paramagnetic solutions, the system now is able by itself, and without being necessary external stimulation, to describe continuous hopping among the different stored patterns. This feature is called *switching behavior*, and it has been studied recently in several models of attractor neural networks [Cortes et al., 2004, Pantic et al., 2002, Torres et al., 2004]. The essential feature in all of them, is that exists a source of noise able to unstabilize the system trapped in an attractor, driving the network to another different one. The same behavior was reported in [Pantic et al., 2002] with solely depressing synapses. However, facilitation incorporates complex and non-trivial modifications of both critical values τ^*_{rec} and τ^{**}_{rec}. The figure 3.4 represents, for fixed β, the mean-field critical value of τ^*_{rec} versus different values of τ_{fac} and U_{SE}. The critical value τ^*_{rec} decreases when τ_{fac} is incremented. This fact produces that the oscillatory behavior is anticipated, and, consequently, occurs a drastic reduction of the ferromagnetic phase. In addition, the width of the oscillatory phase, namely $\delta \equiv \tau^{**}_{rec} - \tau^*_{rec}$, is also diminished, as illustrated by figure 3.5.

After studying the effect of facilitating mechanisms on both the origin and

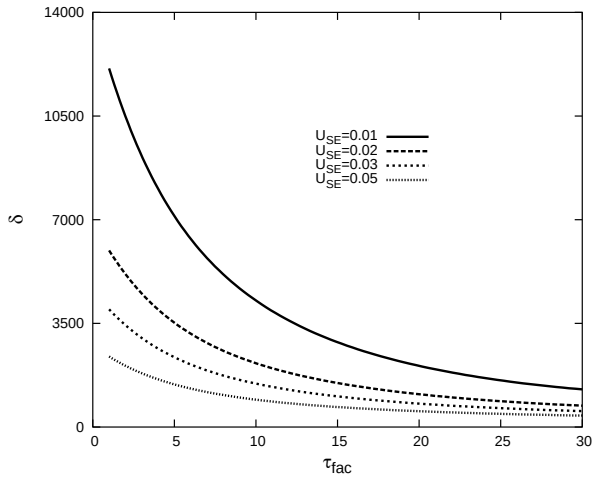

Figure 3.5: The width of the oscillatory phase, as defined in the text, is reduced when τ_{fac} is increased. Here, we take $\beta = 100$ and different values of U_{SE}.

width of the oscillatory region, is interesting to study the frequency of the oscillations for m_+ as a function of both U_{SE} and τ_{fac}. In order to get a suitable normalization in the choices of the parameters, and to ensure the occurrence of the oscillatory behavior, we choose for all different computer-simulations that $\tau_{rec} = \tau^*_{rec} + \epsilon$, being $\epsilon \ll 1$ and fixed to $\epsilon = \delta/20$, where δ is the width of the oscillatory region $(\tau^{**}_{rec} - \tau^*_{rec})$. Then, we compute the average-time between any two consecutive minimum and maximum of the oscillations for m_+, which is the half-period (T/2). The results are shown in figure 3.6. Although the width of the oscillatory region is minor when facilitation is incorporated (see figure 3.5), the frequency of the oscillations is higher, and consequently this can be enhance the network to response to highly changing stimulus.

3.4 Discussion

In this chapter we study the effect of a realistic model for dynamic synapses [Tsodyks et al., 1998] in the retrieval of information in an attractor neural net-

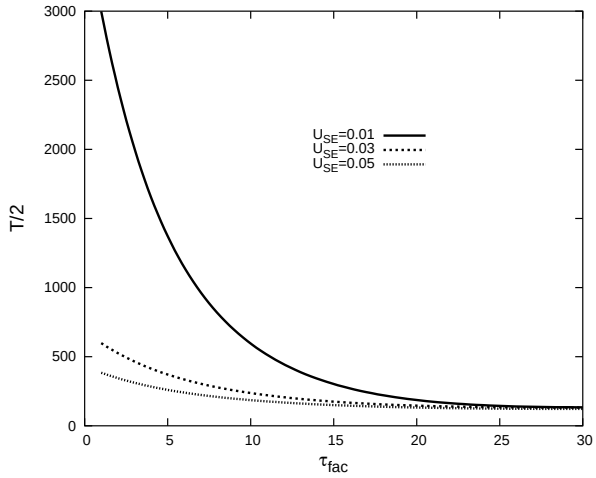

Figure 3.6: The average-time between any consecutive minimum and maximum of the oscillations for m_+ decreases when τ_{fac} increases for different values of U_{SE}. To compute this time, which is the half-period (T/2), we have taken that $\tau_{rec} = \tau^*_{rec} + \epsilon$, being $\epsilon = \delta/20$ and δ as illustrated by figure 3.5. Here, the average has been obtained by counting 1000 different peaks of the stationary time-serie for m_+. Statistical errors are negligible compared to the size of points, which confirms a highly periodic behavior.

works. The synapses intensity can either increases (facilitation) or decreases (depression) by rapid repeated presynaptic activation. We present and solve a general model able to recover previous results of solely depressing synapses [Pantic et al., 2002]. Although preliminary Monte Carlo simulations agree with the mean-field results here presented, a more detailed computational study will be published elsewhere [et. al., 2005]. The main feature is that facilitation gets a stronger depression, and consequently the storage capacity calculated with both facilitating and depressing mechanisms is lower than that computed with solely depressing synapses [Torres et al., 2002]. We have also showed as facilitation enhances easier switching between patterns. The reason is that facilitating mechanism influence strongly on the stability of steady states. The ferromagnetic fixed point or memory solution becomes unstable. The system coalesces in a cycle limit and undergoes stable oscillations. In such dynamics, time play a crucial role. This dimension can be used to encode or decode certain inputs, stimuli or patterns. However, we do not suggest that time is the only coding dimension in this process. Attractor neural networks, for instance with the standard Hebb rule [Hertz et al., 1991], can store and retrieve spatial information. These arguments can suggest that an attractor neural network with dynamic synapses [Tsodyks et al., 1998] can explain and interpretar identification and categorization of spatio-temporal patterns which can be relevant, for instance, to the understanding of early olfactory processing [Laurent et al., 2001]. Different odors can be coded in different attractors and the system can visit continuosly all of them by itself. We have observed that the system always switches describing well-defined periodic trajectories and never with a more complex dynamics, as for example chaotic. This could be negative, nevertheless, to get other technical and industrial applications, as for instance cryptography of signals by using chaos [Klimov et al., 2002].

Bibliography

L. F. Abbott and W. G. Regehr. Synaptic computation. *Nature*, 431:796–803, 2004. 46

D. J. Amit. *Modeling brain function: the world of attractor neural network*. Cambridge University Press, 1989. 45

D. J. Amit, H. Gutfreund, and H. Sompolinsky. Statistical mechanics of neural networks near saturation. *Ann. Phys.*, 173:30–67, 1987. 45, 52

R. Bertram, A. Sherman, and E. F. Stanley. Single-domain/bound calcium hypothesis of transmitter release and facilitation. *J. Neurophysiol.*, 75:1919–1931, 1996. 48

D. Bibitchkov, J.M. Herrmann, and T. Geisel. Pattern storage and processing in attractor networks with short-time synaptic dynamics. *Network: Comput. Neural Syst.*, 13:115–129, 2002. 46

J.M. Cortes, P.L. Garrido, J. Marro, and J.J. Torres. Switching between memories in neural automata with synaptic noise. *Neurocomputing*, 58-60:67–71, 2004. 60

J. J. Torres et. al. Computational abilities of facilitating mechanisms in attractor neural networks. To be published, 2005. 63

T. Geszti. *Physical Models of Neural Networks*. World Scientific, 1990. 45

J. Hertz, A. Krogh, and R.G. Palmer. *Introduction to the theory of neural computation*. Addison-Wesley, 1991. 45, 51, 52, 54, 63

J.J. Hopfield. Neural networks and physical systems with emergent collective computational abilities. *Proc. Natl. Acad. Sci. USA*, 79:2554–2558, 1982. 45, 54

A. Klimov, A. Mityagin, and A. Shamir. Analysis of neural cryptography. In *Lecture Notes in Computer Science*, volume 2501, pages 288–298. Springer-Verlag, 2002. 63

G. Laurent, M. Stopfer, R.W. Friedrich, M.I. Rabinovich, A. Volkovskii, and H.D.I. Abarbanel. Odor encoding as an active, dynamical process: Experiments, computation and theory. *Annual Review of Neuroscience*, 24:263–297, 2001. 46, 63

L. Pantic, J.J. Torres, H.J. Kappen, and S.C.A.M. Gielen. Associative memmory with dynamic synapses. *Neural Comp.*, 14:2903–2923, 2002. xxi, 46, 55, 58, 60, 63

J.J. Torres, J. Marro, P.L. Garrido, J.M. Cortes, F. Ramos, and M.A. Munoz. Effects of static and dynamic disorder on the performance of neural automata. *Biophysical Chemistry. In press*, 2004. 60

J.J. Torres, L. Pantic, and H.J. Kappen. Storage capacity of attractor neural networks with depressing synapses. *Phys. Rev. E.*, 66:061910, 2002. xx, 46, 50, 51, 52, 53, 54, 63

M. V. Tsodyks, K. Pawelzik, and H. Markram. Neural networks with dynamic synapses. *Neural Comp.*, 10:821–835, 1998. 46, 47, 48, 54, 60, 61, 63

Chapter 4

Fast Presynaptic Noise on Attractor Neural Networks

4.1 Introduction

There is multiple converging evidence [Abbott and Regehr, 2004] that synapses play an active role in determining the complex processing of information in the brain. An important aspect of such assertion is well illustrated by attractor neural networks. These show that synapses can efficiently store patterns that are afterwards retrieved with only partial information on them. However, in addition to this long–time effect there is some intriguing "synaptic noise". This refers to short–time fluctuations that seem to compete with other mechanisms during the transmission of information, not to cause unreliability but to ultimately determine a variety of computations [Allen and Stevens, 1994, Zador, 1998]. In spite of some recent efforts (see below and Ref.[Abbott and Regehr, 2004], for instance), a full understanding of how the brain complex processes are influenced by such fast synaptic variations is lacking. A specific matter under discussion concerns the changes induced by short–time noise on the attractor fixed points and other details of the retrieval processes [Bibitchkov

et al., 2002].

The observation that real synapses endure short–time *depression* and/or *facilitation* is likely to be relevant in this context. That is, one may understand some recent observations by assuming that the postsynaptic response may either decrease (*depression*) or increase (*facilitation*) depending on presynaptic neural activity [Thomson et al., 2002, Tsodyks et al., 1998]. It is sensible to expect that these effects, which occur on a short–time scale, are at the basis of a more efficient cooperation between neurons.

Motivated by the neurobiological findings, we report in this chapter on some interesting effects of synaptic noise on the functionality of a neural circuit. We study in detail a network in which the neural activity evolves at random in time regulated by a "temperature" parameter. In addition, the values assigned to the synaptic intensities by a *learning* (e.g., Hebb's) rule are constantly perturbed with *microscopic* fast noise. A new parameter is involved by this perturbation that allows for a continuum transition from depression to facilitation. The simplest versions of the model happen to admit an *effective Hamiltonian description* [Marro and Dickman, 1999]. This leads to some (limited) analytical results. We complement these with an approximate analysis including a series of related computer simulations for some of the more involved cases.

The resulting picture is very interesting; fast synaptic noise during external stimulation may induce the system to scape from the attractor, namely, the stability of fixed point solutions is modified. This mechanism seems most relevant to some computational tasks, as it provides a mean for categorization and class identification. Similar instabilities have been observed in monkeys [Abeles et al., 1995], and they are believed to be a main feature of odor encoding [Laurent et al., 2001].

4.2 Definition of Model

Our interest is in a neural network in which a local stochastic dynamics is constantly influenced by synaptic *noise*. Consider a set of N binary neurons with

configurations $\mathbf{S} \equiv \{s_i = \pm 1; i = 1, \ldots, N\}$. Any two neurons are connected by synapses of intensity

$$w_{ij} = \overline{w}_{ij} x_j \quad \forall i, j. \tag{4.1}$$

Here, $\overline{w}_{ij}$ is fixed, namely, determined in a previous *learning* process, and x_j is a stochastic variable. Once $\mathbf{W} \equiv \{\overline{w}_{ij}\}$ is given, the state of the system at time t is defined by setting $\mathbf{S}$ and $\mathbf{X} \equiv \{x_i\}$. This evolves with time — after the learning process — via the familiar Master Equation, namely,

$$\begin{aligned} \frac{\partial P_t(\mathbf{S}, \mathbf{X})}{\partial t} &= -P_t(\mathbf{S}, \mathbf{X}) \int_{\mathbf{X}'} \sum_{\mathbf{S}'} c[(\mathbf{S}, \mathbf{X}) \to (\mathbf{S}', \mathbf{X}')] \\ &\quad + \int_{\mathbf{X}'} \sum_{\mathbf{S}'} c[(\mathbf{S}', \mathbf{X}') \to (\mathbf{S}, \mathbf{X})] P_t(\mathbf{S}', \mathbf{X}'). \end{aligned} \tag{4.2}$$

We further assume that the *transition rate* or probability per unit time of evolving from $(\mathbf{S}, \mathbf{X})$ to $(\mathbf{S}', \mathbf{X}')$ is

$$c[(\mathbf{S}, \mathbf{X}) \to (\mathbf{S}', \mathbf{X}')] = p\, c^{\mathbf{X}}[\mathbf{S} \to \mathbf{S}'] \delta(\mathbf{X} - \mathbf{X}') + (1 - p)\, c^{\mathbf{S}}[\mathbf{X} \to \mathbf{X}'] \delta_{\mathbf{S},\mathbf{S}'}. \tag{4.3}$$

This choice [Garrido and Marro, 1994, Torres et al., 1997] amounts to consider competing mechanisms. That is, neurons $(\mathbf{S})$ evolve stochastically in time under a noisy dynamics of synapses $(\mathbf{X})$, the latter having an *a priori* relative weight of $(1 - p)/p$. Depending on the value of p, three main classes may be defined [Marro and Dickman, 1999]:

1. For $p \in (0, 1)$ both the synaptic fluctuation and the neuron activity occur on the same temporal scale. This case, which is a candidate for the most involved behavior, has already been preliminary explored in Ref. [Cortes et al., 2004].

2. The limiting case $p \to 1$ corresponds to neurons evolving in the presence of a quenched synaptic configuration, i.e., x_i is constant and independent of i. The *Hopfield model* [Hopfield, 1982] belongs to this class in the simple case that $x_i = 1, \forall i$ and $\mathbf{W}$ is determined by the Hebbian prescription [Hebb, 1949].

3. The limiting case $p \to 0$, which corresponds to an adiabatic elimination of fast variables [Gardiner, 2004], also decouples the two dynamics [Garrido and Marro, 1994]. Consequently, some exact analytical treatment — though not the complete solution — is then feasible. The rest of this chapter is devoted to this class of systems which, in spite of being in principle simpler than case 1, happens to depict intriguing behavior.

For $p \to 0$, the neurons evolve as in the presence of a steady distribution for $\mathbf{X}$, and one may assume $P(\mathbf{S},\mathbf{X}) = P(\mathbf{X}|\mathbf{S})\,P(\mathbf{S})$, where $P(\mathbf{X}|\mathbf{S})$ stands for the conditional probability of $\mathbf{X}$ given $\mathbf{S}$. It then follows from (4.2) and (4.3), after rescaling time $tp \to t$, that

$$\frac{\partial P_t(\mathbf{S})}{\partial t} = -P_t(\mathbf{S}) \sum_{\mathbf{S}'} \bar{c}[\mathbf{S} \to \mathbf{S}'] + \sum_{\mathbf{S}'} \bar{c}[\mathbf{S}' \to \mathbf{S}] P_t(\mathbf{S}'). \tag{4.4}$$

Here,

$$\bar{c}[\mathbf{S} \to \mathbf{S}'] \equiv \int d\mathbf{X}\, P^{st}(\mathbf{X}|\mathbf{S})\, c^{\mathbf{X}}[\mathbf{S} \to \mathbf{S}'], \tag{4.5}$$

and $P^{st}(\mathbf{X}|\mathbf{S})$ is the stationary solution that satisfies

$$P^{st}(\mathbf{X}|\mathbf{S}) = \frac{\int d\,\mathbf{X}'\, c^{\mathbf{S}}[\mathbf{X}' \to \mathbf{X}]\, P^{st}(\mathbf{X}'|\mathbf{S})}{\int d\mathbf{X}'\, c^{\mathbf{S}}[\mathbf{X} \to \mathbf{X}']}. \tag{4.6}$$

Notice that (4.5) is an *effective* rate or superposition that one may interpret to come from the competition between different elementary mechanisms. That is, according to (4.3), there are different underlying dynamics of rate $c^{\mathbf{X}}[\mathbf{S} \to \mathbf{S}']$, each associated to a different realization of the stochasticity $\mathbf{X}$. In the limit $p \to 0$, the effective rate $\bar{c}[\mathbf{S} \to \mathbf{S}']$ results from combining $c^{\mathbf{X}}[\mathbf{S} \to \mathbf{S}']$ with probability $P^{st}(\mathbf{X}|\mathbf{S})$. Each of the elementary dynamics tends to drive the system to a well-defined equilibrium state. However, the competition will impede equilibrium and, in general, the system will asymptotically go towards a non-equilibrium steady state [Marro and Dickman, 1999]. This is known to be a more general condition in nature than the state of thermodynamic equilibrium. The question is if such a competition between synaptic noise and neural activity may be also at the origin of some of the computational strategies in

biological systems. Our study below seems to indicate that this is the case indeed.

For the sake of simplicity, we shall be concerned in this chapter with sequential updating by means of "spin–flip"dynamics. That is, the elementary dynamic step will simply consist of local inversions $s_i \to -s_i$ induced by a bath at temperature T. The elementary rate $c^{\mathbf{X}}[\mathbf{S} \to \mathbf{S}']$ then reduces to a single site rate that one may write as $\Psi[u^{\mathbf{X}}(\mathbf{S}, i)]$. Here, $u^{\mathbf{X}}(\mathbf{S}, i) \equiv 2\beta s_i h_i^{\mathbf{X}}(\mathbf{S})$, where $\beta = 1/T$ and $h_i^{\mathbf{X}}(\mathbf{S}) = \sum_{j \neq i} \overline{w}_{ij} x_j s_j$ is the net synaptic current arriving to the (postsynaptic) neuron i. The function $\Psi(u)$ is arbitrary except that, in order to have a well–defined reference, we shall assume that it satisfies *detailed balance*, namely, $\Psi(u) = \exp(-u)\Psi(-u)$, and $\Psi(0) = 1$ and $\Psi(\infty) = 0$.

4.3 Some Analytical Results

The essential non-equilibrium nature of our model in general prevents one from studying it by the powerful Gibbs ensemble theory. That is, the system is not defined by a unique Hamiltonian but via the stochastic equation (4.4). A Hamiltonian description is hindered because the superposition (4.5), unlike its elements $\Psi(u^{\mathbf{X}})$, does not satisfy detailed balance. Furthermore, in general the synaptic weights w_{ij} in (4.1) are not symmetric. Nevertheless, for $p \to 0$ and some choices of Ψ, an "effective Hamiltonian" may be obtained from the time evolution equation which helps one in extending to the present case some of the tools of (equilibrium) statistical mechanics [Garrido and Marro, 1989, Marro and Dickman, 1999]. Before attempting a more general, numerical treatment below we summarize here some analytical results obtained by this technique.

The following theorem holds. Let a well–behaved description (4.4)–(4.6) under the conditions stated, namely, sequential updating and detailed balance of Ψ. The stationary state for $p \to 0$ may then be described in terms of an *effective Hamiltonian*, $H^{\text{eff}}(S)$, if one assumes that both $\mathbf{c}^{\mathbf{X}}[\mathbf{S} \to \mathbf{S}']$ and $P^{\text{st}}(\mathbf{X}|\mathbf{S})$

appropriately factorize. That is, for

$$\mathbf{P}^{st}\left(\mathbf{X}|\mathbf{S}\right) = \prod_{j} P\left(x_j|s_j\right), \tag{4.7}$$

(4.5) then reduces to

$$\bar{c}[\mathbf{S} \to \mathbf{S}^i] = \prod_{j\neq i} \int dx_j \, P(x_j|s_j) \, \Psi(2\beta s_i \overline{w}_{ij} x_j s_j), \tag{4.8}$$

where $\mathbf{S}^i$ stands for $\mathbf{S}$ after flipping at i, $s_i \to -s_i$. Then, assuming that $H^{eff}(\mathbf{S})$ exists that satisfies detailed balance, namely, that

$$\frac{\bar{c}[\mathbf{S} \to \mathbf{S}^i]}{\bar{c}[\mathbf{S}^i \to \mathbf{S}]} = \exp\left\{-\beta\left[H^{eff}(\mathbf{S}^i) - H^{eff}(\mathbf{S})\right]\right\}, \tag{4.9}$$

it ensues after some algebra that

$$H^{eff}(\mathbf{S}) = -\frac{1}{2}\sum_{i} h_i^{eff}(\mathbf{S}) s_i. \tag{4.10}$$

The effective local fields here are

$$h_i^{eff} = -\beta^{-1}\sum_{j\neq i}\left[\alpha_{ij}^{(+)} s_j + \alpha_{ij}^{(-)}\right], \tag{4.11}$$

where

$$\alpha_{ij}^{(\pm)} \equiv \frac{1}{4}\ln\frac{\bar{c}(2\beta\,\overline{w}_{ij};+)\,\bar{c}(\pm 2\beta\,\overline{w}_{ij};-)}{\bar{c}(-2\beta\,\overline{w}_{ij};\mp)\,\bar{c}(\mp 2\beta\,\overline{w}_{ij};\pm)} \tag{4.12}$$

and

$$\bar{c}(2\beta\,\overline{w}_{ij};s_j) = \int dx_j \, P(x_j|s_j)\,\Psi(2\beta\,\overline{w}_{ij}x_j). \tag{4.13}$$

The above generalizes a previous result [Garrido and Munoz, 1993, Lacomba and Marro, 1994, Marro and Dickman, 1999] to the case of **S**–dependent disorder. For the fast, **S**–independent fluctuations that were considered in the previous literature, one has $\bar{c}(\pm x;+) = \bar{c}(\pm x;-)$, so that $\alpha_{ij}^{(-)} = 0\ \forall i,j$. Instead of, our case amounts to consider a non-zero threshold, $\theta_i \equiv \sum_{j\neq i}\alpha_{ij}^{(-)} \neq 0$.

Some familiar choices for the rate function $\Psi(u)$ that satisfy detailed balance are: the one corresponding to the Metropolis algorithm, i.e., $\Psi(u) = \min[1,\exp(-u)]$; the Glauber case $\Psi(u) = [1+\exp(u)]^{-1}$; and $\Psi(u) = \exp(-u/2)$ [Marro and Dickman, 1999]. Only the latter fulfills $\Psi(u+v) = \Psi(u)\Psi(v)$ which

is required in order to have (4.8). The effective transition rate in this case is simply

$$\bar{c}[\mathbf{S} \to \mathbf{S}^i] = \exp(-\beta s_i h_i^{\text{eff}}). \tag{4.14}$$

One may then derive from (4.4) an equation for the time evolution of the *overlaps*, defined as

$$m^\nu(\mathbf{S}) \equiv \frac{1}{N} \sum_i s_i \xi_i^\nu. \tag{4.15}$$

The result, after using standard techniques [Hertz et al., 1991, Marro and Dickman, 1999], is

$$\partial_t \langle\langle m^\nu \rangle\rangle = 2\langle\langle N^{-1} \sum_i \xi_i^\nu \sinh(\beta h_i^{\text{eff}})\rangle\rangle - 2\langle\langle N^{-1} \sum_i \xi_i^\nu s_i \cosh(\beta h_i^{\text{eff}})\rangle\rangle. \tag{4.16}$$

Here, $\xi^\nu = \{\xi_i = \pm 1, i = 1, \ldots, N\}$ are M random patterns previously stored in the system, $\nu = 1, \ldots, M$, and $\langle\langle F \rangle\rangle$ stands for a double average, namely, over pattern realizations and over the thermal noise.

4.4 Types of Synaptic Noise

The above, e.g., equations (4.11) and (4.12), anticipates an important dependence of emergent properties on the details of the synaptic "noise", i.e., $\mathbf{X}$. Our formalism allows for a simple consideration of different hypothesis concerning the stationary distribution (4.6). A simple specific choice which leads without further assumptions to an explicit effective Hamiltonian is

$$P(x_j|s_j) = \frac{1 + s_j F_j}{2} \delta(x_j + \Phi) + \frac{1 - s_j F_j}{2} \delta(x_j - 1), \tag{4.17}$$

where F_j depends on the properties of the presynaptic neuron j. When this is firing, $s_j = 1$, and one considers the simplest case $F_j = 1 \ \forall j$, the noise modifies $\overline{w}_{ij}$ by a factor $-\Phi$, while the learned synaptic intensity remains unchanged if the neuron is silent. In general, $w_{ij} = -\overline{w}_{ij}\Phi$ with probability $\frac{1}{2}(1 + s_j F_j)$. The resulting local fields are

$$h_i^{\text{eff}} = \frac{1}{2} \sum_{j \neq i} [(1 - \Phi) s_j - (1 + \Phi) F_j] \overline{w}_{ij}. \tag{4.18}$$

This shows that, as compared to the Hopfield case, there is now a non-trivial rescaling of temperature, as well as a threshold $\theta_i \equiv \sum_j \overline{w}_{ij} F_j$ [Hertz et al., 1991]. That is, the effect of fast noise does not seem to be a dramatic one for distribution (4.7) with (4.17).

This choice may be interpreted as a way to model the observed short-term synaptic depression and facilitation [Pantic et al., 2002, Tsodyks et al., 1998]. That is, as indicated above, one is interested in a situation in which increasing the mean firing rate modifies the postsynaptic response resulting in either decreasing or increasing the synaptic weight. A more intriguing behavior consistent with this situation ensues by assuming instead the factorization

$$P^{st}(\mathbf{X}|\mathbf{S}) = \prod_j P(x_j|\mathbf{S}) \tag{4.19}$$

with

$$P(x_j|\mathbf{S}) = \zeta(\vec{\mathbf{m}})\ \delta(x_j + \Phi) + [1 - \zeta(\vec{\mathbf{m}})]\ \delta(x_j - 1). \tag{4.20}$$

Here, $\vec{\mathbf{m}} = \vec{\mathbf{m}}(\mathbf{S}) \equiv \left(m^1(\mathbf{S}), \ldots, m^M(\mathbf{S})\right)$ is the M-dimensional overlap vector, and $\zeta(\vec{\mathbf{m}})$ stands for a function of $\vec{\mathbf{m}}$ to be determined. That is, the magnitude of the depression/facilitation effect depends on the overlap vector, which in turn depends on the net current arriving to postsynaptic neurons. As a consequence of the latter dependence, the non-local choice (4.20) introduces some non-trivial correlations between synaptic noise and neural activity as compared to (4.17).

This system also reduces to the Hopfield case but only in the limit $\Phi \to -1$ for any $\zeta(\vec{\mathbf{m}})$. Otherwise, it results in a rather complex behavior. In particular, the noise lacks the factorization property which is required by our theorem in the previous section. That is, in general, one does not expect an effective Hamiltonian, e.g., condition of symmetric interactions is not fulfilled. Nevertheless, we may still write

$$\frac{\bar{c}[\mathbf{S} \to \mathbf{S}^i]}{\bar{c}[\mathbf{S}^i \to \mathbf{S}]} = \prod_{j \neq i} \frac{\int dx_j\, P(x_j|\mathbf{S})\, \Psi(2\beta\, s_i \overline{w}_{ij} x_j s_j)}{\int dx_j\, P(x_j|\mathbf{S}^i)\, \Psi(-2\beta\, s_i \overline{w}_{ij} x_j s_j)}. \tag{4.21}$$

Using (4.20) and (4.9), this may be linearized around the solution $\overline{w}_{ij} = 0$. One may expect this to be a good approximation for the Hebbian prescription

$\overline{w}_{ij} = N^{-1} \sum_\nu \xi_i^\nu \xi_j^\nu$ as far as this only stores completely uncorrelated, random patterns. In fact, fluctuations in this case are of order $\sqrt{M}/N$ for finite M — of order $1/\sqrt{N}$ for $M \to \infty$ — which tends to vanish for a sufficiently large system, e.g., in the macroscopic (thermodynamic) limit $N \to \infty$. It then follows the effective weights:

$$w_{ij}^{\text{eff}} = \left\{ 1 - \frac{1+\Phi}{2} \left[\zeta(\vec{\mathbf{m}}) + \zeta\left(\vec{\mathbf{m}}^{\mathbf{i}}\right) \right] \right\} \overline{w}_{ij}, \tag{4.22}$$

where $\vec{\mathbf{m}} = \vec{\mathbf{m}}(\mathbf{S})$, $\vec{\mathbf{m}}^{\mathbf{i}} \equiv \vec{\mathbf{m}}(\mathbf{S}^{\mathbf{i}}) = \vec{\mathbf{m}} - 2s_i\vec{\xi}_i/N$, and $\vec{\xi}_i = \left(\xi_i^1, \xi_i^2, ..., \xi_i^M\right)$ is the binary M–dimensional stored pattern. This clearly shows the modification of the intensities which is induced by the noise. The resulting effective local fields are

$$h_i^{\text{eff}} = \sum_{j \neq i} w_{ij}^{\text{eff}} s_j. \tag{4.23}$$

Similar to the case of Hopfield model with asymmetric synapses [Hertz et al., 1991], one may then proceed with the general equations (4.14)–(4.16) after substituting (4.23), even though this is not a true, exact effective Hamiltonian.

This only results in an effective Hamiltonian description when (4.22) has a proper symmetry. This occurs when $\vec{\mathbf{m}}^{\mathbf{i}} = \vec{\mathbf{m}} - 2s_i\vec{\xi}_i/N \simeq \vec{\mathbf{m}}$, which is a good approximation in the thermodynamic limit ($N \to \infty$). The same may be achieved by using a convenient choice for $\zeta(\vec{\mathbf{m}})$. In order to model activity–dependent mechanisms acting on the synapses, $\zeta(\vec{\mathbf{m}})$ should be an increasing function of the total presynaptic current. Furthermore, it should preserve the ± 1 symmetry. A simple, properly normalized choice is

$$\zeta(\vec{\mathbf{m}}) = \frac{1}{1+\alpha} \sum_\nu \left[m^\nu(\mathbf{S}) \right]^2, \tag{4.24}$$

where $\alpha = M/N$. The behavior that ensues from (4.22)–(4.24), which we describe below, correspond to an accurate mean–field description for the case (4.20).

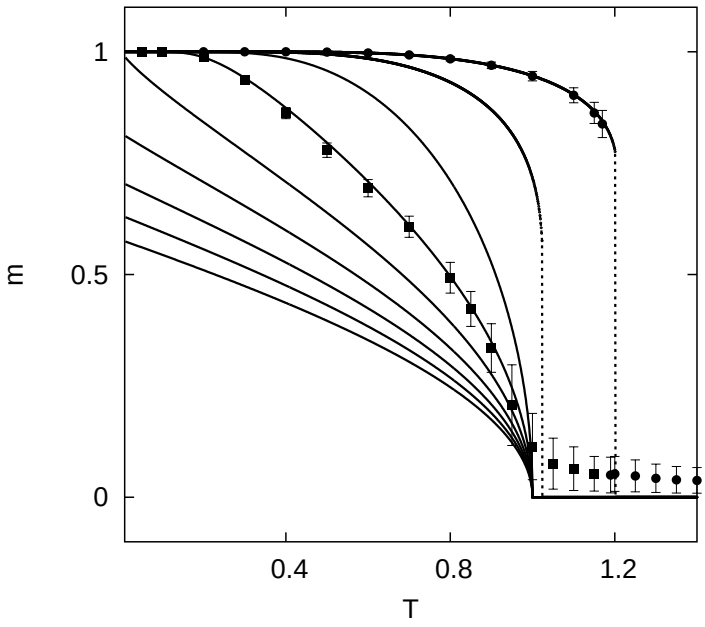

Figure 4.1: The steady overlap $m^*(T)$, as predicted by equation (4.25), for different values of the noise parameter, namely, $\Phi = -2.0, -1.5, -1.0, -0.5, 0.0, 0.5, 1.0, 1.5, 2.0$, respectively, from top to bottom. $\Phi = -1$ corresponds to the Hopfield case, as is explained in the main text. The graphs depict second order phase transitions (solid curves) and, for the most negative values of Φ, first order phase transitions (the discontinuities indicated by dashed lines). The symbols stand for Monte Carlo data corresponding to a network with $N = 1600$ neurons for $\Phi = -0.5$ (filled squares) and -2.0 (filled circles).

4.5 Noise Inducing Phase Transitions

We shall in the following of this chapter be concerned with the consequences of the local fields (4.23) in the retrieval process of the attractor neural network. Let us first consider the case in which the system has just stored a single pattern, $M = 1$. One obtains from (4.14)–(4.16), and taking the mean field assumption $\langle s_i \rangle \approx s_i$, that the steady solution corresponds to the overlap:

$$m^* = \tanh\{\beta m^*[1 - (m^*)^2(1 + \Phi)]\}, \tag{4.25}$$

which preserves the symmetry $\pm m^*$. Figure 4.1 illustrates this behavior for several values of Φ. This figure shows a transition from a *ferromagnetic–like* phase, i.e., solutions $m^* \neq 0$, to a *paramagnetic–like* phase, $m^* = 0$. The transition is continuous or second order only for $\Phi > \Phi_c = -4/3$, and $T_c = 1$. This behavior can be understood by studying the local stability (4.25). That is, it ensues that stable solutions must satisfy

$$|m^*| > m_c^*(T) = \frac{1}{\sqrt{3}} \left(\frac{T_c - T}{\Phi - \Phi_c} \right)^{\frac{1}{2}}. \tag{4.26}$$

Figure 4.2 illustrates the critical temperature as a function of Φ. This shows the tricritical point at (T_c, Φ_c).

It may be remarked that a discontinuous phase transition allows for a much better performance of the retrieval process that a continuous one. This is because the behavior is sharp just below the transition temperature in the former case. Consequently, the above indicates that our model performs better for large facilitation, $\Phi < -4/3$.

We also performed Monte Carlo simulations. These concern a network of $N = 1600$ neurons acted on by the local fields (4.23) and evolving by sequential updating with the effective rate (4.14). Except for some finite–size effects, figure 4.1 shows a good agreement, which confirms that both our simulations and the equations correspond to a mean–field description.

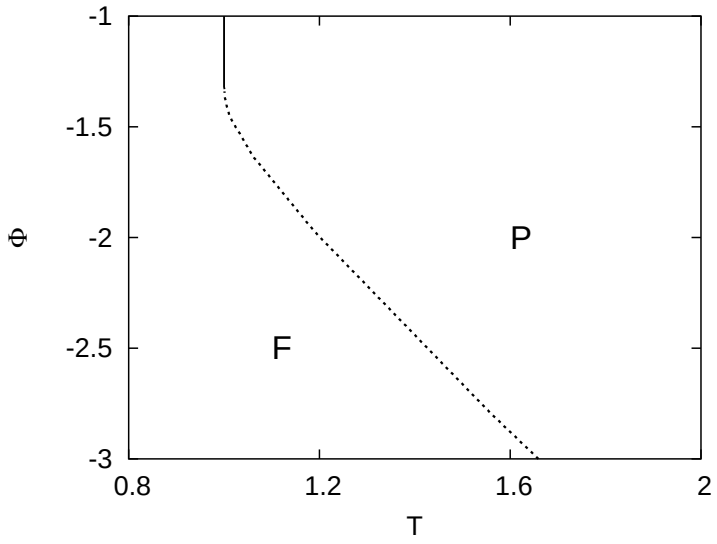

Figure 4.2: Phase diagram depicting T_c as a function of T and Φ. The solid (dashed) curve corresponds to a second (first) order phase transition. The tricritical point is at $(T_c, \Phi_c) = (1, -4/3)$. Here, F and P stand for the *ferromagnetic–like* and *paramagnetic–like* phases, respectively. The best retrieval properties of the model system occur close to the left-lower corner.

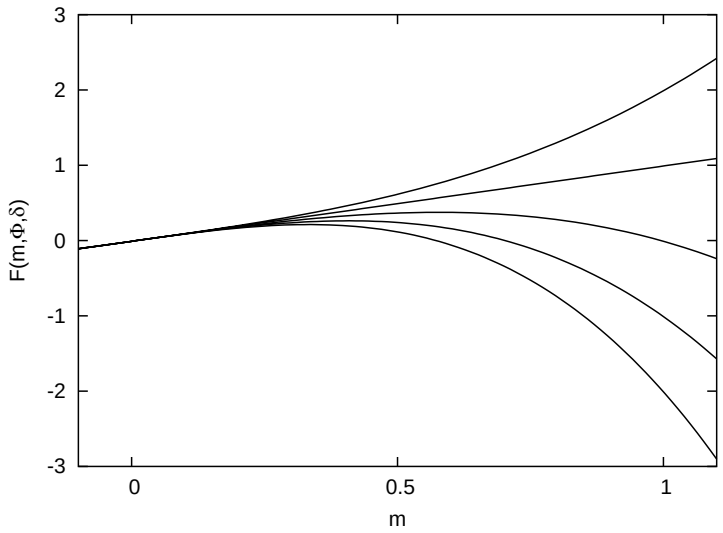

Figure 4.3: The function F as defined in (4.28) for $\delta = 0.01$ and, from top to bottom, $\Phi = -2, -1, 0, 1, 2$. The solution of (4.27) becomes unstable so that the activity will escape the attractor ($m = 1$) for $F < 0$, which occurs for $\Phi > 0$ in this case.

4.6 Sensitivity to External Inputs

As we have seen above, the noise (4.20) is susceptible to model activity-dependent processes reminiscent of short-term synaptic depression. In this section we study the effect of fast noise on the retrieval dynamics under external stimulation. The aim is to check the degree of sensitivity of the network to external inputs. A high value is advantageous in the sense that it facilitates the response of the network to changing stimuli. This could explain, for instance, the observed fast response of animals to continously varying stimuli which are received from their environment.

Consider first the case of one stored pattern ,$M = 1$. A simple external input may be simulated by by adding to each local field a driving term $-\delta\xi_i$, $\forall i$, with $0 < \delta \ll 1$ [Bibitchkov et al., 2002]. A negative drive in this case of a single pattern assures that the network activity may go from the attractor, ξ, to

the antipattern $-\xi$. It then follows the stationary overlap:

$$m^* = \tanh[\beta F(m^*, \Phi, \delta)], \tag{4.27}$$

with

$$F(m^*, \Phi, \delta) \equiv m^*[1 - (m^*)^2(1 + \Phi) - \delta]. \tag{4.28}$$

Figure 4.3 shows this function for (very) small δ and varying Φ. This illustrates two different types of behavior, namely, (local) stability ($F > 0$) and instability ($F < 0$) of the attractor, which corresponds to $m = 1$. That is, the noise induces instability, resulting in this case of switching between the pattern and the antipattern. This is confirmed in figure 4.4 by Monte Carlo simulations. The simulations correspond to a network of $N = 3600$ neurons with one stored pattern, $M = 1$. This evolves from different initial states, corresponding to different distances to the attractor, under an external stimulus $-\delta\xi^1$ for different values of δ. The two left graphs in figure 4.4 show several independent time evolutions for the model with fast noise, namely $\Phi = 1$; the two graphs to the right are for the Hopfield case lacking the noise ($\Phi = -1$). These, and similar graphs one may obtain for other parameters values, clearly demonstrate how the network sensitivity to a simple external stimulus is qualitatively by adding preynaptic noise to the system. Figures (4.5) and (4.6) illustrate a similar behavior in Monte Carlo simulations with several stored patterns. Figure (4.5) is for $M = 3$ correlated patterns, namely, their mutual overlaps are $m^{\nu,\mu} \equiv 1/N \sum_i \xi_i^\nu \xi_i^\mu = 1/3$ for any two of them. The system in this case begins with the first pattern as initial condition and, to avoid dependence on this choice, it is let to relax for 3×10^4 Monte Carlo steps (MCS). It is then perturbed by a drive $-\delta \mathbf{x}\mathbf{i}^\nu$, where the stimulus ν changes ($\nu = 1, 2, 3, 1, \ldots$) every 6×10^3 MCS. The top graph shows the network response in the Hopfield case. There is no visible structure of this signal in the absence of fast noise as far as $\delta \ll 1$. As a matter of fact, in the Hopfield model the depth of the basins of attraction are large enough to prevent any switching phenomena for small δ, except when approaching a critical point ($T_c = 1$), where (thermal) fluctuations diverge. The bottom graph depicts a qualitatively different situation for $\Phi = 1$. That is,

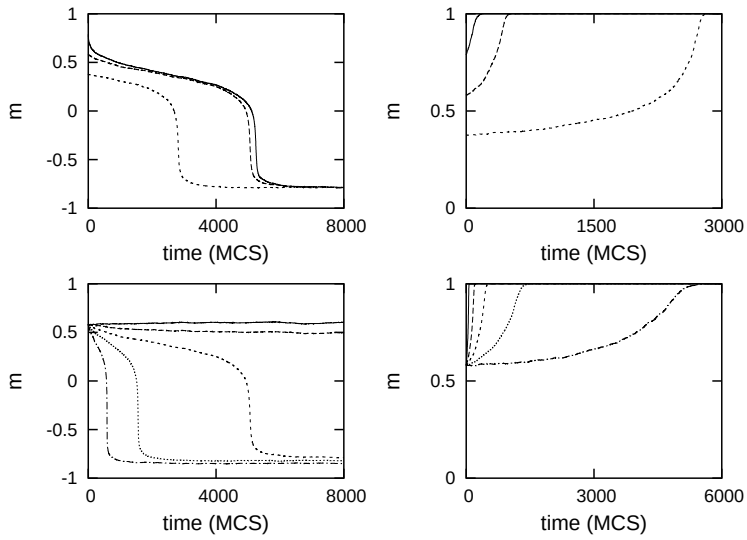

Figure 4.4: Time evolution of the overlap, as defined in (4.15), between the current state and the unique stored pattern ($M = 1$) in Monte Carlo simulations $N = 3600$ and $T = 0.1$. Each graph, for a given set of values for (δ, Φ), shows different curves corresponding to evolutions starting with different initial states. The two top graphs are for $\delta = 0.3$ and $\Phi = 1$ (left) and $\Phi = -1(\mathtt{right})$, the latter corresponding to the Hopfield case lacking the fast noise. This shows the important effect noise has on the network sensitivity to external stimuli. The two bottom graphs illustrate the same for a fixed initial distance from the attractor as one varies the external stimulation, namely, $\delta = 0.1, 0.2, 0.3, 0.4$, and 0.5 from top to bottom.

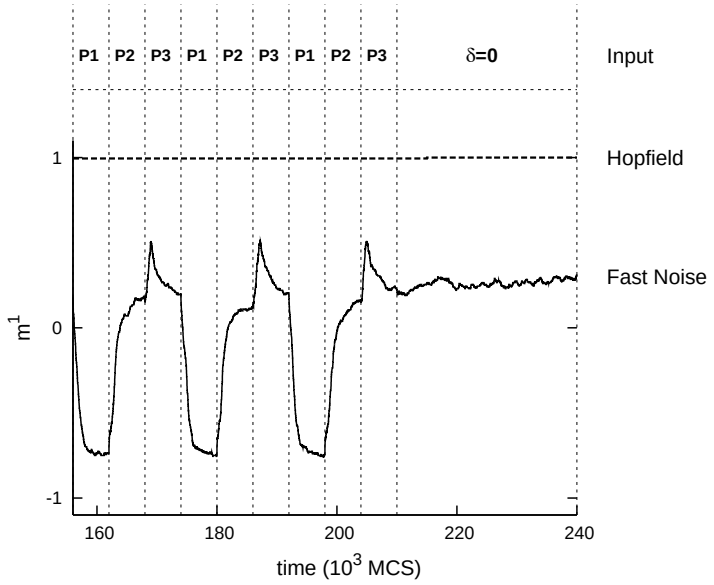

Figure 4.5: Time evolution during a Monte Carlo simulation with $N = 400$ neurons, $M = 3$ correlated patterns, and $T = 0.1$. The system in this case was allowed to relax to the steady state, and then perturbed by the stimulus $-\delta\xi_i^\nu$, $\delta = 0.3$, with $\nu = 1$ for a short time interval, and then $\nu = 2$, and so on. After suppresing the stimulus, the system is again allowed to relax. The graphs show, as a function of time, from top to bottom, (i) the number of the pattern which is used as the stimulus at each time interval; (ii) the resulting response of the network, measured as the overlap of the current state with pattern $\nu = 1$, in the absence of noise, i.e. the Hopfield case $\Phi = -1$; (iii) the same situation for the relevant case of noise $\Phi = 1$.

adding fast noise in general destabilizes the fixed point for the interesting case of small δ far from criticality.

Figure (4.6) shows the response of the network in a similar simulation with 400 neurons at $T = 0.1$ for $M = 3$ random, i.e. (totally) uncorrelated patterns. The initial condition is again $\nu = 1$, and the stimulus is here $\delta\mathbf{xi}^{\nu}$ with ν changed every 1.5×10^5 MCS.

4.7 Discussion

The set of equations (4.4),(4.5) and (4.6) provides a general framework to model activity-dependent processes. Motivated by the behavior of neurobiological systems, we adapted this to study the consequences of fast noise acting on the synapses of an attractor neural network with a finite number of stored patterns. In this chapter we present two different scenarios corresponding to noise distributions fulfilling (4.7) and (4.19), respectively. In particular, assuming a local dependence on activity as in (4.17), one obtains the local fields (4.18), while a global dependence as in (4.20) leads to (4.23). Under certain assumptions, the system in the first of these cases is described by the effective Hamiltonian (4.10). This reduces to a Hopfield system, i.e., the familiar attractor neural network without (fast) synaptic noise, with rescaled temperature and a threshold. This was already studied for a Gaussian distribution of thresholds [Hertz et al., 1991, Horn and Usher, 1989, Litinskii, 2002]. A more intriguing behavior ensues when the noise depends on the total presynaptic current arriving to the postsynaptic neuron. We have studied this case bot analytically by a sort of mean-field treatment and numerically by a series of related Monte Carlo simulations using Glauber, *spin-flip* dynamics [Marro and Dickman, 1999]. The two approaches are fully consistent with and complement each other.

Our model involves two main parameters. One is the *temperature* T which controls the stochastic evolution of the network activity. The other parameter, Φ, controls the fast-noise intensity. Varying this, the system describes from normal operation to depression phenomena. A main result is that the presynaptic

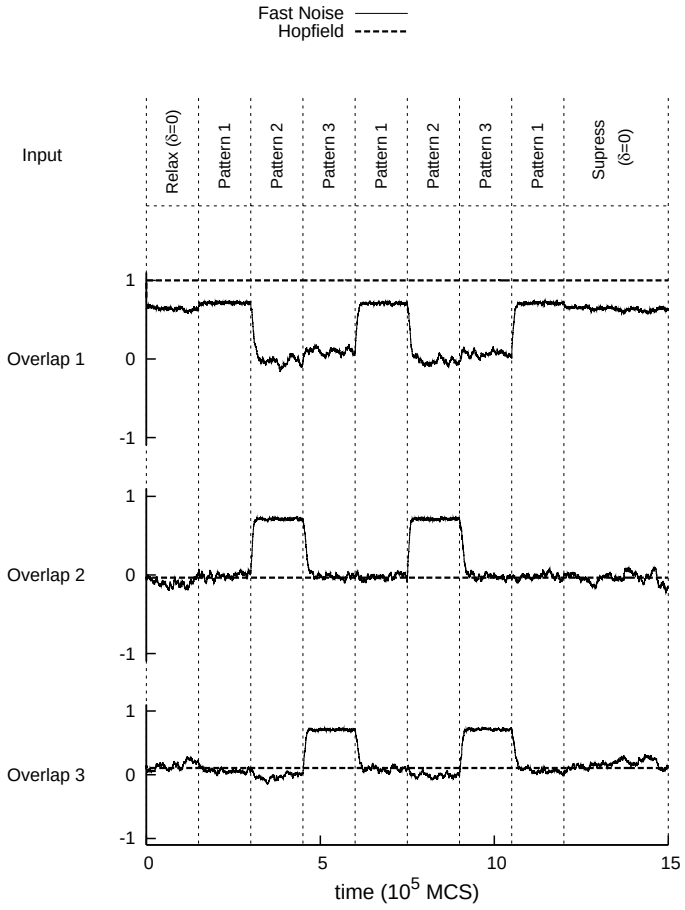

Figure 4.6: The same as in figure 4.5 but for three stored patterns that are orthogonal, i.e. completely uncorrelated. The stimulus is $+\delta\xi^{\nu}$, $\delta = 0.1$, with $\nu = \nu(t)$, as indicated at the top.

noise induces the occurrence of a tricritical point of certain values of these parameters $(T_c, \Phi_c) = (1, -4/3)$. This separates (in the limit $\alpha \to 0$) first from second order phase transitions between a ferromagnetic -like, retrieval phase and a paramagnetic-like, non-retrieval phase.

The principal conclusion in this chapter is that fast noise seems indeed to importantly enhance the network sensitivity to external stimulation. We explicitly show the noise may turn unstable the *attractor* of fixed point solution of the retrieval process, and the system then seeks for another attractor. In particular, one observes switching from the stored pattern to corresponding antipattern for $M = 1$, and switching between patterns for a larger number of stored patterns, M. This behavior is most interesting because improves the network ability to be very sensitive to the forcing stimulus, but rather independent of the network initial state or the thermal noise. It seems sensible to argue that, besides recognition, the processes of class identification and categorization in nature might follow a similar strategy. That is, different attractor may correspond to different objects, and a dynamics conveniently perturbed by fast noise may keep visiting the attractors belonging to a class which is characterized by a certain degree of correlation between its elements. In fact, a similar mechanism seems at the basis of early olfactory processing of insects [Laurent et al., 2001], and instabilities of the same sort have been described in the cortical activity of monkeys [Abeles et al., 1995].

Finally we mention that the above complex behavior seems confirmed by preliminary Monte Carlo simulations for a macroscopic number of stored patterns, i.e., a finite loading parameter $\alpha = M/N \neq 0$. A mean-field approximation (see below) shows that the storage capacity of the network is similar to the Hopfield case ($\alpha_c = 0.138$) for any $\Phi < 0$, while it is always smaller for $\Phi > 0$. This is in agreement with previous results concerning the effect of synaptic depression in Hopfield-like systems [Bibitchkov et al., 2002, Torres et al., 2002]. The fact that a positive value of Φ tends to shallow the basin thus destabilizing the attractor may be understood by a simple (mean-field) argument which is confirmed by Monte Carlo simulations. Assume that the stationary activity

shows just one overlap with the rest, $M-1$ stored patters is of order $(1/\sqrt{N})$ (*non-condensed patterns*) [Hertz et al., 1991]. The resulting probability of change of the synaptic intensity, namely, $(1+\alpha)\sum_{\nu=1}^{M}(m^{\nu})^2$ is order unity, and the local fields (4.23) follow as $h_i^{\text{eff}} \sim -\Phi h_i^{\text{Hopfield}}$. Therefore, the storage capacity, which is computed at $T=0$, is the same as in the Hopfield case for any $\Phi < 0$, and always lower otherwise.

Bibliography

L. F. Abbott and W. G. Regehr. Synaptic computation. *Nature*, 431:796–803, 2004. 67

M. Abeles, H. Bergman, I. Gat, I. Meilijson, E. Seidemann, N. Tishby, and E. Vaadia. Cortical activity flips among quasi-stationary states. *Proc. Natl. Acad. Sci. USA*, 92:8616–8620, 1995. 68, 85

C. Allen and C.F. Stevens. An evaluation of causes for unreliability of synaptic transmission. *Proc. Natl. Acad. Sci. USA*, 91:10380–10383, 1994. 67

D. Bibitchkov, J.M. Herrmann, and T. Geisel. Pattern storage and processing in attractor networks with short-time synaptic dynamics. *Network: Comput. Neural Syst.*, 13:115–129, 2002. 67, 79, 85

J.M. Cortes, P.L. Garrido, J. Marro, and J.J. Torres. Switching between memories in neural automata with synaptic noise. *Neurocomputing*, 58-60:67–71, 2004. 69

C. W. Gardiner. *Handbook of Stochastic Methods: for Physics, Chemistry and the Natural Sciences*. Springer-Verlag, 2004. 70

P.L. Garrido and J. Marro. Effective hamiltonian description of nonequilibrium spin systems. *Phys. Rev. Lett.*, 62:1929–1932, 1989. 71

P.L. Garrido and J. Marro. Kinetic lattice models of disorder. *J. Stat. Phys.*, 74: 663–686, 1994. 69, 70

P.L. Garrido and M.A. Munoz. Nonequilibrium lattice models: A case with effective hamiltonian in d dimensions. *Phys. Rev. E*, 48:R4153–R4155, 1993. 72

D. O. Hebb. *The Organization of Behavior: A Neuropsychological Theory*. Wiley, 1949. 69

J. Hertz, A. Krogh, and R.G. Palmer. *Introduction to the theory of neural computation*. Addison-Wesley, 1991. 73, 74, 75, 83, 86

J.J. Hopfield. Neural networks and physical systems with emergent collective computational abilities. *Proc. Natl. Acad. Sci. USA*, 79:2554–2558, 1982. 69

D. Horn and M. Usher. Neural networks with dynamical thresholds. *Phys. Rev. A*, 40:1036–1044, 1989. 83

A.I. Lopez Lacomba and J. Marro. Ising systems with conflicting dynamics: Exact results for random interactions and fields. *Europhys. Lett.*, 25:169–174, 1994. 72

G. Laurent, M. Stopfer, R.W. Friedrich, M.I. Rabinovich, A. Volkovskii, and H.D.I. Abarbanel. Odor encoding as an active, dynamical process: Experiments, computation and theory. *Annual Review of Neuroscience*, 24:263–297, 2001. 68, 85

L. B. Litinskii. Hopfield model with a dynamic threshold. *Theoretical and Mathematical Physics*, 130:136–151, 2002. 83

J. Marro and R. Dickman. *Nonequilibrium Phase Transitions in Lattice Models*. Cambridge University Press, 1999. 68, 69, 70, 71, 72, 73, 83

L. Pantic, J.J. Torres, H.J. Kappen, and S.C.A.M. Gielen. Associative memmory with dynamic synapses. *Neural Comp.*, 14:2903–2923, 2002. 74

A.M. Thomson, A.P. Bannister, A. Mercer, and O.T. Morris. Target and temporal pattern selection at neocortical synapses. *Philos. Trans. R. Soc. Lond. B Biol. Sci.*, 357:1781–1791, 2002. 68

J.J. Torres, P.L. Garrido, and J. Marro. Neural networks with fast time-variation of synapses. *J. Phys. A: Math. Gen.*, 30:7801–7816, 1997. 69

J.J. Torres, L. Pantic, and H.J. Kappen. Storage capacity of attractor neural networks with depressing synapses. *Phys. Rev. E.*, 66:061910, 2002. 85

M. V. Tsodyks, K. Pawelzik, and H. Markram. Neural networks with dynamic synapses. *Neural Comp.*, 10:821–835, 1998. 68, 74

A. Zador. Impact of synaptic unreliability on the information transmitted by spiking neurons. *J. Neurophysiol.*, 79:1219–1229, 1998. 67

Chapter 5

Fast Presynaptic Noise on Neural Automata

5.1 Motivation and Antecedents

Analysis of brain waves indicates that *strange attractors* might be dominant for some of the neural activity. For instance, the reported chaotic activity in electroencephalogram or EEG time series [Babloyantz and Destexhe, 1986, Barrie et al., 1996, Elbert et al., 1994] might reflect an efficiently search between many patterns of activity which can encode information, as in olfactory processes [Freeman, 1987], or perhaps a state of collective synchronization of the network during expectation and attention [Hansel and Sompolinsky, 1992, 1996]. In fact, different sorts of constructive chaos have already been incorporated in some neural networks models [Bolle and Vink, 1996, Dominguez, 1996, Poon and Barahona, 2001, Wang et al., 1990]. However, a demonstration of chaos out of extremely bursting EEG signals is still a difficult task, and a conclusion of the significance and the functional role of chaos in neurobiological systems is an open issue [Faure and Korn, 2001, Korn and Faure, 2003, Rabinovich and Abarbanel, 1998].

We address here this problem by simulating a *neural automata* which exhibits chaotic behavior. The model is a bio-inspired cellular automata [Frisch et al., 1986, Wolfram, 1984] in which dynamics concerns a large number of neurons simultaneously updated, instead of sequentially updating a small neighborhood at each time step. The automata strategy has already shown to be efficient in modeling some neural tasks, as for instance associative memory [Cortes et al., 2004, Ganguly et al., 2003, Torres et al., 2004]. In the present paper, our motivation follows the recent observation that fast presynaptic noise may importantly modify the stability of attractors in Hopfield–like neural networks [Cortes et al., 2005]. Trying to generalize this important issue, we demonstrate that short time–scale fluctuations depending on neural presynaptic activity may importantly affect the retrieval dynamics in this class of neural automata. More precisely, we show that not only the attractor may turn unstable but even *strange,* so that a chaotic dynamics between the stored patterns sets in. The inherent instability in chaotic motions facilitates the extraordinary ability of neural systems to adapt, make transitions among different kinds of behavior when the environment is altered, and consequently to create a rich variety of spatio-temporal patterns. This might be one the nature strategies for efficient computation [Lu et al., 2003, Schweighofer et al., 2004, Stam et al., 1994]. However, there are some another evidences showing that neural systems can control chaos [Freeman et al., 1997, Molgedey et al., 1992, Schiff et al., 1994], by incorporating an external contribution of noise, as for instance in stochastic resonance phenomena. Here, we report on the relation between emerging chaoticity and fast synaptic noise. Depending on its intensity, the neural automata exhibits different regimes from high to low chaoticity which can be relevant to solve autonomously and efficiently some problems in nature.

5.2 The Model

Consider a network of binary neurons (firing or silent) whose configurations are $\mathbf{S} \equiv \{s_i = \pm 1; i = 1, \ldots, N\}$. Any two neurons are connected by synapses of

intensity

$$w_{ij} = w^L_{ij} x_j \quad \forall i, j, \tag{5.1}$$

where w^L_{ij} are fixed *weights* determined in a previous *Learning* process (for instance, Hebb's). The equation (5.1) ensures that weights are constantly perturbed by the variables $\mathbf{X} \equiv \{x_j\}$, which incorporate stochastic fluctuations modeling the existence of a microscopic noise. The local field $h_i(\mathbf{S}, \mathbf{X}) \equiv \sum_{j \neq i} w_{ij} x_j s_j$ represents the total presynaptic current arriving to the postsynaptic neuron s_i. In order to construct a stochastic neural dynamics, we introduce a noise parameter $T \equiv \beta^{-1}$ driving changes of neurons states. In the limit of $T \to 0$ the dynamics becomes deterministic and satisfies that $\mathrm{sig}(h_i) = s_i$.

We consider the case of *fast* fluctuations on the microscopic variables $\mathbf{X}$. This limit allows to consider the neurons evolving in presence of a steady distribution of $\mathbf{X}$ (for technical details see for instance [Marro and Dickman, 1999, Torres et al., 1997]). We are interested in such distributions of probability, namely $P^{st}(\mathbf{X}|\mathbf{S})$, which allow to model activity-dependent processes based on recent neurobiological findings [Abbott and Regehr, 2004]. In this context, synapses intensities are assumed to be modified by rapid repeated presynaptic activation, which is typically required to produce appreciable synaptic plasticity. The aim is to understand how short-term synaptic *depression* [Pantic et al., 2002, Tsodyks et al., 1998] could affect the neural automata dynamics. Synaptic depression ensures that an increase of the mean firing rate modifies the postsynaptic response decreasing the synaptic weight. Considering this, we assume the choice

$$P^{st}(\mathbf{X}|\mathbf{S}) = \prod_j P(x_j|\mathbf{S}), \tag{5.2}$$

with

$$P(x_j|\mathbf{S}) = \zeta(\vec{\mathbf{m}})\ \delta(x_j + \Phi) + [1 - \zeta(\vec{\mathbf{m}})]\ \delta(x_j - 1). \tag{5.3}$$

Here, $\vec{\mathbf{m}} = \vec{\mathbf{m}}(\mathbf{S}) \equiv \left(m^1(\mathbf{S}), \ldots, m^\mu(\mathbf{S}), \ldots, m^M(\mathbf{S})\right)$ is the M-dimensional overlap vector with $m^\mu(\mathbf{S}) \equiv 1/N \sum_i \xi^\mu_i s_i$, where ξ^μ_i are M binary–patterns

stored in the weights. The function $\zeta(\vec{\mathbf{m}})$ stands for a probability function of $\vec{\mathbf{m}}$ to be determined. In practice, the choice (5.3) means that the depression effect depends on the net current arriving to postsynaptic neurons, which in turn depends on the overlap vector $\vec{\mathbf{m}}$. As a consequence, the probability (5.3) introduces some non–trivial correlations between synaptic noise and neural activity. The model has as a natural limit the Hopfield model [Hertz et al., 1991] for $\Phi \to -1$. Otherwise, it results in a rather complex behavior. In order to model activity–dependent mechanisms acting on synapses, $\zeta(\vec{\mathbf{m}})$ should be an increasing function of the total presynaptic current. A simple, properly normalized choice is $\zeta(\vec{\mathbf{m}}) = \frac{1}{1+\alpha}\sum_{\nu}\left[m^{\nu}(\mathbf{S})\right]^2$, where $\alpha = M/N$ is the load parameter of the network [Hertz et al., 1991].

In the following, we shall assume that postsynaptic neuron, s_i, receives an *effective* presynaptic current $\overline{h_i}(\mathbf{S})$ given by

$$\overline{h_i}(\mathbf{S}) \equiv \int_{\mathbf{X}} h_i(\mathbf{S},\mathbf{X}) P^{st}(\mathbf{X}|\mathbf{S}) d\mathbf{X}. \tag{5.4}$$

Under the scenario described above, where fluctuations in the $\mathbf{X}$–variables are very fast, the equation (5.4) becomes justified [Bibitchkov et al., 2002, Gardiner, 2004]. That is due to neurons evolve in time observing an average contribution of all different realizations of the local field $h_i(\mathbf{S},\mathbf{X})$. In the case of assuming the Hebb's learning rule in (5.1), it is possible to obtain the local fields in terms of the overlaps. Thus, after some straightforward algebra, the result is

$$\overline{h_i}(\mathbf{S}) = \left[1 - \frac{(1+\Phi)\sum_{\nu}\left[m^{\nu}(\mathbf{S})\right]}{1+\alpha}\right]\sum_{\nu'}\xi_i^{\nu'} m^{\nu'}(\mathbf{S}). \tag{5.5}$$

In the next section we construct a stochastic neural automata driven by the local fields given by (5.5).

5.3 Analysis of Neural Automata

We concern a stochastic neural automata which evolves in time according to the master equation [Marro and Dickman, 1999, Peretto, 1992]

$$P_{t+1}(\mathbf{S}) = \sum_{\mathbf{S}'} P_t(\mathbf{S}')\Omega(\mathbf{S}' \to \mathbf{S}). \tag{5.6}$$

The jumping probability from configuration $\mathbf{S}'$ to $\mathbf{S}$ is defined as

$$\Omega(\mathbf{S}' \to \mathbf{S}) = \prod_{i=1}^{N^*(t)} \omega(s'_{l(i)} \to s_{l(i)}), \tag{5.7}$$

and we shall assume that $\omega(s'_{l(i)} \to s_{l(i)}) \propto \Psi[\beta \overline{h_{l(i)}}(\mathbf{S}')(s'_{l(i)} - s_{l(i)})]$ and that $\overline{h_{l(i)}}(\mathbf{S}')$ is independent on $s'_{l(i)}$, which is a good approximation in the thermodynamic limit ($N \to \infty$). In principle, the function Ψ is arbitrary, unless it satisfies that $\Psi(u) = \Psi(-u)\exp(u)$ and the boundary conditions $\Psi(0) = 1$ and $\Psi(\infty) = 0$ [Marro and Dickman, 1999]. In the equation (5.7), $N^*(t)$ is the total number of change trials and $l(i)$ denotes the position occupied by the neuron involved in the i-th trial. The required normalization constraint ensures that $\sum_{\mathbf{S}} \Omega(\mathbf{S}' \to \mathbf{S}) = 1$ and one possibility to satisfy it is to take [Cortes et al., 2004]

$$\omega(s'_{l(i)} \to s_{l(i)}) = \frac{\Psi[\beta \overline{h_{l(i)}}(\mathbf{S}')(s'_{l(i)} - s_{l(i)})]}{1 + \Psi[2\beta s'_{l(i)} \overline{h_{l(i)}}(\mathbf{S}')]}. \tag{5.8}$$

We report on two different types of SNA characterized by considering in (5.7) either

$$\begin{aligned} N^*(t) &= N, \\ &\text{or} \\ N^*(t) &< N. \end{aligned} \tag{5.9}$$

The first one considers $N^*(t) = N$ (parallel updating) and the second takes N^* as non-constant in time and satisfying $N^*(t) < N$. For the first case, we present both mean field theory and Monte Carlo simulations in full agreement. Because is not possible to advance analytically further in the second situation, we present Monte Carlo simulations and different measures which show a picture which is interesting and stimulating. Both cases illustrate emergent behavior which is complex; in particular, it depicts fixed points, P–cycles, hopping between memorized patterns [Cortes et al., 2004, Pantic et al., 2002], and even chaotic dynamics which can be, in several different situations, convenient in order to be possible to visit a huge number of different spatio-temporal patterns.

The chaotic dynamics is aperiodic, and this can be useful to store and retrieve different spatio-temporal patterns [Freeman, 1994]. An example of this kind of systems where spatio-temporal stimulus or odors can be coded in attractors is the olfactory bulb in insects [Laurent et al., 2001].

5.4 Case $N^*(t) = N$

In this section we report on results of considering the first stochastic neural automata defined in (5.10). The algorithm is as follows:

1. Store the M different binary patterns ξ_i^μ in the learning rule

$$w_{ij}^L \equiv \frac{1}{N} \sum_\mu \xi_i^\mu \xi_j^\mu. \tag{5.10}$$

2. Set in the state of the network at random.

3. Compute and store the N different effective local fields $\overline{h_i}(\mathbf{S})$ by using (5.5).

4. Do the change $s_i \to -s_i$ with the standard jumping probability per site given by (5.8).

5. Do $t = t + 1$.

6. Go to (3).

Now, we have $N^*(t) = N$, and this situation is corresponded with the synchronous *Little* dynamics [Peretto, 1992]. In order to go analytically further, we study the case of only one pattern stored. Starting at (5.6), using the Eqs. (5.7), (5.8) and (5.5), it is possible to obtain the discrete map [Hertz et al., 1991, Marro and Dickman, 1999] describing the time evolution for the overlap between the network activity and the stored pattern, namely $m^1 \equiv m$. The result is

$$m_{t+1} = \tanh\{\beta m_t [1 - m_t^2 (1 + \Phi)]\}. \tag{5.11}$$

Note that the Eq. (5.11) is symmetrical with respect to solutions $m_t = \pm 1$.

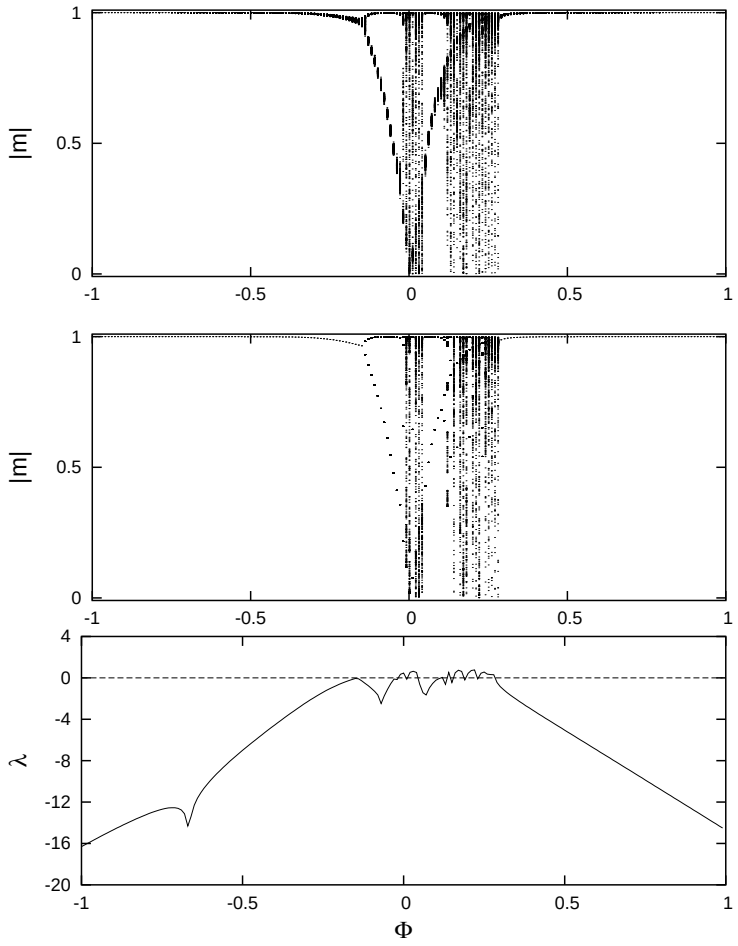

Figure 5.1: We represent the absolute value for the steady overlap versus the fast noise parameter Φ (bifurcation diagram). We store only one pattern $M = 1$ and the measures have been computed either by using Monte Carlo simulations in a network of $N = 10000$ neurons (top graphics) or iterating the (mean field) discrete time map (5.11) (represented in the middle). Both results are in full agreement. On the bottom, we represent the corresponding Lyapunov exponent, namely λ, showing the existence of a chaotic window, as characterized by a positive value. Here, the temperature parameter T is low and fixed to 0.1 in order to negligee thermal fluctuations and observe just the influence of fast noise.

The fixed point solutions of (5.11) were studied in [Cortes et al., 2005]; depending on the fast noise parameter Φ, the system is able to show both first and second order phase transitions in the retrieval process. Attending to the dynamical properties, in [Cortes et al., 2005] is studied the effects of considering the updating as sequential (see for details [Marro and Dickman, 1999, Peretto, 1992]) and the main result is that the system is not able to jump between different attractors in the retrieval dynamics by itself. That is, in order to reach it, we have to introduce external stimulation. On the contrary, the dynamical properties are very different and intriguing when the updating is considered non-sequential; we observe fixed points, $P-$cycles where the system is hopping among all attractors corresponding each one to the stored patterns, and even, chaotic switching. The dynamical mean field map (5.11) shows a very complex behavior depending on both temperature, T, and the fast noise, Φ, parameters. In figure 5.1 we compare the result between steady measures of the absolute value for the overlap between the network and the unique pattern stored obtained by either Monte Carlo simulations or by using the mean field discrete map (5.11). They are both in full agreement. The temperature is fixed to $T = 0.1$, which is small in order to make the thermal fluctuations negligible. The bottom graph appearing in figure 5.1 shows the Lyapunov exponent, λ, corresponding to the same discrete map (5.11). It detects different chaotic windows ($\lambda > 0$) in the plane (T,Φ) when we fixed T and vary the fast noise parameter Φ. It is important to remark that in the case of absence of fast noise acting on the synapses intensity , which is equivalent to consider $\Phi = -1$ [Cortes et al., 2005], the system dynamics is stable ($\lambda < 0$) and only is possible the fixed point solutions. This situation is corresponded to a Hopfield neural network with parallel updating [Hopfield, 1982, Peretto, 1992]. This is not the first time where chaos appears in the retrieval process in an attractor neural network. In [Bolle and Vink, 1996] is studied the retrieval dynamics attending to the shape of the gain functions as a modeling parameter. This gain function is defined as

$$m_{t+1} \equiv G(m_t) \tag{5.12}$$

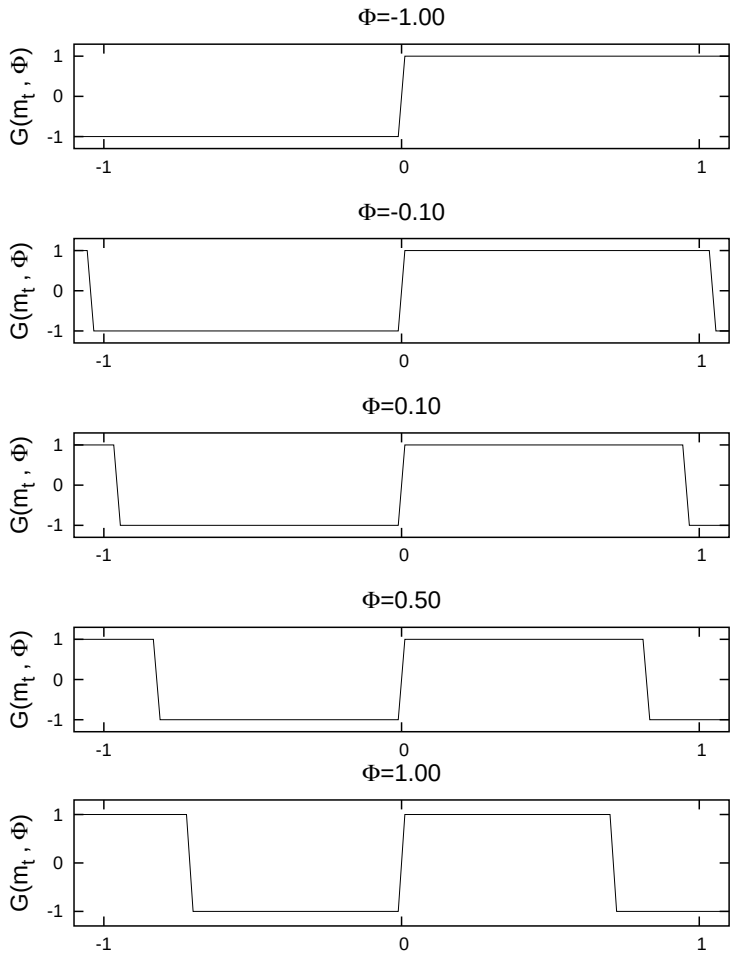

Figure 5.2: The gain function (5.13) versus m_t for different values of Φ, as indicated. Note that in the case $\Phi > 0$, the gain function becomes non-sigmoidal and consequently appears the possibility to show chaotic behavior in the retrieval processes as is explained in the text. Note that, in the Hopfield situation or equivalently $\Phi = -1$, the gain function is monotonic as is well-known.

Many different dynamical behaviors are observed, covering the full range from point attractors to chaotic dynamics. It is shown that after introducing non-sigmoidality in the gain function does not improve the performance of the network in comparison to the standard networks of analogous neurons with monotonic gain functions, as for example the Hopfield case (see figure 5.2). That is due to non-sigmoidal gain functions incorporate an oscillatory behavior[Bolle and Vink, 1996] in which the system is visiting continuosly the set of different stored patterns [Cortes et al., 2004, Pantic et al., 2002]. Measures as for example the storage capacity cannot be improved incorporating this switching behavior [Torres et al., 2002], because the fixed points (attractors) become unstable and consequently the basin attraction associated to each pattern is less deep. These results suggest to define new measures of storage capacity able to incorporate the possibility to code and retrieve spatio-temporal information. In our case, also is possible to obtain from Eq. (5.11) the associated gain function. The result, in $T = 0$, is

$$G(m_t, \Phi) = \text{sign}\left(m_t\left[1 - m_t^2(1+\Phi)\right]\right). \tag{5.13}$$

Note that now the gain function depends on both m_t and Φ. Figure 5.2 depicts the function (5.13) for varying Φ. This reveals that the gain is non-sigmoidal for $\Phi > 0$ and, consequently, may then lead to chaotic behavior of the overlap dynamics [Bolle and Vink, 1996]. The figure 5.1 is coherent with these results, because chaotic regions appear only in the case $\Phi > 0$ or equivalently when the gain function becomes non-sigmoidal.

Another feature important in the switching behavior appearing in the retrieval dynamics, is related to the remaining time in each attractor (in the case of only one pattern we have the pattern and antipattern or equivalently the solutions $m = \pm 1$). In order to be possible to define any kind of retrieval or associative memory is necessary to remain a certain interval of time before jumping to another attractor. Under a mathematical point of view, this is equivalent to have dynamical attractors which are metastable, and never highly unstable. Monte Carlo simulations of this system reveal that in the case of $\Phi > 0$ and

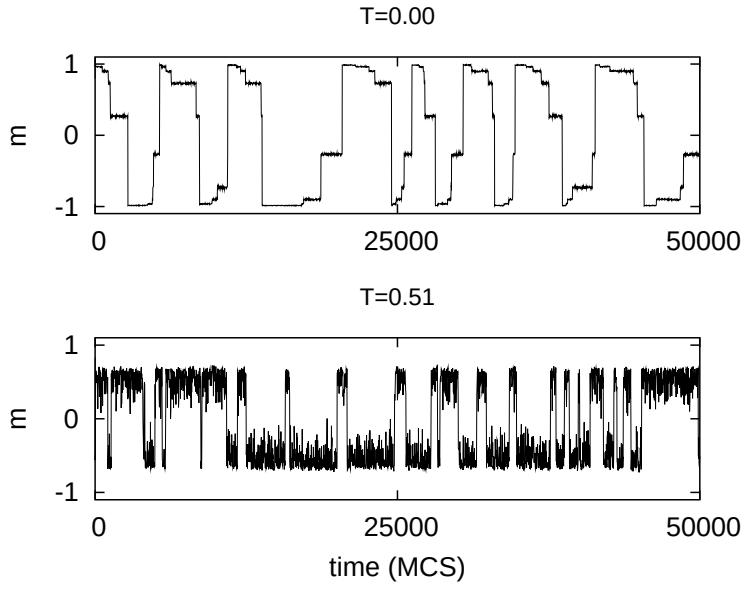

Figure 5.3: Monte Carlo simulations for a single pattern ($\alpha \to 0$) and $N = 3600$ neurons show the effect of fast noise on experiments of recalling for $\Phi = 0.043$. The top panel illustrates oscillations at $T = 0$, e.g. in absence of thermal fluctuations, and the bottom one at $T = 0.51$. Here, m is the overlap of the neural activity with the pattern 1, namely $m^1(\mathbf{S})$.

driving the system with parallel updating we never get to remain in the attractor more than a few temporal steps and in this sense we need to control and introduce less instability in the system in order to be possible to study associative memory processes. In the next section we formulate another stochastic neural automata where, depending on the fast noise parameter, oscillations between different attractors can be with low frequency and consequently there is associative memory and swithching behavior properly defined.

5.5 Case $N^*(t) < N$

Another possibility to construct neural automatas is by considering in (5.10) the second choice $N^*(t) < N$. The algorithm is as follows:

1. Store the M different binary patterns ξ_i^μ in the learning rule (5.10).
2. Set in the state of the network at random.
3. Compute and store the N different effective local fields $\overline{h_i}(\mathbf{S})$ by using (5.5).
4. Compute $N^*(t)$ defined as the total different sites chosen at random after N trials. Note, that in general $N^*(t) \leq N$.
5. Do the change $s_{l(i)} \to -s_{l(i)}$ with the standard jumping probability per site given by (5.8). Here, $l(i)$ denotes the site position occupied by the neuron involved in the i-th trial.
6. Do $t = t + 1$.
7. Go to (3).

Monte Carlo simulations of the system described above show complex behavior. It depicts fixed points, regular hopping between memorized patterns [Cortes et al., 2004, Pantic et al., 2002], and even chaotic dynamics. For a single pattern, e.g. in the limit $\alpha \to 0$, figure 5.3 shows that a complex switching

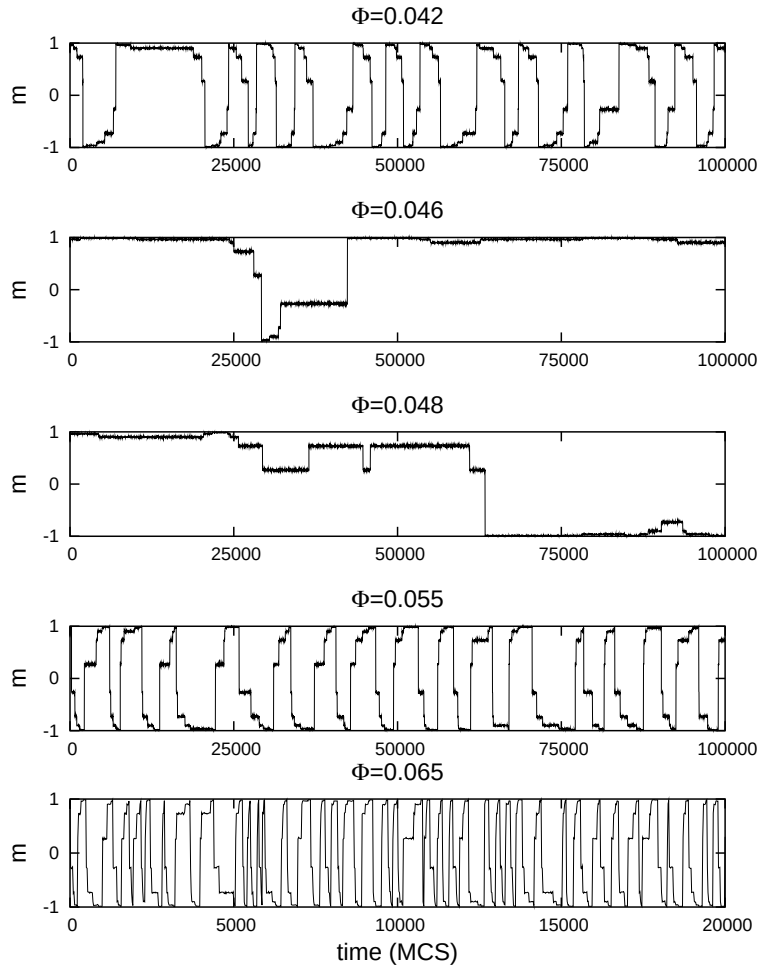

Figure 5.4: Monte Carlo simulations in absence of thermal fluctuations ($T = 0$) for a single pattern, $N = 3600$ neurons and different values of the fast noise parameter Φ. Depending on its value, the emergent oscillations can show different temporal scales and degrees of complexity.

among pattern (ξ^{μ}) and antipattern ($-\xi^{\mu}$) emerges. More precisely, it depicts that these oscillations are not induced by thermal noise. Indeed, they are a consequence of fast synaptic noise. Therefore, we shall restrict in the following to simulate the system at $T = 0$. Figure 5.4 illustrates the main results, that is, the shape and frequency of the oscillations can be modulated by tuning the fast noise parameter Φ.

In order to get a quantitative description of the complexity of these oscillations, we measure the entropy for their harmonics. Using a standard Fast Fourier Transform algorithm (FFT), we computed the power spectra $P(n)$, and then we normalized it to define the probability $p_n = P(n)/\sum P(n)$. This allows to define a regular entropy in bits $S \equiv -\sum_n p_n \log_2 p_n$. This measure has been usually considered to explain the appearance of some regularity in chaotic activity of real neurons [Varona et al., 2001]. Note that $S > 0$ gives chaoticity while $S = 0$ corresponds to a periodic behavior. In figure 5.5, we represent the entropy as a function of Φ.

The minimum corresponds to the smallest degeneration in time series of figure 5.4 (second graph from top to bottom). A decrease of S is an indication of regularization or smaller chaoticity, while a increase means higher chaos and irregularity in time series.

5.6 Discussion

We have introduced a class of bio-inspired neural automata in presence of fast synaptic noise. Depending on the noise details, the model presents a rich emergent behavior including chaotic switching among attractors. This results in complex patterns of neural activity. An increase of the coding rate of spatio-temporal information to be retrieved has high computational interest. For instance, there are some evidences [Freeman, 1994] of chaos being essential in the searching dynamics of new patterns to learn. In this sense, entropy could take an important role to detect the optimal noise parameter which allows to learn new patterns. Moreover, a decrease of S allows the neural automata to

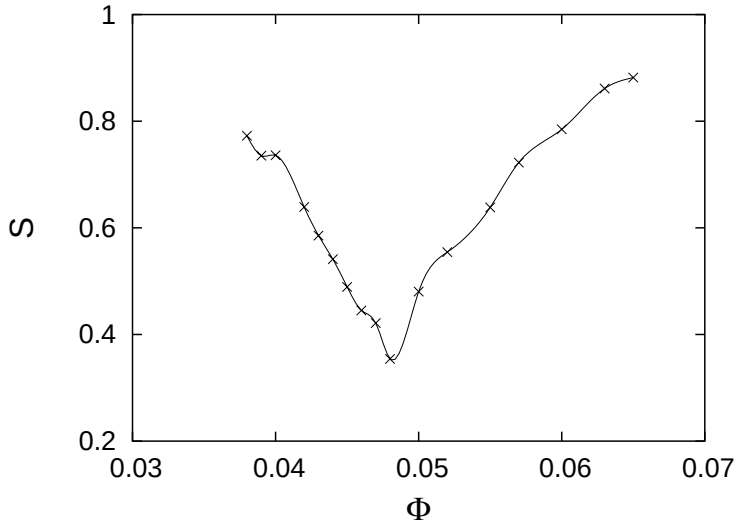

Figure 5.5: Entropy function, as defined in the main text, for different time series of the neural automata and different values of Φ. A decrease of the entropy is a measure of regularization on complexity of times series and consequently, the graphs shows different regimes of chaoticity.

control chaos by a regularization of neural activity which has been reported to be relevant in living systems [Garfinkel et al., 1992, Schiff et al., 1994]. This can achieve by tuning the fast noise parameter. The design of a mechanism in which noise intensity varies autonomously (without an external input/noise) can be useful to self-control of chaos. This strategy could be computationally efficient to solve different tasks in nature.

Bibliography

L. F. Abbott and W. G. Regehr. Synaptic computation. *Nature*, 431:796–803, 2004. 93

A. Babloyantz and A. Destexhe. Low-dimensional chaos in an instance of epilepsy. *Proc. Natl. Acad. Sci. USA*, 83:3513–3517, 1986. 91

J. M. Barrie, W. J. Freeman, and M. Lenhart. Modulation by discriminative training of spatial patterns of gamma eeg amplitude and phase in neocortex of rabbits. *J. Neurophysiol.*, 76:520–539, 1996. 91

D. Bibitchkov, J.M. Herrmann, and T. Geisel. Pattern storage and processing in attractor networks with short-time synaptic dynamics. *Network: Comput. Neural Syst.*, 13:115–129, 2002. 94

D. Bolle and B. Vink. On the dynamics of analogue neurons with nonsigmoidal gain functions. *Physica A*, 223:293–308, 1996. 91, 98, 100

J. M. Cortes, J. J. Torres, J. Marro, P. L. Garrido, and H. J. Kappen. Effects of fast presynaptic noise in attractor neural networks. To be published, 2005. 92, 98

J.M. Cortes, P.L. Garrido, J. Marro, and J.J. Torres. Switching between memories in neural automata with synaptic noise. *Neurocomputing*, 58-60:67–71, 2004. 92, 95, 100, 102

D. R. C. Dominguez. Inference and chaos by a network of nonmonotonic neurons. *Phys. Rev. E*, 54:4066–4070, 1996. 91

T. Elbert, W. J. Ray, Z. J. Kowalik, J. E. Skinner, K. E. Graf, and N. Birbaumer. Chaos and physiology: deterministic chaos in excitable cell assemblies. *Physiol. Rev.*, 74:1–47, 1994. 91

P. Faure and H. Korn. Is there chaos in the brain? i. concepts of nonlinear dynamics and methods of investigation. *C. R. Acad. Sci. III*, 324:773–793, 2001. 91

W. J. Freeman. Simulation of chaotic eeg patterns with a dynamic model of the olfactory system. *Biol. Cybern.*, 56:139–150, 1987. 91

W. J. Freeman. Neural networks and chaos. *J. Theor. Biol.*, 171:13–18, 1994. 96, 104

W. J. Freeman, H. J. Chang, B. C. Burke, P. A. Rose, and J. Badler. Taming chaos: Stabilization of aperiodic attractors by noise. *IEEE Transactions on Circuits and Systems-I: Fundamental theory and Applications*, 44, 1997. 92

U. Frisch, B. Hasslacher, and Y. Pomeau. Lattice-gas automata for the navier-stokes equation. *Phys. Rev. Lett.*, 56:1505–1508, 1986. 92

N. Ganguly, A. Das, P. Maji, B. K. Sikdar, and P. P. Chaudhuri. Evolving cellular automata based associative memory for pattern recognition. In B. Monien, V.K. Prasanna, and S. Vajapeyam, editors, *High Performance Computing - HiPC 2001 : 8th International Conference*, volume 2228, pages 115–124. Springer-Verlag, 2003. 92

C. W. Gardiner. *Handbook of Stochastic Methods: for Physics, Chemistry and the Natural Sciences*. Springer-Verlag, 2004. 94

A. Garfinkel, M. L. Spano, W. L. Ditto, and J. N. Weiss. Controlling cardiac chaos. *Science*, 257:1230–1235, 1992. 106

D. Hansel and H. Sompolinsky. Synchronization and computation in a chaotic neural network. *Phys. Rev. Lett.*, 68:718–721, 1992. 91

D. Hansel and H. Sompolinsky. Chaos and synchrony in a model of a hypercolumn in visual cortex. *J. Comput. Neurosci.*, 3:7–34, 1996. 91

J. Hertz, A. Krogh, and R.G. Palmer. *Introduction to the theory of neural computation*. Addison-Wesley, 1991. 94, 96

J.J. Hopfield. Neural networks and physical systems with emergent collective computational abilities. *Proc. Natl. Acad. Sci. USA*, 79:2554–2558, 1982. 98

H. Korn and P. Faure. Is there chaos in the brain? ii. experimental evidence and related models. *C. R. Biol.*, 326:787–840, 2003. 91

G. Laurent, M. Stopfer, R.W. Friedrich, M.I. Rabinovich, A. Volkovskii, and H.D.I. Abarbanel. Odor encoding as an active, dynamical process: Experiments, computation and theory. *Annual Review of Neuroscience*, 24:263–297, 2001. 96

Q. Lu, G. Shen, and R. Yu. A chaotic approach to maintain the population diversity of genetic algorithm in network training. *Comput. Biol. Chem.*, 27: 363–371, 2003. 92

J. Marro and R. Dickman. *Nonequilibrium Phase Transitions in Lattice Models*. Cambridge University Press, 1999. 93, 94, 95, 96, 98

L. Molgedey, J. Schuchhardt, and H. G. Schuster. Suppressing chaos in neural networks by noise. *Phys. Rev. Lett.*, 69:3717–3719, 1992. 92

L. Pantic, J.J. Torres, H.J. Kappen, and S.C.A.M. Gielen. Associative memmory with dynamic synapses. *Neural Comp.*, 14:2903–2923, 2002. 93, 95, 100, 102

P. Peretto. *An Introduction to the modeling of neural networks*. Cambridge University Press, 1992. 94, 96, 98

C. S. Poon and M. Barahona. Titration of chaos with added noise. *Proc. Natl. Acad. Sci. USA*, 98:7107–7112, 2001. 91

M. I. Rabinovich and H. D. I. Abarbanel. The role of chaos in neural systems. *Neuroscience*, 87:5–14, 1998. 91

S. J. Schiff, K. Jerger, D. H. Duong, T. Chang, M. L. Spano, and W. L. Ditto. Controlling chaos in the brain. *Nature*, 370:615–620, 1994. 92, 106

N. Schweighofer, K. Doya, H. Fukai, J. V. Chiron, T. Furukawa, and M. Kawato. Chaos may enhance information transmission in the inferior olive. *Proc. Natl. Acad. Sci. USA*, 101:4655–4660, 2004. 92

K. J. Stam, D. L. Tavy, B. Jelles, H. A. Achtereekte, J. P. Slaets JP, and R. W. Keunen. Non-linear dynamical analysis of multichannel eeg: clinical applications in dementia and parkinson's disease. *Brain Topogr.*, 7:141–150, 1994. 92

J.J. Torres, P.L. Garrido, and J. Marro. Neural networks with fast time-variation of synapses. *J. Phys. A: Math. Gen.*, 30:7801–7816, 1997. 93

J.J. Torres, M.A. Munoz, J. Marro, and P.L. Garrido. Influence of topology on the performance of a neural network. *Neurocomputing*, 58-60:229–234, 2004. 92

J.J. Torres, L. Pantic, and H.J. Kappen. Storage capacity of attractor neural networks with depressing synapses. *Phys. Rev. E.*, 66:061910, 2002. 100

M. V. Tsodyks, K. Pawelzik, and H. Markram. Neural networks with dynamic synapses. *Neural Comp.*, 10:821–835, 1998. 93

P. Varona, J.J. Torres, R. Huerta, H.D.I. Abarbanel, and M. I. Rabinovich. Regularization mechanisms in the dynamics of spiking-bursting neurons. *Neural Networks*, 14:865–875, 2001. 104

L. Wang, E. E. Pichler, and J. Ross. Oscillations and chaos in neural networks: An exactly solvable model. *Proc. Natl. Acad. Sci. USA*, 87:9467–9471, 1990. 91

S. Wolfram. Cellular automata as models of complexity. *Nature*, 311:419–424, 1984. 92

Chapter 6

Neural Automata with Two Temperatures Parameters

6.1 Introduction and Model

The understanding of how the processing of information in neural media is influenced by the biophysical processes that take place at the synaptic level is an open question. In particular, the effect of synaptic dynamics and noise on complex functions such as associative memory is not yet well understood. In relation to this, it has been reported that short-term synaptic plasticity has a main role in the ability of some systems to exhibit switching between stored memories [Pantic et al., 2002]. The same behavior ensues assuming dynamics of the neuron threshold to fire [Horn and Usher, 1989]. The origin of the switching mechanism seems in both cases as a sort of fatigue of the postsynaptic neuron under repeated presynaptic simulation. This destabilizes the current attractor which may result in a transition to a new one. It would be interesting to put this on a more general perspective concerning the role of noise in associative memory tasks. With this aim, we present in this chapter a *stochastic neural automata* that involves two independent competing dynamics, one for

neurons and other for synapses.

Consider N (binary) neuron variables, $s_i = \pm 1$, any two of them linked by synapses of intensity w_{ij}; $i, j = 1, \ldots, N$. The interest is on the configurations $\mathbf{S} \equiv \{s_i\}$ and $\mathbf{W} \equiv \{w_{ij}\}$. In order to have a well–defined reference, we assume that interactions are determined by the Hopfield *energy* function. Furthermore, consistent with the observation that memory is a global dynamic phenomenon, we take the model dynamics determined at each time step by a single pattern, say μ. Consequently, $H(\mathbf{S}, \mathbf{W}; t) = -\frac{1}{2} \sum_i \sum_{j \neq i} w_{ij}^{\mu} s_i s_j$ with $\mu = \mu(t)$ and assuming the Hebbian learning rule, for example, $w_{ij}^{\mu} = \frac{k}{N} \xi_i^{\mu} \xi_j^{\mu}$, where, $\xi_i^{\mu} = \pm 1$ are the variables that characterize the μ pattern, one out of the P considered ones, and k is a proportionality constant. Therefore, each configuration $\mathbf{W}$ is unambiguously associated to a single μ, and we write $\mathbf{W} \equiv \mu$ in the following.

The above may be formulated by stating that the probability of any configuration $(\mathbf{S}, \mu)$ evolves in discrete time according to

$$P_{t+1}(\mathbf{S}, \mu) = \sum_{\mathbf{S}'} \sum_{\mu'} T[(\mathbf{S}, \mu)|(\mathbf{S}', \mu')] P_t(\mathbf{S}', \mu'), \tag{6.1}$$

where $T[(\mathbf{S}, \mu)|(\mathbf{S}', \mu')]$ represents the probability of jumping from $(\mathbf{S}', \mu')$ to $(\mathbf{S}, \mu)$. We explicitly consider here the case in which

$$T[(\mathbf{S}, \mu)|(\mathbf{S}', \mu')] \equiv T_0^{\mu'}[\mathbf{S}|\mathbf{S}'] \; T_1^{\mathbf{S}}[\mu|\mu'] \tag{6.2}$$

with $T_0^{\mu'}[\mathbf{S}|\mathbf{S}']$ corresponding to *Little dynamics*, i.e., parallel updating, so that $T_0^{\mu'}[\mathbf{S}|\mathbf{S}'] = \prod_{i=1}^{N} t_0^{\mu'}[s', i]$. Furthermore, $t_0^{\mu'}[s', i] \equiv \Psi[\beta_0 \Delta H^{\mu'}(s_i' \to s_i = \pm s_i')]$, where $\Psi(X)$ is an arbitrary function, except that it is taken to satisfy *detailed balance* and a suitable normalization (see Ref. [Marro and Dickman, 1999] for a discussion), β_0 is an (inverse) temperature parameter, and ΔH denotes the *energy* change brought about by the indicated transition. For changes in the synapses, we take $T_1^{\mathbf{S}}[\mu|\mu'] \equiv \Psi[\beta_1 \Delta H^{\mathbf{S}}(\mu' \to \mu)]$. After some algebra, one has that

$$\Delta H^{\mu'}(s_i' \to s_i = \pm s_i') = -k \xi_i^{\mu'} (s_i - s_i')(m'^{\mu'} - s_i' \xi_i^{\mu'}/N) \tag{6.3}$$

and

$$\Delta H^{\mathbf{S}}(\mu' \to \mu) = -\frac{1}{2} k N [(m^{\mu})^2 - (m^{\mu'})^2], \tag{6.4}$$

where $m^{\mu}(\mathbf{S}) \equiv m^{\mu}$ is the overlap between the current state $\mathbf{S}$ and pattern μ. The factor N in $\Delta H^{\mathbf{S}}$ appears because we assume *global* energy variations (i.e., all synapses are attempted to be changed at each step) instead of the energy variation per site in $\Delta H^{\mu'}$.

This model differs essentially from apparently close proposals, e.g., [Coolen et al., 1993, Marro et al., 1998, Torres et al., 1997]. Firstly, because it assumes the same time scale for changes in both $\mathbf{S}$ and μ. Secondly, the choice here for $T[(\mathbf{S}, \mu)|(\mathbf{S}', \mu')]$ amounts to drive neurons activity and synaptic intensities by different temperature, $\beta_0^{-1} \equiv T_0$ and $\beta_1^{-1} \equiv T_1$, respectively. The case of our model with a single pattern is equivalent to the equilibrium Hopfield model with $P = 1$; for more than one pattern, however, new non-equilibrium steady states ensue. This is closely due to the fact that $T[(\mathbf{S}, \mu)|(\mathbf{S}', \mu')]$ does not satisfy detailed balance [Marro and Dickman, 1999].

6.2 Monte Carlo Simulations

We report on some Monte Carlo simulations of this model which reveals an intriguing situation. Different regimes are shown in figure 6.1 depending on the values of temperatures T_0 and T_1. To distinguish between them, we introduce the overlap ($\mathbf{m}$) and the total number of jumps (j); there are three different phases occur that are close to the ones reported in [Pantic et al., 2002]: the *Ferromagnetic*, for $T_0 < T_0^3(T_1)$, with $\mathbf{m} \neq 0$ and $j = 0$. The system has *static* associative memory. The *Paramagnetic* , for $T_0 > T_0^1(T_1)$, with $\mathbf{m} = 0$ and $j = 0$, without any kind of associative memory and the *Oscillatory*, for $T_0^3(T_1) < T_0 < T_0^1(T_1)$, with $\mathbf{m} = 0$, $j \neq 0$. In this oscillatory phase which is illustrated in figure 6.2 the system has associative memory, like in Hopfield model. However, here it is a dynamic process, in the sense that the system trapped in any attractor corresponding with a pattern is able to jump to the

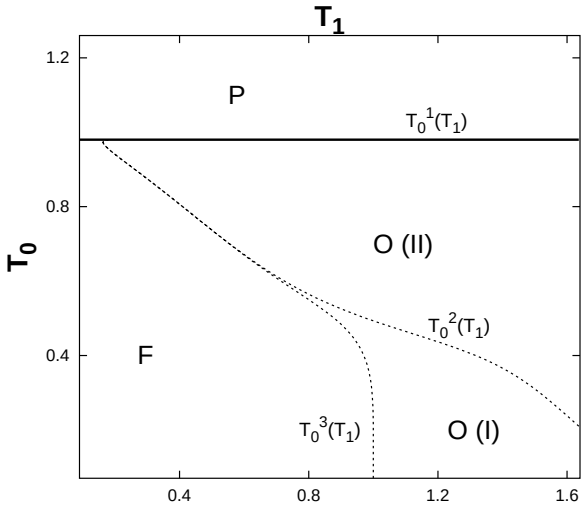

Figure 6.1: Phase diagram for the Neural Automata depicting three coexistence curves that define several phases; see the main text. Solid (dashed) lines means second (first) order transition. Here, $N = 16384$ and $P = 3$ spatial-correlated patterns with 20% of average overlap between any two of them.

other stored patterns. Because the probability of jumping depends on the overlaps, which is the total presynaptic current arriving to the postsynaptic neuron, this mechanism is, in general, a complex process. In order to study in detail the oscillatory phase, it turned out convenient to look at time correlations. Therefore, we used correlated patterns, namely, there was an average overlap $C^{\nu^1\nu^2} \equiv \frac{1}{N}\sum_{i=1}^{N} \xi_i^{\nu^1}\xi_i^{\nu^2}$, with $\nu^1, \nu^2 = 1, \ldots, P$, of 20% between any two of the stored patterns. The goal was to detect non-trivial correlations between jumps, so that we computed the time $\tau_{\nu\gamma}$ the system *remains* in pattern ν before jumping to pattern γ; $\sum_{\gamma=1}^{P} \tau_{\nu\gamma} = \tau_\nu$ is the total time the system stays in pattern ν. This reveals the existence of two different kinds of oscillatory behavior. One is such that $\tau_{\nu\gamma} \simeq \tau$, independent of ν and γ. That is, the system stays the same time at each pattern, so that jumping behaves as a completely random process, without any time correlation. This is denoted by *O(II)* in figure 6.1 . Even more interesting is phase *O(I)*. As the probability of jumping between patterns is activity dependent, lowering T_0 leads to non-trivial time correlations, namely, $\tau_{\nu\gamma}$ depends on both ν and γ. We also observe that $\tau_{\nu\gamma}$ differs from $\tau_{\gamma\nu}$. This peculiar behavior in O(I) suggests using our algorithm to code spatial–temporal information [Laurent et al., 2001, Rabinovich et al., 2001]. Consequently, the jumps between patterns can be either uncorrelated ($O(II)$) or time-correlated ($O(I)$) and the transition between them is discontinuous (first order).

6.3 Coarse-Graining Procedure

In principle, one may estimate from (6.1) how any observable $F(\mathbf{S}, \mu)$ evolves in time. The result is an equation $\langle F\rangle_{t+1} = f(\bar{K}, \langle F\rangle_t)$, where $\bar{K}$ is the set of control parameters and $\langle\cdots\rangle$ denotes statistical average with $P(\mathbf{S}, \mu)$ [Marro and Dickman, 1999].

Alternatively, one may be directly concerned with the time evolution for the probability of jumping in terms of the overlaps $\mathbf{m} \equiv \{m^\nu; \nu = 1, \ldots, P\}$.

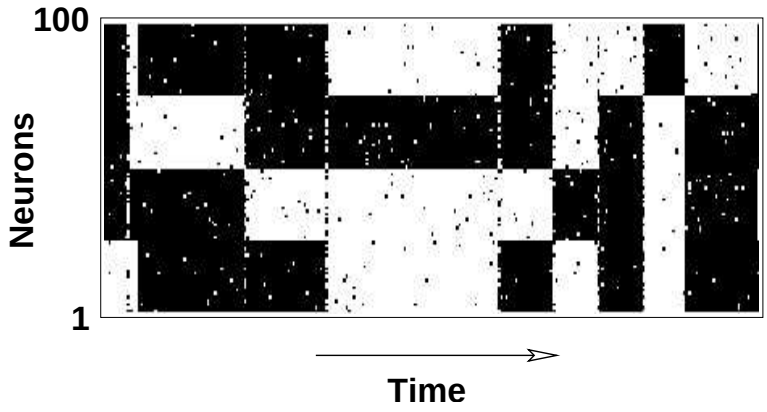

Figure 6.2: Activity of neurons versus time for $N = 100$ neurons and $P = 4$ patterns. Here, $T_0 = 0.9T_0^c$ and $T_1 = 1.69T_1^c$, where T_0^c and T_1^c are the corresponding critical values of temperatures.

One has that

$$\Pi_{t+1}(\mathbf{m}, \mu) \equiv \sum_{S} \delta[\mathbf{m} - \mathbf{m}(\mathbf{S})] P_{t+1}(\mathbf{S}, \mu) \tag{6.5}$$

satisfies

$$\Pi_{t+1}(\mathbf{m}, \mu) = \int d\mathbf{m}' \sum_{\mu'} \bar{T}[(\mathbf{m}, \mu)|(\mathbf{m}', \mu')]\, \Pi_t(\mathbf{m}', \mu'). \tag{6.6}$$

This amounts to reduce the degrees of freedom, from a number of order $2^N + 1$ in $(\mathbf{S}, \mu)$ to $P + 1$ in $(\mathbf{m}, \mu)$. Dealing with this sort of coarse–grained master equation requires an explicit expression for $\bar{T}[(\mathbf{m}, \mu)|(\mathbf{m}', \mu')]$. Starting in the equation (6.1), it is necessary to have an appropriate normalization for $T[(\mathbf{S}, \mu)|(\mathbf{S}', \mu')]$. This implies that $\sum_{\mathbf{S}} \sum_{\mu} T[(\mathbf{S}, \mu)|(\mathbf{S}', \mu')] = 1$. Besides, because $\mathbf{W} \equiv \mu$ is assumed, we have in addition that $\sum_{\mathbf{S}} T_0^{\mu'}[\mathbf{S}|\mathbf{S}'] = 1$ for any $\mu' = 1, \ldots, P$ and $\sum_{\mu} T_1^{\mathbf{S}}[\mu|\mu'] = 1$ for any $\mathbf{S}$. In the case of parallel updating, it is enough to consider that

$$t_0^{\mu'}[s', i] = \frac{\Psi[\beta_0 \Delta H^{\mu'}(s_i' \to s_i = \pm s_i')]}{1 + \Psi[2\beta_0 \xi_i^{\mu'} s_i' k(m_{\mu'}' - \frac{1}{N} \xi_i^{\mu'} s_i')]} \tag{6.7}$$

and for changes in synapses that

$$T_1^{\mathbf{S}}[\mu|\mu'] = \frac{\Psi[\beta_1 \Delta H^{\mathbf{S}}(\mu' \to \mu)]}{1 + \sum_{\nu \neq \mu'} \Psi[\beta_1 \Delta H^{\mathbf{S}}[(\mu' \to \nu)]}\ . \tag{6.8}$$

In the following we will write that $T_1^S[\mu|\mu'] \equiv \bar{\Psi}\{\beta_1 \Delta H^S[(\mu' \rightarrow \mu)]\}$, being $\bar{\Psi}$ normalized according to equation (6.8). The energy cost corresponding to each transition is introduced in the equations (6.3) and (6.4).

Taking into account that the equation (6.7) only depends on the sign variables $\xi_i^{\mu'} s_i$ and $\xi_i^{\mu'} s'_i$ it is possible to rewrite it as

$$t_0^{\mu'}[s', i] \equiv \exp(A') \exp(B' \xi_i^{\mu'} s_i) \exp(C' \xi_i^{\mu'} s'_i) \exp(D' s'_i s_i). \tag{6.9}$$

We have denoted $\mathcal{F}(\mathbf{m}) \equiv \mathcal{F}$ and $\mathcal{F}(\mathbf{m}') \equiv \mathcal{F}\prime$, being $\mathcal{F}$ any generic function. Note that the set of constants A', B', C' and D' depend on $m'^{\mu'}$, β_0, N and the function $\Psi(X)$ chosen in the equation (6.7). For the constants, after some algebra, it is possible to get

$$\begin{aligned}
\exp(4A'^{\mu'}) &\equiv \frac{\Psi[r'^{\mu'}(-,\beta_0)]\ \Psi[-r'^{\mu'}(+,\beta_0)]}{\{1+\Psi[r'^{\mu'}(-,\beta_0)]\}^2\ \{1+\Psi[-r'^{\mu'}(+,\beta_0)]\}^2} \\
\exp(4B'^{\mu'}) &\equiv \frac{\Psi[-r'^{\mu'}(+,\beta_0)]}{\Psi[r'^{\mu'}(-,\beta_0)]} \\
\exp(4C'^{\mu'}) &\equiv \frac{\{1+\Psi[-r'^{\mu'}(+,\beta_0)]\}^2\ \Psi[r'^{\mu'}(-,\beta_0)]}{\{1+\Psi[r'^{\mu'}(-,\beta_0)]\}^2\ \Psi[-r'^{\mu'}(+,\beta_0)]} \\
\exp(4D'^{\mu'}) &\equiv \frac{1}{\Psi[r'^{\mu'}(-,\beta_0)]\ \Psi[-r'^{\mu'}(+,\beta_0)]}\ ,
\end{aligned} \tag{6.10}$$

where we have defined

$$r'^{\mu'}(\pm,\beta_0) \equiv 2\beta_0 k(m'^{\mu'} \pm \frac{1}{N}). \tag{6.11}$$

As a consequence of parallel updating, T_0 factorizes and remains in the form

$$T_0^{\mu'}[\mathbf{S}|\mathbf{S}'] = \exp(NA'^{\mu'}) \exp(NB'^{\mu'} m^{\mu'}) \exp(NC'^{\mu'} m'^{\mu'}) \prod_{i=1} \exp(D'^{\mu'} s'_i s_i) \tag{6.12}$$

In order to get equation (6.6) we follow the same procedure reported in [Coolen, 2001]. We start at equation (6.5) and substitute the time evolution of $P_{t+1}(\mathbf{S}, \mu)$ defined by the master equation (6.1). Considering the jumping probability given by (6.2) and taking into account the properties $\delta(x) = \int \frac{dk}{2\pi} \exp(jkx)$ and $\int d\mathbf{m}' \delta[\mathbf{m}' - \mathbf{m}(\mathbf{S}')] = 1$ finally we get

$$\begin{aligned}
\Pi_{t+1}(\mathbf{m}, \mu) &= (\frac{1}{2\pi})^P \int\int d\mathbf{m}' d\mathbf{k} \sum_{\mathbf{S}} \sum_{\mathbf{S}'} \sum_{\mu'} \delta[\mathbf{m}' - \mathbf{m}(\mathbf{S}')] \exp(j \sum_{\nu=1} k^\nu m^\nu) \times \\
&\quad \times \exp[-j \sum_{\nu=1} k^\nu m^\nu(\mathbf{S})]\ T_0^{\mu'}[\mathbf{S}|\mathbf{S}']\ T_1^S[\mu|\mu'] P_t(\mathbf{S}', \mu'),
\end{aligned} \tag{6.13}$$

where **k** is the conjugated momentum of **m** and j the imaginary unit.

To get easier expressions, we substitute the equations (6.8) and (6.12) in (6.13) and collect all $\mathbf{S}'$–dependence introducing the function

$$I(\mathbf{S}', \mu') \equiv \sum_{\mathbf{S}} \exp[-j \sum_{\nu} k^{\nu} m^{\nu}(\mathbf{S})] \prod_{i=1} \exp(D'^{\mu'} s'_i s_i). \tag{6.14}$$

In the most cases, almost never it is possible to add exactly all terms implied in the *entropic* contribution given by equation (6.14). However, applying the overlap definition it is possible to rewrite $I'(\mathbf{S}', \mu')$ like

$$I(\mathbf{S}', \mu') = \exp\{N[\frac{1}{N} \sum_{i=1}^{N} (\nu'^{0}_{i,\mu'} + s'_i \nu'^{1}_{i,\mu'})]\} \tag{6.15}$$

with

$$\begin{aligned} \exp(2\nu'^{0}_{i,\mu'}) &\equiv 4\cosh(D'^{\mu'} - j\eta_i)\cosh(D'^{\mu'} + j\eta_i) \\ \exp(2\nu'^{1}_{i,\mu'}) &\equiv \frac{\cosh(D'^{\mu'} - j\eta_i)}{\cosh(D'^{\mu'} + j\eta_i)} \end{aligned} \tag{6.16}$$

and $\eta_i \equiv \sum_{\nu} \frac{k^{\nu} \xi_i^{\nu}}{N}$.

Theorem 1 *If* $D = 0$, *the system evolves exactly through its overlaps.*

Proof. *In effect, assuming* $D = 0$ *the equations (6.16) give that* $\nu_i^1 = 0$ *and* $\exp(\nu_i^0) = 2\cosh(j\eta_i)$. *Therefore, the function given by (6.14) does not depend on* $\mathbf{S}'$ *and all terms implied in the equation (6.13) can be add exactly.*

Corollary 1 *An exact description of the mesodynamics (6.6) dealt by (6.12) assume to take* $\Psi(X) = \exp(-X/2)$.

Proof. *As a consequence of Theorem* 1, *the definition (6.10) gives for* $D = 0$ *that*

$$\Psi(r_0 - \zeta)\Psi(r_0 + \zeta) = \exp(-r_0)\exp(-\zeta), \tag{6.17}$$

for all Ψ *satisfying that* $\Psi(X) = \Psi(-X)\exp(-X)$ *(detailed balance). We have denoted, besides,* $r_0 \equiv 2\beta_0 k m'^{\mu'}$ *and* $\zeta \equiv 2\beta_0 k \frac{1}{N}$, *in order to have separately the solution of its size-dependent corrections, which can be controlled by expanding the constraint (6.17) around* $\zeta \approx 0$, *i.e.* $N \to \infty$ *(thermodynamic limit). The result is*

$$(1+\zeta)\Psi^2(r_0) + [\frac{\Psi^2(r_0)}{2} - \Psi'^2(r_0) + \Psi(r_0)\Psi''(r_0)]\zeta^2 + \mathcal{O}(\zeta^3) = \exp(-r_0) \tag{6.18}$$

Note that orders ζ^2 are negligible for enoughly large finite-systems. Therefore, after rescaling the constant $(1+\zeta)$ in time at(6.6) , we obtain that $\Psi(X) = \exp(-X/2)$.

Corollary 1 guarantees the explicit form of the function $\Psi(X)$ to simulate the system and define the set of constants (6.10) appearing at (6.12). Under the conditions of Theorem 1, one has that the jumping probability (6.6) is

$$\bar{T}[(\mathbf{m},\mu)|(\mathbf{m}',\mu')] = (\frac{1}{2\pi})^P \int d\mathbf{k} \exp(j\sum_{\nu=1} k^\nu m^\nu) I(\mu')\, T_0^{\mu'}(\mathbf{m}|\mathbf{m}')\, T_1^{\mathbf{m}}(\mu|\mu') \quad (6.19)$$

where after using the δ–function properties the quantities

$$T_0^{\mu'}(\mathbf{m}|\mathbf{m}') = \exp(NA'^{\mu'}) \exp(NB'^{\mu'} m^{\mu'}) \exp(NC'^{\mu'} m'^{\mu'}) \quad (6.20)$$

and

$$T_1^{\mathbf{m}}(\mu|\mu') = \bar{\Psi}\{\beta_1 \Delta H^{\mathbf{m}}[(\mu' \to \mu)]\} \quad (6.21)$$

do not depend on $\mathbf{S}$ and $\mathbf{S}'$ anymore. For a practical convenience, in order to be possible apply the steepest descends method as was explained in [Coolen, 2001], we introduce in (6.13) the change of variable $k^\nu \equiv Nq^\nu$ to obtain

$$\bar{T}[(\mathbf{m},\mu)|(\mathbf{m}',\mu')] \equiv \mathcal{K} \int d\mathbf{q} \exp[N\Phi(\beta_0,\beta_1,\mathbf{m},\mathbf{m}',\mathbf{q},\mu,\mu',N)] \quad (6.22)$$

with $\Phi \equiv \Phi_0 + \Phi_1$. Here, $\mathcal{K} \equiv (\frac{N}{2\Pi})^P$ is a constant and we have defined

$$\begin{aligned} \Phi_0(\beta_0,\mathbf{m},\mathbf{m}',\mathbf{q},\mu',N) &\equiv j\sum_\nu q^\nu m^\nu + A'^{\mu'} + B'^{\mu'} m^{\mu'} + C'^{\mu'} m'^{\mu'} + \nu^0, \\ \Phi_1(\beta_1,\mathbf{m},\mu,\mu',N) &\equiv \frac{1}{N}\log[\bar{\Psi}\{\beta_1 \Delta H^{\mathbf{m}}[(\mu' \to \mu)]\}] \end{aligned} \quad (6.23)$$

and $N\nu^0 \equiv \sum_{i=1}^N \nu_i^0$. It is convenient to note that the dynamics driven by (6.22) allows to evolve the variables μ and $\mathbf{m}$ separately in time. Changes in μ, given $\mathbf{m}$, are controlled by Φ_1 while $\mathbf{m}$ evolves with a fixed μ' influenced by Φ_0.

The form of (6.22) allows to apply the saddle point method to obtain the steady states. In the thermodynamic limit it is satisfied that

$$\lim_{N\to\infty} \bar{T}[(\mathbf{m},\mu)|(\mathbf{m}',\mu')] = \delta[\mathbf{m} - \mathbf{m}^*(\mathbf{m}',\mu')]\delta[\mu - \mu^*(\mathbf{m}',\mu')] \quad (6.24)$$

where $\mathbf{m}^*$ and μ^* defines the saddle point solution, which ensures that the 2ν different derivatives

$$\begin{aligned}\frac{\partial\Phi_0}{\partial q^\nu} &= jm^\nu + \frac{j}{N}\sum_i \xi_i^\nu \tanh(j\eta_i)\\ \frac{\partial\Phi_0}{\partial m^\nu} &= jq^\nu + \frac{\beta_0 k m'^{\mu'}}{2}\delta_{\mu',\nu}\end{aligned} \tag{6.25}$$

with $\nu = 1,\ldots,P$, are all equal to 0 and an extremal condition of Φ_1. The variable η_i was introduced in equations (6.16). The saddle point solution is

$$m^{*\nu}(\mathbf{m}',\mu') = C^{\nu\mu'}\tanh(\frac{\beta_0 k}{2}m'^{\mu'}) \tag{6.26}$$

and

$$\mu^*(\mathbf{m},\mu') = \{\mu\in P \;/\; [(m^\mu)^2-(m^{\mu'})^2] \text{ is max}\}. \tag{6.27}$$

where we have introduced $C^{\nu\gamma}\equiv\frac{1}{N}\sum_{i=1}^N \xi_i^\nu\xi_i^\gamma$, which is the spatial correlation between the patterns ν and γ. *Orthogonal* (uncorrelated) patterns means that $C^{\nu\gamma}\simeq\delta_{\nu\gamma}$. Two comments about the equations (6.26) and (6.27). First, because the argument of the tanh in equation (6.26) does not depend on the site i, averaging over patterns realizations is not necessary in this model. Secondly, due to (6.27), the dynamics is completely determined through the initial condition, i.e μ^* at $time = 0$, that unless some special restriction is in principle chosen randomly. However, Monte Carlo simulations of the system [Cortes et al., 2004] show how the temperature controlling changes in synapses intensity β_1 scales clearly with N. This solves the apparently *trivial* dynamical behavior, completely determined by its initial condition. Consequently, this assumption changes essentially the form of equations (6.22) and (6.24). Now, they are

$$\bar{T}[(\mathbf{m},\mu)|(\mathbf{m}',\mu')] = \bar{\Psi}[\beta_1\Delta H^{\mathbf{m}}(\mu'\to\mu)]\mathcal{K}\int d\mathbf{q}\exp[N\Phi_0(\beta_0,\mathbf{m},\mathbf{m}',\mathbf{q},\mu',N)] \tag{6.28}$$

and

$$\lim_{N\to\infty}\bar{T}[(\mathbf{m},\mu)|(\mathbf{m}',\mu')] = \delta[\mathbf{m}-\mathbf{m}^*(\mathbf{m}',\mu')]\bar{\Psi}[\beta_1\Delta H^{\mathbf{m}}(\mu'\to\mu)]. \tag{6.29}$$

With this in mind, the dynamical equations for any generic observable $F\equiv F(\mathbf{m},\mu)$ can be obtained using equations (6.6), (6.29) and (6.26). They have the

form

$$\langle F\rangle_{t+1} = \sum_{\mu} \langle F\bar{\Psi}[\beta_1 \Delta H(\mu' \to \mu)]\rangle_t^* \tag{6.30}$$

where $\langle\cdots\rangle_t$ denotes statistical average over $\Pi_t(\mathbf{m}', \mu')$ and * which is evaluated in the saddle point m^*. As an example, we consider the observable overlap m^γ, with fixed γ and consequently independent of μ. Directly from (6.30) one has that

$$\langle m^\gamma\rangle_{t+1} = \int d\mathbf{m}' \sum_{\mu} \sum_{\mu'} C^{\gamma\mu'} \tanh(\frac{\beta_0 k}{2} m'^{\mu'})\bar{\Psi}[\beta_1 \Delta H^*(\mu' \to \mu)]\Pi_t(\mathbf{m}', \mu') \tag{6.31}$$

Together this equation, the probability $\Pi_t(\mathbf{m}', \mu')$ evolves in time according to (6.6). This set of coupled *continuous* maps describes a complex *mesodynamics*. In the next chapter we study some approximations to this problem.

6.4 Discussion

We have introduced a neural automata with synaptic noise modulated by two different thermal baths. The time evolution of the system is dealt by (6.28) and allows to have two independent mechanisms to evolve the system: one, given a pattern, which defines a configuration of synaptic intensities, explains how the system changes between different configurations on the neural activity. The other, is responsible of changes between any two different patterns, fixed an neural activity configuration. The main approach after applying a coarse-graining procedure is that to average over patterns realizations is not necessary in this model, because the dependence on patterns can be extracted of the tanh functions which characterize an steepest descend solution in attractor neural networks. We present also Monte Carlo simulations which depict an intriguing phase-diagram. For $\alpha \to 0$ (load parameter), we find three phases: ferromagnetic, paramagnetic and oscillatory. The switching can be uncorrelated or time-correlated. Therefore, chosen properly the system parameters values, it seems to be useful to model dynamical processes taken place, for instance, in the olfactory bulb of insects, where it is possible to associate different

odors to different spatio–temporal patterns of neuronal activity. There are a increasing belief [Laurent et al., 2001, Rabinovich et al., 2001], that those patterns are associated to the fact of the neural dynamics is visiting a particular set of unstable attractors, each one corresponding with a particular odor.

Bibliography

A.C.C. Coolen. Statistical mechanics of recurrent neural networks: Ii. dynamics. In F. Moss and C. Gielen, editors, *HandBook of Biological Physics*, volume 4, pages 597–662. Elsevier Science, 2001. 117, 119

A.C.C. Coolen, R.W. Penney, and D. Sherrington. Coupled dynamics of fast spins and slow interactions: An alternative perspective on replicas. *Phys. Rev. B*, 48:16116–16118, 1993. 113

J.M. Cortes, P.L. Garrido, J. Marro, and J.J. Torres. Switching between memories in neural automata with synaptic noise. *Neurocomputing*, 58-60:67–71, 2004. 120

D. Horn and M. Usher. Neural networks with dynamical thresholds. *Phys. Rev. A*, 40:1036–1044, 1989. 111

G. Laurent, M. Stopfer, R.W. Friedrich, M.I. Rabinovich, A. Volkovskii, and H.D.I. Abarbanel. Odor encoding as an active, dynamical process: Experiments, computation and theory. *Annual Review of Neuroscience*, 24:263–297, 2001. 115, 122

J. Marro and R. Dickman. *Nonequilibrium Phase Transitions in Lattice Models*. Cambridge University Press, 1999. 112, 113, 115

J. Marro, P. L. Garrido, and J. J. Torres. Effect of correlated fluctuations of synapses in the performance of neural networks. *Phys. Rev. Lett.*, 81:2827–2830, 1998. 113

L. Pantic, J.J. Torres, H.J. Kappen, and S.C.A.M. Gielen. Associative memmory with dynamic synapses. *Neural Comp.*, 14:2903–2923, 2002. 111, 113

M.I. Rabinovich, A. Volkovskii, P. Lecanda, R. Huerta, H.D.I. Abarbanel, and G. Laurent. Dynamical encoding by networks of competing neuron groups: Winnerless competition. *Phys. Rev. Lett.*, 87:068102, 2001. 115, 122

J.J. Torres, P.L. Garrido, and J. Marro. Neural networks with fast time-variation of synapses. *J. Phys. A: Math. Gen.*, 30:7801–7816, 1997. 113

Chapter 7

Neural Automata which allows for Categorization

7.1 Motivation and Model

Nowadays, there is a multitude of technical applications requiring for "categorization", e.g. assigning of objects to zero or more predefined classes. In all of them massive storage of data must be firstly preserved for then being consulted. The most emergent situation in recent times is text-categorization on WWW searchers, due to the availability of ever larger numbers of text documents in digital form and to the ensuing need to organize them for easier use. Examples include from classifying web documents to search articles or researchers in data bases of science [Berners-Lee et al., 1994]. The dominant aim is to build software tools capable of classifying by learning the characteristics of the categories from a training set of pre-classified documents [Aphinyanaphongs et al., 2004, Doolittle, 2004]. In biotechnology, the need for accurate, automated protein classification still remains unsolved, due to extreme diversity among its members [Cheng et al., 2005]. Other industrial devices which need optimal algorithms for classification are the electronic noses, e.g chemical sensors with

a pattern recognition system (normally, artificial neural networks). They are being developed as systems for the automated detection and classification of odors, vapors and gases, which can play a main role for defense in "chemical wars". In civil applications, as for instance, the food industry use such devices as aids for quality control or process-monitoring tools [Vazquez et al., 2004]. Moreover, multitude of biological frameworks need of these (natural) strategies to make possible categorization, for instance, the early olfactory processing [Laurent et al., 2001]. Against machine learning methods, as for instance decision trees and naive Bayes classifiers, we present an alternative for categorization based on stochastic neural automatas. We (computationally) explore the complex spatio-temporal dynamics and suggest by using the described trajectories for the neural automata as a a tool for categorization. We observe that depending on correlations among stored patterns, is possible to establish a hierarchical classification among its elements.

7.2 Mean-field Analysis

In the next lines we study the consequences of assuming a mean field treatment, e.g $\langle \mathbf{m} \rangle \approx \mathbf{m}$, in equations (6.31) and (6.6). By construction, $\Pi_t(\mathbf{m}', \mu')$ is properly normalized, and this implies that $\int d\mathbf{m}' \Pi_t(\mathbf{m}'|\mu') = 1$ and $\sum_{\mu'} \Pi_t(\mu') = 1$, where $\Pi_t(m'|\mu')$ stands for the conditional probability of $\mathbf{m}'$ given μ' and is defined like $\Pi_t(\mathbf{m}', \mu') \equiv \Pi_t(\mathbf{m}'|\mu')\Pi_t(\mu')$. To obtain how overlaps evolve in time according to equation (6.30) we take that $F(\mathbf{m}, \mu) = m^\gamma$ with $\gamma = 1, \ldots, P$ and we denote $\bar{\Psi}[\beta_1 \Delta H^*(\mu' \to \mu)] \equiv \omega^\mu_{\mu'}(\mathbf{m}^*)$. The result is

$$m^\gamma_{t+1} = \sum_\mu \sum_{\mu'} C^{\gamma\mu'} \omega^\mu_{\mu'}(\mathbf{m}^*_t) \tanh(\bar{\beta_0} m^{\mu'}_t) \Pi_t(\mu'), \tag{7.1}$$

where $2\bar{\beta_0} \equiv \beta_0 k$. By construction of the jumping probability (6.28) we have in addition the constraint $\sum_\mu \omega^\mu_{\mu'} = 1$ for any $\mu' = 1, \ldots, P$, which allows to rewrite (7.1) as

$$m^\gamma_{t+1} = \sum_\mu C^{\gamma\mu} \tanh(\bar{\beta_0} m^\mu_t) \Pi_t(\mu). \tag{7.2}$$

Hence, the unique dependence on β_1 is through the probability $\Pi_t(\mu)$. To close the equations given by (7.2), we need to determine how the probability $\Pi_t(\mu')$ evolved in time. Summing over $\mathbf{m}$ in both sides of equation (6.6), and taking into account (6.29), mean field assumption for overlaps gives

$$\Pi_{t+1}(\mu) = \sum_{\mu'} \omega^{\mu}_{\mu'}(\mathbf{m}^*)\Pi_t(\mu') \tag{7.3}$$

The dynamical (mean-field) behavior of overlaps is defined trough equations (7.1) and (7.3). As an example, we consider the simplest case of two patterns, e.g. $\gamma = 1, 2$. The set of (mean-field) dynamical equations for overlaps is

$$\begin{aligned}
m^{\gamma}_{t+1} &= C^{\gamma 1}\tanh(\beta_0 m^1_t)\Pi^1_t + C^{\gamma 2}\tanh(\beta_0 m^2_t)\Pi^2_t, \\
\Pi^{\gamma}_{t+1} &= \omega^{\gamma}_1\Pi^1_t + \omega^{\gamma}_2\Pi^2_t, \\
\omega^{j}_{i} &= \frac{\Psi[\beta_1\Delta H^*(i\to j)]}{1+\sum_{k\neq i}\Psi[\beta_1\Delta H^*(i\to k)]}, \\
\Delta H^*(i\to j) &= [1-(C^{ij})^2]\tanh(\beta_0 m^i_t)^2,
\end{aligned} \tag{7.4}$$

where we have denoted $\Pi^{\gamma}_t \equiv \Pi_t(\gamma)$ with $\gamma = 1, 2$. Some comments about this set of equations. Firstly, they do not show switching behavior, and therefore a mean-field assumption in the equations (6.31) and (6.6) is too strong, and some necessary correlations to jump among different patterns must be destroyed. However, they show two important facts. (1) As is expected from a jumping probability given by (6.28), all dependences on the temperature controlling synaptic changes β_1 appears in the probability Π^{γ}_t and (2) appear terms which depend on C^{ij}, for any two patterns i and j, and this reveals the importance of these (spatial) correlations on the system dynamics.

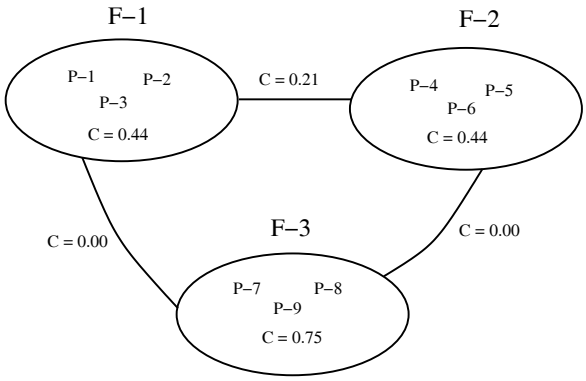

Figure 7.1: Three different families (F) of pattens (P) defined according to the partial correlation (C) defined in main the text.

7.3 Mesodynamics combined with Monte Carlo Simulations

In the next section, we combine a mesodynamics defined by the saddle point solution (6.26) with a Monte Carlo dynamics for the pattern μ. The reason is going a next step further, in order to show switching behavior, of the mean-field assumption studied in the previous section. We have seen that equation (6.28) allows to have two independent mechanisms to deal the system: one, given a pattern μ' defining an intensity synapses configuration, which is controlled by T_0 explains how the system goes from $\mathbf{m}'$ to $\mathbf{m}$. The other, monitored by T_1 is responsible of changes between any two different patterns μ' and μ, fixed an overlaps configuration. This allows to apply a combination between a mesodynamics for overlaps, coming from a coarse-graining procedure over $\mathbf{S}$–variables, and Monte Carlo simulations for the dynamics of μ. The result is in agreement of simulations. The procedure is the next:

1. Define P patterns in the system. Compute the correlation matrix $C^{\nu^1\nu^2}$, with $\nu^1, \nu^2 = 1, \ldots, P$ appearing in the equation (6.26) and defined as $\frac{1}{N}\sum_{i=1}^{N} \xi_i^{\nu^1}\xi_i^{\nu^2}$.

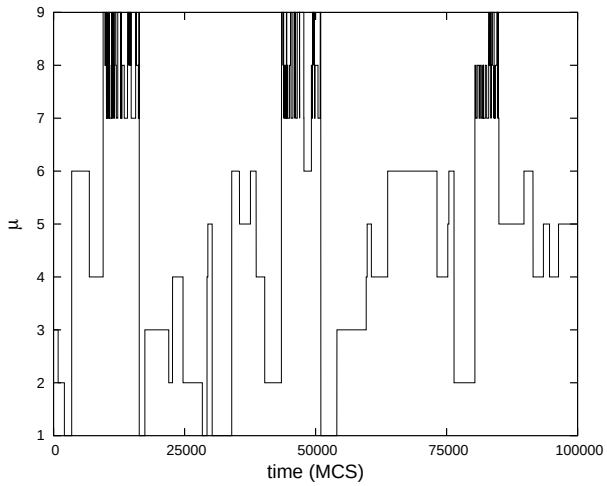

Figure 7.2: Time evolution for the index μ which, defining different synaptic intensities, shows swithching between the different patterns represented in figure 7.1. The neural automata identifies, by detecting correlations among them, patterns 7, 8 y 9 for constituting the same family.

2. Given a pattern, μ^{initial} and a configuration $\mathbf{m}_t$, obtain a new one μ^{final} with probability $\bar{\Psi}[\beta_1 \Delta H^{\mathbf{m}_t}(\mu^{\text{initial}} \rightarrow \mu^{\text{final}})]$ defined in (6.21).

3. Iterate all overlaps applying $m_{t+1}^{\gamma} = C^{\gamma\mu^{\text{final}}} \tanh(\bar{\beta_0} m_t^{\mu^{\text{final}}})$, being $\bar{\beta_0} \equiv \frac{\beta_0 k}{2}$.

4. Do $\mu^{\text{initial}} = \mu^{\text{final}}$ and $t = t + 1$.

5. Go to (2) and so on.

This dynamics has a peculiar spatio-temporal behavior. To study it, we are going to simulate different cases. In the first one, we introduce $P = 9$ patterns with partial correlations $C^{\nu^1\nu^2}$ as illustrated by figure 7.1. In figure 7.2 we represent the temporal evolution of the index μ as a function of time, e.g. $\mu(t)$. The trajectory in time allows for identification of all the different patterns ($P = 9$). However, after following its time trajectory, solely is possible include the 7, 8 y 9 to constitute the same family (F3). Thus, we have a mechanism to

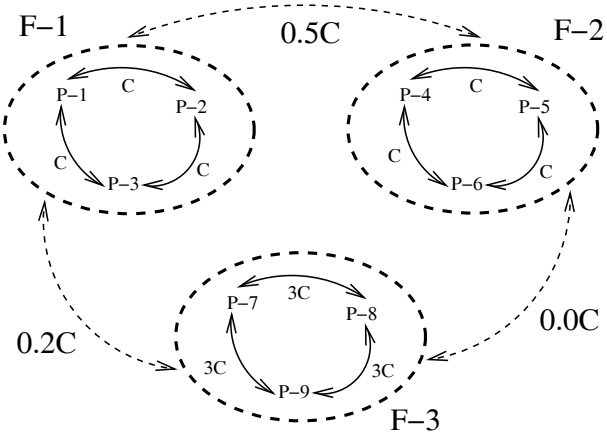

Figure 7.3: Similar to figure 7.1, we represent three different families defined as a function of a free parameter C.

detect correlations between different elements, which can be used to establish a hierarchical search on different systems. However, in figure 7.1 families 1st and 2nd are indistinguibles respecting the 3th one, and consequently the system is not able to show (temporal) differences between them.

In order to go quantitatively further, to measure this feature which allows for classification and categorization, depending on the correlations among the different elements, we compute the time $\tau_{\nu\gamma}$ in which the system remains in pattern ν before jumping to pattern γ. Thus, $\sum_{\gamma=1}^{P} \tau_{\nu\gamma} = \tau_\nu$ is the total time the system stays in pattern ν. We consider the sketch illustrated in figure 7.3, which does not establishes any ambiguity as occurred in figure 7.1. The synaptic noise is chosen inside the region $O(I)$ in the phase-diagram 6.1. Note, that although those values depicted in 6.1 have been obtained by Monte Carlo simulations of the system, e.g. microscopic dynamics, extensive Monte Carlo simulations show that both the microscopic and mesoscopic dynamics defined in this section are in full agreement. In figure 7.4 we illustrate how the temporal evolution of the index μ is strongly correlated inside of $O(I)$. For that, we represent the autocorrelation function in the steady state for different values of synaptic noise (T_1) , e.g. $\mathrm{corr}(\delta) \equiv \langle \mu(t^* + \delta)\mu(t^*)\rangle - \langle \mu(t^*)\rangle^2$,

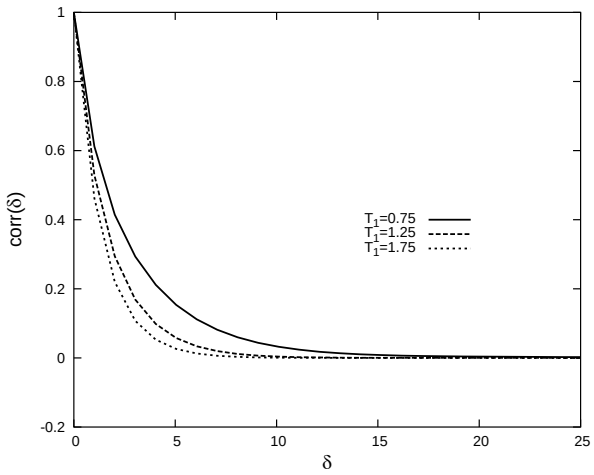

Figure 7.4: Autocorrelation function of the index μ for different values of the synaptic noise, e.g. from top to bottom, $T_1 = 0.75, 1.25, 1.75$ in units of the critical value T_1^c, as illustrated in figure 6.1 and delimiting the beginning of the oscillatory phase. The set of patterns is that illustrated in figure 7.3 for $C = 40\%$. The temperature in neurons activity is fixed to $T_0 = 0.05$. We divide the total number of Monte Carlo Steps (MCS) in the steady state in $50 \cdot 10^4$ different intervals of size 10^2. Statistical errors are negligible.

where $\langle \cdots \rangle$ denotes standard average and t^* denotes any time in the steady state. We are interested in the point T_1 such as the correlation temporal remains during a longer time. Therefore, we take the point of the phase-diagram, $\{T_0, T_1\} = \{0.05T_0^c, 0.75T_1^c\}$, and we present a systematic computational study. We compute the probability distribution, namely $P(\tau_{\nu\gamma})$, for any ν, γ patterns. Figure 7.5 illustrates both probability distributions for patterns belonging to the same and different families for a fixed C. The neural automata is able to detect, during the time-trajectory, patterns constituenting a same family. We are interesting precisely in this hierarchical search. In figure 7.6 we compute the probability distribution of $\tau_{\nu\gamma}$, but, however, this time ν and γ indicate any two different families. The resulting probability distribution represented in figure 7.6 fits to Poisson, which characterizes a large number of counting

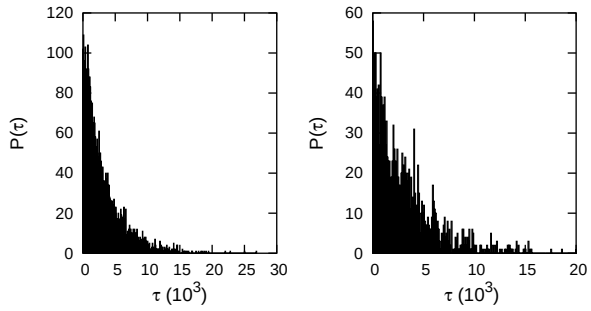

Figure 7.5: Probability distribution for the time the system stays in a pattern before jumping to another one in the phase O(I). The configuration of patterns has been chosen according to the sketch illustrated in figure 7.3 for $C = 40\%$. The left graph is for transitions from $\mu = 1$ to $\mu = 2$ (inside the same family) and the right one from $\mu = 1$ to $\mu = 9$ (belonging to different family).

processes, as radioactive nuclear disintegration, the number of phone calls to a phone central office, the number of arrived cosmic rays, etc. In all of them the important variable is the number of events. Therefore, the system can classify different patterns for constituting a same group, simplely for monitoring the frequency between jumps from any two elements, which is larger when their (spatial) correlation increases. As a test of Poisson distribution, in figure 7.7 we represent the fraction between the mean and the standard deviation for different values of the (partial) correlation C appearing in figure 7.3 and for three values of T_1.

7.4 Some Simulations in Real Systems

In previous sections we have simulated sets of different patterns, constituting different families as illustrated by figures 7.1 and 7.3. Both of them have been made in the computer, by using an algorithm able to add some correlations to the patterns, which initially are chosen totally uncorrelated. In this section, we simulate a real system, e.g. a set of 15 patterns such represented in figure 7.8. Different persons form different families, each one with 5 different shots

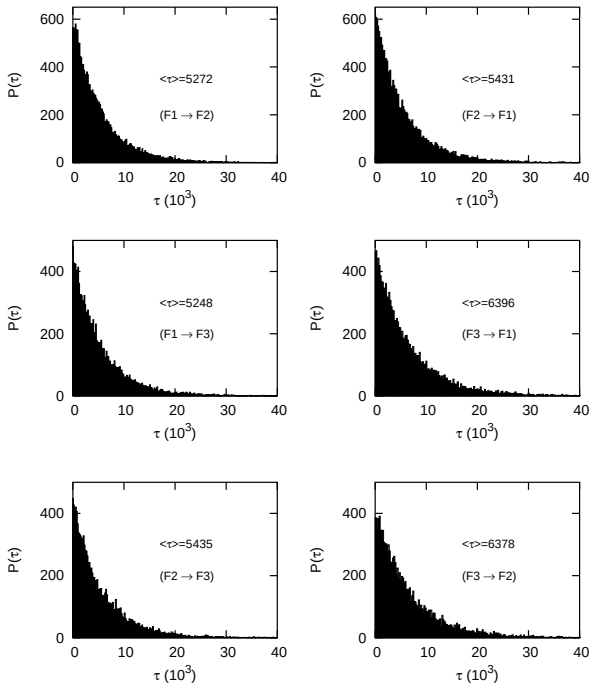

Figure 7.6: Probability distribution for the remaining time in a family before jumping to another one. Different families follows the sketch represented in figure 7.3 for $C = 40\%$. The time-average and different transitions among each respective family are indicated in the graph. We take $T_1 = 0.75T_1^c$ and $T_0 = 0.05T_0^c$.

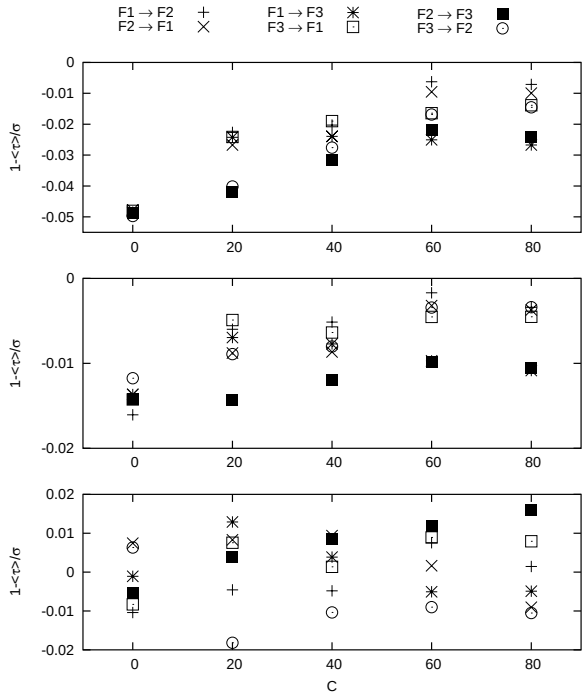

Figure 7.7: The relation between the mean and the standard deviation for the probability distributions depicted in figure 7.6 as a (numerical) test of a Poisson distribution. The different families of patterns, characterized by the the partial correlation C are those represented in the sketch in figure 7.3. Here, we take $C(\%) = 0, 20, 40, 60, 80$ and from bottom to top $T_1 = 0.75, 1.25, 1.75$, normalized by T_1^c and the transitions between families are showed on the top.

Figure 7.8: Different families associated to different persons. Each family is formed for patterns, which correspond with different shots for each individuo. The photos has been obtained from The Laboratory for Communications Engineering within the Cambridge University Department of Engineering.

at different positions corresponding to the same individuo. We analyse the system with a similar procedure than that reported in previous sections.

Firstly, we represent the probability distribution function between different individuos or families. The result is represented in figure 7.9.

Finally, in order to show a fitted data following a Poisson distribution we represent in figure 7.10 the relation between the mean of the remaining time inside families before jumping to another ones, and its standard deviation against different values of T_1.

7.5 Discussion

We have presented Monte Carlo simulations for the neural automata introduced in previous chapter 6. We analyse the system by combining a mesoscopic dynamics obtained in chapter 6 and Monte Carlo simulations for the chosen pattern, which defines a configuration of synaptic intensities. In special, we study the time-correlations showed in the oscillatory phase. This switching behavior has been explained in different places in the development of this the-

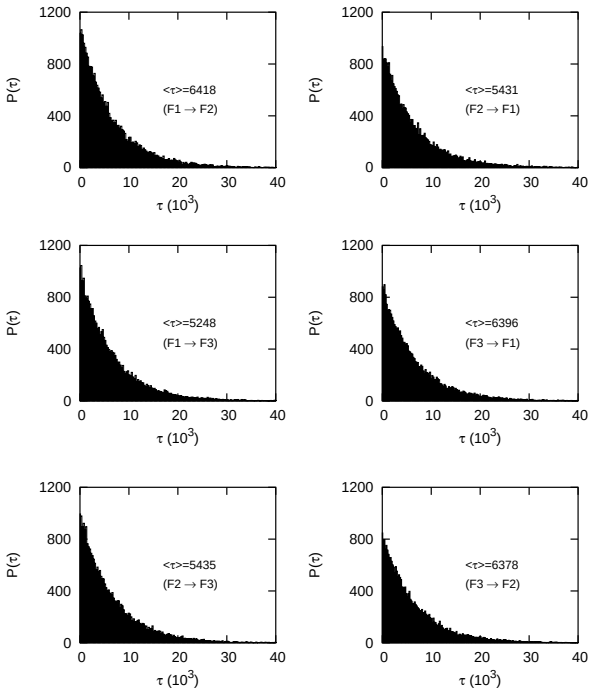

Figure 7.9: Similar than figure 7.6 we represent the probability distribution of the remaining time in a family before jumping to another one. Now, families correspond to different shots of the same individuo as illustrated by figure 7.8. The time-average and different transitions among each respective family are indicated in the graph. We take $T_1 = 0.75T_1^c$ and $T_0 = 0.05T_0^c$.

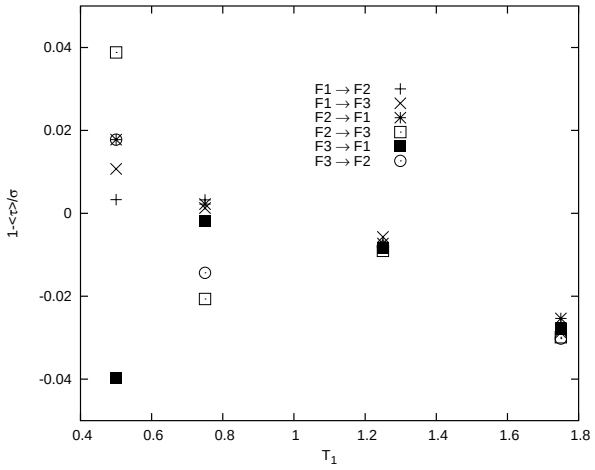

Figure 7.10: The relation between the mean and the standard deviation for probability distributions appearing in figure 7.9 versus different values of the synaptic temperature, namely, T_1 (normalized by the critical value). Poisson distributions ensure that this relation is equal to the unit. Therefore, data show a high interval of fidelity.

sis (chapters 3,5,6), and the main concussion is that it is an advantage because improves the network ability to detect changing stimuli which are received from the environment. In this phase, is possible to code and/or decode in the temporal dimension. Furthermore, we have seen as spatial information in attractor neural networks can be stored in synapses. Hence, this mechanism can explain and understand identification and categorization of spatio-temporal patterns which can be relevant, for instance, to the understanding of early olfactory processing [Laurent et al., 2001]. Thus, different odors could be coded in different attractors and the neural automata is able to extract and segment the components of complex odor patterns which are spatiotemporal sequences of neural activity. Note that the meaning of categorization, implies, firstly, identify the different patterns for then classify them constituting the same family and establishing thus a hierarchy of correlations among its elements.

Bibliography

Y. Aphinyanaphongs, I. Tsamardinos, A. Statnikov, D. Hardin, and C. F. Aliferis. Text categorization models for high quality article retrieval in internal medicine. *J. Am. Med. Inform. Assoc.*, Nov 23, 2004. 125

T. Berners-Lee, R. Cailliau, A. Luotonen, H. F. Nielsen, and A. Secret. The world-wide web. *Communications of the ACM*, 37:76–82, 1994. 125

B. Y. Cheng, J. G. Carbonell, and J. Klein-Seetharaman. Protein classification based on text document classification techniques. *Proteins*, Jan 11, 2005. 125

N. D. Doolittle. State of the science in brain tumor classification. *Semin. Oncol. Nurs.*, 20:224–230, 2004. 125

G. Laurent, M. Stopfer, R.W. Friedrich, M.I. Rabinovich, A. Volkovskii, and H.D.I. Abarbanel. Odor encoding as an active, dynamical process: Experiments, computation and theory. *Annual Review of Neuroscience*, 24:263–297, 2001. 126, 138

M. J. Vazquez, R. A. Lorenzo, and R. Cela. Chlorophenols identification in water using an electronic nose and anns (artificial neural networks) classification. *Water Sci. Technol.*, 49:99–105, 2004. 126

Chapter 8

Summary and Conclusions

We have studied by using tools from non-equilibrium statistical mechanics how in recurrent neural networks some collective phenomena, measured by a few observables, emerge from cooperation between the whole system (neurons and synapses). Some examples can be long-term memory, pattern recognition, presynaptic noise acting on synapses, switching phenomena, or identification and categorization. All these global properties of the system depend on the complexity or assumed realism of synaptic interactions among different neurons. We have studied three different levels on the s description of synapses.

The highest or most realistic degree was analyzed in chapter 3. The motivation of this modell is the Tsodyks's phenomenological model [Tsodyks et al., 1998]. We assume that the intensity of the synapse can either increase (facilitation) or decrease (depression) by rapid repeated presynaptic activation which is typically required to produce appreciable synaptic plasticity [Abbott and Regehr, 2004]. We consider a stochastic neural network of N binary neurons and we assume that the state of each neuron evolves in time with a probabilistic Glauber dynamics [Peretto, 1992] associated to local fields given by $h_i = \sum_j \omega_{ij} x_j s_j$. These local fields represent the total presynaptic current arriving to the postsynaptic neuron i. The variables ω_{ij} are static weights and represent the synaptic strength between neurons i and j. They are defined ac-

cording to the standard Hebb rule [Hebb, 1949, Hertz et al., 1991]. The variable $x_j(t)$ is a dynamical quantity representing the current state of the synapse and its probability of producing a postsynaptic response [Tsodyks et al., 1998]. In particular, it represents the fraction of neurotransmitters that are in a *recovering* state. Depending on its dynamics this variable can include short term depression and facilitation mechanisms. When $x_j = 1$, for any j we recover the standard Hopfield model, e.g. under this scenario an attractor neural network with static synapses. If one wants to include facilitation, it is necessary to use a new dinamical variable $u_j(t)$, which increases after each presynaptic spike and takes into account the opening of calcium channels in the presynaptic neuron near the neurotransmitter release sites. Consequently, Ca^2+ ions enter into the cell and bind to an acceptor close to the release sites gating the neurotransmitter quantal release [Bertram et al., 1996]. This system is defined by a set of dynamical equations in which appear both coupled-dynamics $u_j(t)$ and $x_j(t)$, each one characterized respectively by the constant of times τ_{fac} and τ_{rec} [Tsodyks et al., 1998]. We report on the mean-field analysis of the model. Using similar techniques to those explained in [Hertz et al., 1991, Marro and Dickman, 1999, Pantic et al., 2002] we study both stationary and dynamical properties. The steady solutions (fixed points) recover the previous results of only depression appearing [Torres et al., 2002], simply taking the limit τ_{fac} going to 0. In the steady states, we observe that the effect of facilitation is considerable only when the initial probability of neurotransmitter release, namely U_{SE}, is low [Tsodyks et al., 1998]. It seems facilitation and depression coexist at synapses, with their relative weight depending largely on U_{SE}. A high (low) value favors depression (facilitation).

Another quantity that in attractor neural networks takes a relevant importance and that is measured in the steady state, is the maximum number of stable patterns that the system is able to store and retrieve, e.g. the *storage capacity*. To calculate it, we use the standard method explained in [Hertz et al., 1991], which assumes that in the steady state the network has a set of macroscopic overlaps, $\mathcal{O}(1)$, with a finite number of patterns (condensed patterns)

whereas the overlap is $\mathcal{O}(1/\sqrt{N})$ for the rest of patterns (non-condensed patterns). We apply similar technical details to those reported in [Torres et al., 2002]. The result is a set of closed macroscopic and stationary equations for the order parameters $\mathbf{m}, \mathbf{q}, \mathbf{r}$, called respectively, overlap, Edwards-Anderson (EA) and Amit-Gutfreund-Sompolinsky (AGS) [Amit et al., 1987, Hertz et al., 1991]. We recover previous results existing in the literature. First, by taking the limit τ_{rec} going to 0, the case of static synapses or equivalently, the Hopfield situation [Hertz et al., 1991] and second, when τ_{fac} going to 0, the choice of considering only depressing synapses [Torres et al., 2002]. Compared to this last one, in our case, which includes facilitating mechanisms, the storage capacity of stable patterns decreases. This is due to the effect of facilitation is the reduction of depression, and consequently the stability of the attractors is changed considerably. Thus, we have two sources of noise in the storage capacity calculation; the usual noise originated by the increase of the number of patterns, and a new contribution caused by the unstability of patterns. This fact gets a meaningful decrease in the critical value for the storage capacity. Following this reasoning, the case of static synapses or Hopfield situation [Hertz et al., 1991, Hopfield, 1982] (recovered in the limit $\tau_{rec} \to 0$) gives the largest storage capacity, $\alpha_c = 0.138$. The next value corresponds to the case of only depressing synapses [Torres et al., 2002] and finally, the smallest storage is achieved when both depressing and facilitating mechanisms are incorporated.

In relation to dynamical properties, we study for $\alpha = 0$ the local stability around the steady states and we investigate an oscillatory phase, where the system is able to jump between the stored patterns in the retrieval dynamics. Similar to the results reported in [Pantic et al., 2002], we show that there are two critical or bifurcation values of τ_{rec} , namely, τ^{*}_{rec} and τ^{**}_{rec}. For $\tau_{rec} < \tau^{*}_{rec}$, the system has three fixed points, two stable which correspond with the memory solution or ferromagnetic, and one unstable, which gives the no-memory solution or paramagnetic. For $\tau^{*}_{rec} < \tau_{rec} < \tau^{**}_{rec}$ stable oscillations occur (limit cycle attractor). Finally, when $\tau_{rec} > \tau^{**}_{rec}$ only the paramagnetic fixed point is stable. Therefore, in addition to the fixed-point (ferromagnetic and param-

agnetic) attractors, we show that the network dynamics reveals a limit cycle attractor, which enables a periodic kind of oscillatory behavior. Compared to the situation of static synapses for $\alpha = 0$, which lonely shows the ferromagnetic and paramagnetic solutions, the system now is able by itself, without external stimulation, of describing continuous hopping among the different stored patterns. This feature is called *switching behavior*. Other important fact, is that facilitation incorporates, compared to [Pantic et al., 2002], complex and non-trivial modifications of both critical values τ^{*}_{rec} and τ^{**}_{rec}. The critical value τ^{*}_{rec} decreases when τ_{fac} is incremented. This fact brings forward the oscillatory behavior, and, consequently, a drastic reduction of the ferromagnetic phase occurs . In addition, the width of the oscillatory phase, namely $\delta \equiv \tau^{**}_{rec} - \tau^{*}_{rec}$, is also diminished. However, the frequency of the oscillations is higher, and consequently this can be enhance the network to response to highly changing stimulus.

An intermediate level of complexity on synapses assumes that (fast) presynaptic noise affects to synapses. This fact can model short-term plasticity or working memory [Abbott and Regehr, 2004] and unreliable synapses [Zador, 1998]. The case of sequential updating has been studied in chapter 4. There is multiple converging evidence [Abbott and Regehr, 2004] that synapses play an active role in determining the complex processing of information in the brain. One may understand some recent observations by assuming that the postsynaptic response may either decrease (*depression*) or increase (*facilitation*) depending on presynaptic neural activity [Thomson et al., 2002, Tsodyks et al., 1998]. It is reasonable to expect that these effects, which occur on a short–time scale, are at the basis of a more efficient cooperation between neurons. In our model the values assigned to the synaptic intensities by a *learning* (e.g., Hebb's) rule are constantly perturbed with *microscopic* fast noise. A new parameter is involved by this perturbation that allows for a continuum transition from depressing to static synapses.

Our interest is in a neural network in which a local stochastic dynamics is constantly influenced by synaptic *noise*. Consider a set of N binary neurons

with configurations $\mathbf{S} \equiv \{s_i = \pm 1; i = 1, \ldots, N\}$. Any two of them connected by synapses $w_{ij} = \overline{w}_{ij} x_j, \forall i, j$. Here, $\overline{w}_{ij}$ is fixed, namely, determined in a previous *learning* process, and x_j is a stochastic variable. Once $\mathbf{W} \equiv \{\overline{w}_{ij}\}$ is given, the state of the system at time t is defined by setting $\mathbf{S}$ and $\mathbf{X} \equiv \{x_i\}$. This evolves with time — after the learning process — via a familiar Master Equation [Marro and Dickman, 1999]. We restrict our analysis to the case of fast fluctuations on $\mathbf{X}$. Here, the neurons evolve in the presence of a steady distribution for $\mathbf{X}$. The dynamics is characterized by an *effective* rate or superposition that one may interpret to come from the competition between different elementary mechanisms. Each of the elementary dynamics tends to drive the system to a well-defined equilibrium state. In general, the competition will impede the equilibrium and, the system will asymptotically go towards a non-equilibrium steady state [Marro and Dickman, 1999]. This is known to be a more general condition in nature than the state of thermodynamic equilibrium. We show that such competition between synaptic noise and neural activity may be the origin of some of the computational strategies in biological systems. In this chapter we are concerned with sequential updating. That is, the elementary dynamic step will simply consist of local inversions $s_i \to -s_i$ induced by a bath at temperature T. We formulate an stochastic scenario given by the equations (4.4),(4.5) and (4.6) and propose it as a tool to model activity-dependent processes.

We present in this chapter two different frameworks; the first one assumes for the steady probability of X a local dependence on activity, and the second one assumes a global dependence. Under certain assumptions, the system in the first of these cases is described by the effective Hamiltonian. This reduces to a Hopfield system, i.e., the familiar attractor neural network without (fast) synaptic noise, with rescaled temperature and a threshold. A more intriguing behavior shows the second situation, e.g. the noise depends on the total presynaptic current arriving to the postsynaptic neuron. We study this case both analytically by a sort of mean-field treatment and numerically by a series of related Monte Carlo simulations using Glauber, *spin-flip* dynamics [Marro and

Dickman, 1999]. The two approaches are in full agreement and complement each other. Our model involves two main parameters. One is the *temperature*, T, and controls the stochastic evolution of the network activity. The other, Φ, controls the fast-noise intensity. Varying this, the system describes from normal operation to depression phenomena. A main result is that the presynaptic noise induces the occurrence of a tricritical point of certain values of these parameters $(T_c, \Phi_c) = (1, -4/3)$. In the limit $\alpha \to 0$, this separates first from second order phase transitions between a ferromagnetic-like (retrieval) phase and a paramagnetic-like (non-retrieval) phase. In this chapter, the main achievement is that fast noise drastically enhances the network sensitivity to external stimulation. We explicitly show how the noise may cause instability to the *attractor* and the system consequently will seek for another one. In particular, one observes for a single pattern switching to the associated antipattern , and for several stored patterns jumps among different ones. This behavior is most interesting because it improves the network's ability to be very sensitive to the forcing stimulus. However, it is rather independent of the network's initial state. It seems reasonable to argue that, in nature pattern recognition and processes of identification and categorization in classes might follow a similar strategy. That is, different attractors may correspond to different objects, and a dynamics conveniently perturbed by fast noise may keep visiting the attractors belonging to a class which is characterized by a certain degree of correlation between its elements. In fact, a similar mechanism seems at the basis of early olfactory processing of insects [Laurent et al., 2001], and the same sort of instabilities have been described in the cortical activity of monkeys [Abeles et al., 1995].

In chapter 5, we discuss the consequences of considering the presynaptic noise (studied and analyzed in the previous chapter 4) in *stochastic neural automatas* (SNA), namely, lattice models of attractor neural networks which is simultaneously updated[1], instead of sequential updating where solely a small

[1]For details of different kind of updatings and their effects on the system dynamics see for instance [Marro and Dickman, 1999, Peretto, 1992].

neighborhood is updated at each time step. We consider a network with binary neurons represented by configurations $\mathbf{S} \equiv \{s_i = \pm 1\}_{i=1}^{N}$, each one at each node $i = 1, \ldots, N$, and assume synapses intensities w_{ij} connecting the neurons i and j. They are defined as $w_{ij} = \overline{w}_{ij} x_j$, being x_j a stochastic variable and $\overline{w}_{ij}$ fixed intensities (or weights), which are determined in a previous *learning* process. After defining the local field $h_i = \sum_{j \neq i} w_{ij} x_j s_j$ or the total presynaptic current reaching the postsynaptic neuron (s_i), in absence of thermal fluctuations the system dynamics is deterministic and assures that $\mathrm{sig}(h_i) = s_i$. In order to construct a stochastic dynamics, we introduce a noise parameter $T \equiv \beta^{-1}$ (note that the deterministic dynamics is again recovered just taking the limit $T \to 0$). It is important to remark that the intensities $w_{ij} = \overline{w}_{ij} x_j$ are asymmetric, and therefore, the system behavior cannot described by using a (equilibrium) Hamiltonian description. Under certain assumptions, enumerated and showed in the previous chapter 4 is shown the possibility to describe the system in terms of *effective* local fields. Compared to the previous chapter 4, non-sequential updating allows to switch the system among the different attractors, without external stimulation.

We discuss two types of SNA characterized by taking different total number of change trials in the jumping probability appearing in the master equation. The first family, assumes $N^*(t) = N$ and is equivalent to parallel updating *(Little dynamics)*. The second one, takes N^* as non-constant in time and satisfying $N^*(t) < N$. For the first case, we present both mean field theory and Monte Carlo simulations in full agreement. For the second choice we solely present Monte Carlo simulations. Both of them illustrate an emergent behavior which is complex; in particular, it depicts fixed points, P–cycles, hopping between memorized patterns [Cortes et al., 2004, Pantic et al., 2002], and even chaotic dynamics which in several different situations can be convenient in order to be possible to visit a huge number of different patterns. The chaotic dynamics is aperiodic, and this can be useful to store and retrieve different spatio-temporal patterns [Freeman, 1994]. An example of this kind of systems where spatio-temporal stimuli can be coded is the olfactory bulb in insects [Laurent et al.,

2001]. We want to remark that this is not the first time where chaos appears in retrieval processes in attractor neural networks. For instance, in [Bolle and Vink, 1996] is studied the retrieval dynamics attending to the shape of the gain functions as a modeling parameter. Many different dynamical behaviors are observed, covering from point attractors to chaotic dynamics. In our case, also is possible to obtain an associated gain function, which is non-sigmoidal for $\Phi > 0$ and, consequently, may lead to chaotic behavior for the overlap dynamics [Bolle and Vink, 1996]. In order to get a quantitative description of these chaotic oscillations, we measure the power spectrum and an entropy for its harmonics. Using FFT, we computed the harmonic power spectra $P(n)$, and then we converted it to its probability $p(n) = P(n)/\sum P(n)$. The entropy function is then given in bits as $S \equiv -\sum p \log_2(p)$ [Varona et al., 2001]. This measures regularization; a decrease of S is an indication of regularization or a lower chaoticity, while an increase of S means a higher chaos or an irregularity in the time series. For practical convenience, to increase the maximum coding rate of spatio-temporal information able of being retrieved is very interesting. There are experimental evidences [Freeman, 1994] showing that chaos is essential in the dynamics of searching new patterns to learn. In this sense, entropy has a main role to look for the noise parameter which is optimum to learn new and more spatio-temporal patterns. If S increases, the chaoticity in time series is larger. A mechanism based on the coding of spatio-temporal patterns is the olfactory bulb of, for instance, insects. It is able to discriminate and categorize different odors [Laurent et al., 2001].

Finally, the lowest level on the complexity of synapses has been studied in chapter 6 and the main (computational) consequences of this dynamics has been explored in chapter 7. In chapter 6, we present another *stochastic neural automata* which involves two independent competing dynamics, one for neurons and the other for synapses. Consider N (binary) neuron variables, $s_i = \pm 1$, any two of them linked by synapses of intensity w_{ij}; $i, j = 1, \ldots, N$. The interest is on the configurations $\mathbf{S} \equiv \{s_i\}$ and $\mathbf{W} \equiv \{w_{ij}\}$. In order to have a well–defined reference, we assume that interactions are determined by

the Hopfield *energy* function. Furthermore, consistent with the observation that memory is a global dynamic phenomenon, we take the model dynamics determined at each time step by a single pattern, say μ. Consequently, $H(\mathbf{S}, \mathbf{W}; t) = -\frac{1}{2}\sum_i \sum_{j\neq i} w_{ij}^{\mu} s_i s_j$ with $\mu = \mu(t)$ and assuming the Hebbian learning rule, for example, $w_{ij}^{\mu} = \frac{k}{N}\xi_i^{\mu}\xi_j^{\mu}$, where, $\xi_i^{\mu} = \pm 1$ are the variables that characterize the μ binary pattern, one out of the P considered ones, and k is a proportionality constant. Therefore, each configuration $\mathbf{W}$ is unambiguously associated with a single μ, and we write $\mathbf{W} \equiv \mu$ in the following. This scenario may be formulated by stating that the probability of any configuration $(\mathbf{S}, \mu)$ evolves in discrete time according to a master equation [Marro and Dickman, 1999]. The associated jumping probability amounts to drive neurons activity and synaptic intensities by different temperature, $\beta_0^{-1} \equiv T_0$ and $\beta_1^{-1} \equiv T_1$, respectively. We report on some Monte Carlo simulations of this model which reveals an intriguing situation. Depending on the values of temperatures T_0 and T_1 different regimes occur. To distinguish them, we introduce the overlap ($\mathbf{m}$) and the total number of jumps (j). Three different phases appear: (1) the *Ferromagnetic*, satisfying $\mathbf{m} \neq 0$ and $j = 0$, and where the system has *static* associative memory. (2) The *Paramagnetic*, with $\mathbf{m} = 0$ and $j = 0$, and where there is no any kind of associative memory and (3) the *Oscillatory* for $\mathbf{m} = 0$, $j \neq 0$. In this last phase, similar to the Hopfield situation, the system has associative memory. However, here it is a dynamic process, in the sense that the system trapped in any attractor is able to jump to another one. Because the probability of jumping depends on the overlaps, which is the total presynaptic current arriving to the postsynaptic neuron, in general this mechanism is a complex process. In order to study in detail the oscillatory phase, it was convenient to look at time correlations. We compute the time $\tau_{\nu\gamma}$ in which the system *remains* in the pattern νth before jumping to the γth. This reveals the existence of two different kinds of oscillatory behavior. One is such that $\tau_{\nu\gamma} \simeq \tau$, independent of ν and γ. That is, the system stays the same time at each pattern. Thus, jumping behaves as a completely random process, without any time correlation. Instead of, lowering T_0 leads to non-trivial time correla-

tions, namely, $\tau_{\nu\gamma}$ depends on both ν and γ. This peculiar behavior suggests to use our algorithm to code spatial–temporal information.

To explain the phenomenology observed in Monte Carlo simulations, we develop a coarse-graining procedure. It is possible to estimate from the master equation for $P(\mathbf{S}, \mu)$ how any observable $F(\mathbf{S}, \mu)$ evolves in time[2]. Alternatively, one may be directly concerned with the time evolution for the probability of jumping in terms of the overlaps $P(\mathbf{m}, \mu)$. This reduces the degrees of freedom, from a number of order $2^N + 1$ in $(\mathbf{S}, \mu)$ to $P+1$ in $(\mathbf{m}, \mu)$. After coarse-graining, the time evolution of the system is dealt by an *effective* jumping probability which allows us to have two independent mechanisms to evolve the system: one, given a pattern, explains how the system changes between different configurations on the neural activity. The other, is responsible of changes between any two different patterns, for fixed neural activities. After applying the coarse-graining procedure, the main approach is that averaging over patterns realizations is not necessary. That is due to the dependence on patterns can be extracted from tanh functions which characterize the steepest descend solution [Amit et al., 1987, Hertz et al., 1991].

In chapter 7, we present a computational study of the stochastic neural automata defined in chapter 6. As a matter of fact, this chapter can be understood like an extension of the previous one. The motivation of these simulations lies on a multitude of technical applications requiring for categorization, e.g. assigning of objects to zero or more predefined classes. In all of them, firstly is necessary to storage a huge amount of data, and after being consulted. In recent times, the most emergent necessity is text-categorization on WWW searchers, due to the availability of ever larger numbers of text documents in digital form and to the ensuing need to organize them for easier use. Some examples can include classification of web documents, or searchs of articles and researchers in data bases of science [Berners-Lee et al., 1994]. The dominant aim is to build software tools capable of classifying by learning

[2]See [Marro and Dickman, 1999] for the discussion of different systems

the characteristics of the categories from a training set of pre-classified documents [Aphinyanaphongs et al., 2004, Doolittle, 2004]. In biotechnology, the need for accurate, automated protein classification still remains unsolved, due to extreme diversity among its members [Cheng et al., 2005]. Other industrial devices which need optimal algorithms for classification are the electronic noses, e.g chemical sensors with a pattern recognition system (normally, artificial neural networks). They are being developed as systems for the automated detection and classification of odors, vapors and gases, which can play a main role for defense in "chemical wars". There are also civil applications requiring for classification. For instance, food industries use such devices as aids for quality control or process-monitoring tools [Vazquez et al., 2004]. In addition, a multitude of biological frameworks need of these (natural) strategies to make possible categorization, for instance, the early olfactory processing [Laurent et al., 2001]. Instead of machine learning methods, as for instance decision trees and naive Bayes classifiers, we present an alternative for categorization based on stochastic neural automatas. We (computationally) explore the complex spatio-temporal dynamics. For different sets of families of patterns, we illustrate the time-trajectory described by the neural automatas. We propose that this spatio-temporal evolutions can be a tool allowing for categorization. Depending on correlations among the stored patterns, we observe that is possible to establish a hierarchical classification among its elements.

In sum, we have studied stationary and dynamical properties of recurrent neural networks which depend on the assumed realism to describe synaptic interactions among different neurons. We have studied three different levels on the synaptic description. The most realistic case has been presented in the chapter 3. Here, we present the effects of both facilitating and depressing mechanisms on synapses [Tsodyks et al., 1998] and its influence in attractor neural networks. This is the first time where an attractor neural model includes a facilitating mechanism. We solve the general case and recover previous results of solely depressing synapses [Pantic et al., 2002]. Our results reinforce the fact of facilitation gets a stronger depression and consequently, enhances

easier switching between patterns, because influences strongly on the stability of steady states. The intermediate level, has been analyzed in the chapters 4 and 5. In chapter 4 we study both computational and analytically the effect of (fast) presynaptic noise on the transmission of information in attractor neural networks. This is inspired in recent neurobiological findings that show that synaptic strength may either increase or decrease, on a short-time scale depending on presynaptic activity. We thus model short-term plasticity or working memory [Abbott and Regehr, 2004] and unreliable synapses [Zador, 1998] and describe a mechanism by which fast presynaptic noise enhances the neural network sensitivity to an external stimulus. The reason is that the presynaptic noise induces nonequilibrium behavior and, consequently, the space of fixed points is modified in such a way that the system can easily scape from the attractor. In addition of pattern recognition, the model shows class identification and categorization, which may be relevant to the understanding of some of the brain complex tasks. In chapter 5, we present and study a family of stochastic neural automatas which are affected by fast noise. Depending on the parameter which controls the noise intensity, the system can show very different types of dynamics, ranging from totally ordered to chaotic. In chapter 6 we introduce other stochastic neural automata in which fluctuations of neural activity and synaptic intensities evolve at different temperature. The competition between two thermal baths impedes one reaching the thermodynamic equilibrium [Marro and Dickman, 1999]. The complex non-linear dynamics is solved via a coarse-graining procedure. The network exhibits various retrieval phases, including switching among different attractors, which can be either uncorrelated (random) or correlated in time. We present a computational study of these time-correlations observed in the oscillatory phase. In chapter 7 we analyse the system inside the oscillatory phase by combining a mesoscopic dynamics obtained in chapter 6 and Monte Carlo simulations. In special, we study the time-correlations showed in the oscillatory phase. This switching behavior has been explained in different places in the development of this thesis (chapters 3,5,6), and the main concussion is that it is an advantage because improves the

network ability to detect changing stimuli which are received from the environment.

Under different approaches, switching behavior appears in the development of this thesis. Sometimes, oscillations in the system are produced by external stimulation (non-autonomous), othertimes by itself (autonomous). The time-trajectory is in general complex, presenting fixed points, P-cycles or even chaotic. The main achievement is the possibility to code and/or decode certain inputs, stimuli or patterns in the temporal dimension which together the spatial information's susceptibility of being stored/retrieved for attractor neural systems, allows this mechanism explain and interpret identification and categorization of spatio-temporal patterns which can be relevant, for instance, to the understanding of early olfactory processing [Laurent et al., 2001]. Thus, different odors can be coded in different attractors and the neural system is able to extract and segment the components of complex odor patterns which are spatiotemporal sequences of neural activity. Note that the meaning of categorization, implies, firstly, the identification for different patterns, for then being classified by belonging to the same family; this then establishes a hierarchy of correlations among its elements.

The last comment concerns the main objectives which were formulated in the beginning of this thesis, namely, (1) To understand and analyse by (non-equilibrium) statistical mechanics, how from interactions of (infinitely) large number of neurons emerge (essential) learning processes, such as, storage and retrieval of information, classification in families of patterns, (long-term) memory, or switching phenomena, and (2) To develop both theory and simulation of stochastic neural automatas, which may allow new studies, either analytical or for applications, including the possibility to implement in hardware these kind of neural systems to solve problems in biology or engineering. About the achievements, readers only should judge it.

Bibliography

L. F. Abbott and W. G. Regehr. Synaptic computation. *Nature*, 431:796–803, 2004. 141, 144, 152

M. Abeles, H. Bergman, I. Gat, I. Meilijson, E. Seidemann, N. Tishby, and E. Vaadia. Cortical activity flips among quasi-stationary states. *Proc. Natl. Acad. Sci. USA*, 92:8616–8620, 1995. 146

D. J. Amit, H. Gutfreund, and H. Sompolinsky. Statistical mechanics of neural networks near saturation. *Ann. Phys.*, 173:30–67, 1987. 143, 150

Y. Aphinyanaphongs, I. Tsamardinos, A. Statnikov, D. Hardin, and C. F. Aliferis. Text categorization models for high quality article retrieval in internal medicine. *J. Am. Med. Inform. Assoc.*, Nov 23, 2004. 151

T. Berners-Lee, R. Cailliau, A. Luotonen, H. F. Nielsen, and A. Secret. The world-wide web. *Communications of the ACM*, 37:76–82, 1994. 150

R. Bertram, A. Sherman, and E. F. Stanley. Single-domain/bound calcium hypothesis of transmitter release and facilitation. *J. Neurophysiol.*, 75:1919–1931, 1996. 142

D. Bolle and B. Vink. On the dynamics of analogue neurons with nonsigmoidal gain functions. *Physica A*, 223:293–308, 1996. 148

B. Y. Cheng, J. G. Carbonell, and J. Klein-Seetharaman. Protein classification based on text document classification techniques. *Proteins*, Jan 11, 2005. 151

J.M. Cortes, P.L. Garrido, J. Marro, and J.J. Torres. Switching between memories in neural automata with synaptic noise. *Neurocomputing*, 58-60:67–71, 2004. 147

N. D. Doolittle. State of the science in brain tumor classification. *Semin. Oncol. Nurs.*, 20:224–230, 2004. 151

W. J. Freeman. Neural networks and chaos. *J. Theor. Biol.*, 171:13–18, 1994. 147, 148

D. O. Hebb. *The Organization of Behavior: A Neuropsychological Theory*. Wiley, 1949. 142

J. Hertz, A. Krogh, and R.G. Palmer. *Introduction to the theory of neural computation*. Addison-Wesley, 1991. 142, 143, 150

J.J. Hopfield. Neural networks and physical systems with emergent collective computational abilities. *Proc. Natl. Acad. Sci. USA*, 79:2554–2558, 1982. 143

G. Laurent, M. Stopfer, R.W. Friedrich, M.I. Rabinovich, A. Volkovskii, and H.D.I. Abarbanel. Odor encoding as an active, dynamical process: Experiments, computation and theory. *Annual Review of Neuroscience*, 24:263–297, 2001. 146, 147, 148, 151, 153

J. Marro and R. Dickman. *Nonequilibrium Phase Transitions in Lattice Models*. Cambridge University Press, 1999. 142, 145, 146, 149, 150, 152

L. Pantic, J.J. Torres, H.J. Kappen, and S.C.A.M. Gielen. Associative memmory with dynamic synapses. *Neural Comp.*, 14:2903–2923, 2002. 142, 143, 144, 147, 151

P. Peretto. *An Introduction to the modeling of neural networks*. Cambridge University Press, 1992. 141, 146

A.M. Thomson, A.P. Bannister, A. Mercer, and O.T. Morris. Target and temporal pattern selection at neocortical synapses. *Philos. Trans. R. Soc. Lond. B Biol. Sci.*, 357:1781–1791, 2002. 144

J.J. Torres, L. Pantic, and H.J. Kappen. Storage capacity of attractor neural networks with depressing synapses. *Phys. Rev. E.*, 66:061910, 2002. 142, 143

M. V. Tsodyks, K. Pawelzik, and H. Markram. Neural networks with dynamic synapses. *Neural Comp.*, 10:821–835, 1998. 141, 142, 144, 151

P. Varona, J.J. Torres, R. Huerta, H.D.I. Abarbanel, and M. I. Rabinovich. Regularization mechanisms in the dynamics of spiking-bursting neurons. *Neural Networks*, 14:865–875, 2001. 148

M. J. Vazquez, R. A. Lorenzo, and R. Cela. Chlorophenols identification in water using an electronic nose and anns (artificial neural networks) classification. *Water Sci. Technol.*, 49:99–105, 2004. 151

A. Zador. Impact of synaptic unreliability on the information transmitted by spiking neurons. *J. Neurophysiol.*, 79:1219–1229, 1998. 144, 152

Articles and preprints

1. J. Marro, J. M. Cortes and P. I. Hurtado. Modeling nonequilibrium phase transitions and critical behavior in complex systems. *Computer Physics Communications*, 147:115-119, 2002.

2. J.M. Cortes, P.L. Garrido, J. Marro and J.J. Torres. Switching between memories in neural automata with synaptic noise. *Neurocomputing*,58-60:67-71, 2004.

3. J.J. Torres, J. Marro, P.L. Garrido, J.M. Cortes, F. Ramos and M.A. Munoz. Effects of static and dynamic disorder on the performance of neural automata. *Biophysical Chemistry*. In press. 2004.

4. J. M. Cortes, J. J. Torres, J. Marro, P. L. Garrido and H. J. Kappen. Effects of Fast Presynaptic Noise in Attractor Neural Networks. *Neural Comp.* Submitted. 2005.

5. J. M. Cortes, J. J. Torres and J. Marro. Chaotic Switching Phenomena in Stochastic Neural Automata. *Phys. Rev. E.* Submitted. 2005.

6. J. J. Torres, J. M. Cortes and J. Marro. Facilitating mechanisms on attractor neural networks. *Phys. Rev. E.* Submitted. 2005.

7. J. J. Torres, J. M. Cortes and J. Marro. Instability of attractors in auto–associative networks with bio–inspired, fast synaptic noise. *Neurocomputing*. Submitted. 2005.

8. J. M. Cortes, J. J. Torres and J. Marro. Controlling neural chaos by synaptic noise. *Biosystems* Submitted. 2005.

9. J. Marro, J. J. Torres, P. L. Garrido and J. M. Cortes. Neural automata with two temperatures. *Phys. Rev. Lett.*. Submitted. 2005.

10. J. M. Cortes, J. J. Torres, P. L. Garrido and J. Marro. A Neural Automata alternative for categorization. In preparation.

11. J. J. Torres, J. M. Cortes and J. Marro. A Formulation of Dynamic Synapses based on Statistical Mechanics. In preparation.